Two–Loop Techniques in Rare Decays

Dissertation
zur
Erlangung der naturwissenschaftlichen Doktorwürde
(Dr. sc. nat.)

vorgelegt der
Mathematisch-naturwissenschaftlichen Fakultät
der
Universität Zürich
von
Sabine Schilling
aus Deutschland

Promotionskomitee

Prof. Dr. Daniel Wyler (Vorsitz)
Prof. Dr. Thomas Gehrmann

Zürich 2005

Abstract

In the Standard Model (SM) rare decays are forbidden at the tree level by various mechanisms. Loop decays, which then become the dominant contribution, are sensitive to new physics phenomena due to a strong dependence on virtually exchanged particles. Thus they serve as an excellent test area of the SM and often discussed extensions of it, like Two-Higgs-Doublet models (THDMs) or supersymmetric models. In this thesis we calculate rare one- and two-loop B-decays in the SM and THDMs as well as the decay of the supersymmetric partner of the tau-lepton, the $\tilde{\tau}$, into an axino, the supersymmetric partner of the axion, in modern versions of supersymmetric models:
Flavour changing neutral current (FCNC) B-decays arise in the SM first at the one-loop level, as FCNC are forbidden at the tree-level by the GIM mechanism. We derive the Wilson coefficients $C_7(\mu_W)$, $C_9(\mu_W)$ and $C_{10}(\mu_W)$ of the operators

$$\mathcal{O}_7 = \frac{e}{g_s^2} m_b (\bar{s}\sigma^{\mu\nu} P_L b) F_{\mu\nu}, \quad \mathcal{O}_9 = \frac{e^2}{g_s^2} (\bar{s}\gamma_\mu P_L b) \sum (\bar{l}\gamma^\mu l), \quad \mathcal{O}_{10} = \frac{e^2}{g_s^2} (\bar{s}\gamma_\mu P_L b) \sum (\bar{l}\gamma^\mu \gamma_5 l)$$

of the effective Hamiltonian up to $\mathcal{O}(\alpha_s)$-precision in the SM and type-I and type-II THDMs at the matching scale μ_W. The $\mathcal{O}(\alpha_s)$-corrections are important ingredients for next-to-next-to-leading logarithmic predictions of various observables related to the inclusive decays $B \to X_s\gamma$ and $B \to X_s l^+ l^-$.
Axinos are well-motivated candidates for the lightest supersymmetric particle (LSP) and for cold dark matter in the universe. Assuming the $\tilde{\tau}$ to be the next-to lightest-supersymmetric (NLSP) particle, we show how the NLSP decays can be used to probe the axino LSP scenario in KSVZ axion models by calculating the one-loop induced decay rate of the $\tilde{\tau} \to \tau\ \tilde{a}\ \gamma$ decay as well as the two-loop induced decay $\tilde{\tau} \to \tau\ \tilde{a}$. The corresponding tree-level processes are forbidden as axinos can couple only to the heavy quarks introduced in KSVZ models.

In order to calculate the numerous one- and two-loop integrals appearing in the calculation of the B- and $\tilde{\tau}$-decays, we have written a software package which enables us to perform the integration of all occurring integrals automatically. A detailed documentation of the written software is given in the appendix.

Zusammenfassung

Im Standard-Modell (SM) der Teilchenphysik sind seltene Zerfälle auf Baum-Graphen-Niveau aufgrund verschiedener Mechanismen verboten. Schleifen-Diagramme, die in seltenen Zerfällen den dominante Beitrag zum Wirkungsquerschnitt liefern, hängen stark von den virtuellen Teilchen im Schleifen-Diagramm ab. Sie eignen sich somit besonders für Präzisions-Tests des Standard-Modells sowie häufig diskutierten Erweiterungen des Standard-Modells wie Zwei-Higgs-Dublett-Modellen (2HDM) und modernen Versionen von supersymmetrischen Modellen. In dieser Doktorarbeit werden seltene Ein- und Zwei-Schleifen B-Zerfälle im SM und 2HDM sowie seltene Zerfälle des Staus ($\tilde{\tau}$) in ein Axino ($\widetilde{a}$, den supersymmetrischen Partner des Axions, untersucht:
"Flavour changing neutral current" (FCNC) B-Zerfälle sind im SM auf Baum-Graphen-Niveau aufgrund des GIM-Mechanismus verboten und treten somit in niedrigster Ordnung auf Ein-Schleifen-Niveau auf. Wir berechnen die Wilson-Koeffizienten $C_7(\mu_W)$, $C_9(\mu_W)$ und $C_{10}(\mu_W)$ der Operatoren

$$\mathcal{O}_7 = \frac{e}{g_s^2} m_b (\bar{s}\sigma^{\mu\nu} P_L b) F_{\mu\nu}, \quad \mathcal{O}_9 = \frac{e^2}{g_s^2} (\bar{s}\gamma_\mu P_L b) \sum (\bar{l}\gamma^\mu l), \quad \mathcal{O}_{10} = \frac{e^2}{g_s^2} (\bar{s}\gamma_\mu P_L b) \sum (\bar{l}\gamma^\mu \gamma_5 l)$$

der effektiven Hamilton-Dichte bis zur Ordnung $\mathcal{O}(\alpha_s)$ im SM und in Typ-I- und Typ-II-2HDMs. $\mathcal{O}(\alpha_s)$-Korrekturen sind wichtige Beiträge zur Berechnung von "next-to-next-leading-logarithmic"-Vorhersagen verschiedener Messgrössen in inklusiven $B \to X_s\gamma$- und $B \to X_s l^+ l^-$-Zerfällen.
Axinos sind sowohl gut motivierte Kandidaten für das leichteste supersymmetrische Teilchen (LSP) als auch für kalte dunkle Materie im Universum. Unter der Annahme, dass das $\tilde{\tau}$ dasjenige supersymmetrische Teilchen sei, das mit seiner Masse derjenigen des LSP am nächsten läge, zeigen wir, dass die Zerfälle des $\tilde{\tau}$s dazu geeignet sind, das Axino-LSP-Szenario zu überprüfen. Hierzu berechnen wir den Drei-Körper-Zerfall $\tilde{\tau} \to \tau\ \tilde{a}\ \gamma$, der zuerst auf Ein-Schleifen-Niveau auftritt, sowie den Zwei-Körper-Zerfall $\tilde{\tau} \to \tau\ \tilde{a}$, der erstmals auf Zwei-Schleifen-Niveau auftritt. Der entsprechende Baum-Graphen-Beitrag ist verboten, da Axinos nur an schwere Quarks, die in supersymmetrischen KSVZ-Modellen eingeführt werden, koppeln können.

In den betrachteten seltenen Zerfällen von B- und $\tilde{\tau}$ treten zahlreiche Ein- und Zwei-Schleifen-Integrale auf. Deren Berechnung wurde mittels eines Programmpaketes, dessen ausführliche Dokumentation im Anhang vorzufinden ist, automatisiert.

Contents

Chapter 1

Introduction

The current description of particle physics - the so called Standard Model (SM) - has been formed as a result of a combination of many theoretical concepts combined with experimental observations. As a locally gauge invariant quantum field theory the ideas of quantum theory, relativistic field theory and group theory are incorporated. The SM successfully includes almost all known properties of three out of the four known fundamental interactions - the strong, the weak and the electro-magnetic force. This is reflected by invariance under local transformations of the non-Abelian gauge symmetry $SU(3)_C \otimes SU(2)_W \otimes U(1)_Y$.

In principle local gauge invariance implies massless gauge bosons and consequently predicts long range forces. Thus local gauge theories do not seem to be at the first sight the proper description of the observed short range weak force mediated by massive gauge bosons. This apparent drawback can be solved with the help of spontaneous symmetry breaking achieved through the Higgs mechanism [1–3]. Furthermore, the proof of renormalisability of local non-Abelian (Yang-Mills) gauge theories [4] was extended to spontaneously broken gauge theories [5]. The Higgs mechanism and the proof of renormalisability were the foundations of the application of local gauge theories to describe short range weak interactions and the starting point of the formulation of the SM. The spontaneous breaking of the gauge symmetries is necessary to model accurately the short range interactions. It requires the introduction of at least one scalar particle - the so called Higgs particle. Up to now the Higgs particle has escaped the direct detection at high energy colliders [6] and is the last missing part of the experimental confirmation of the SM. The formally massless introduced gauge and "matter" fields (leptons and quarks) acquire masses due to their coupling to the Higgs field. Thus the Higgs mechanism represents the mass generation of gauge and "matter" fields.

As a consequence of the spontaneous symmetry breaking the couplings of the W and Z boson to quarks are given in terms of the elements of the Cabbibo-Kobayashi-Maskawa (CKM) matrix V_{ij} [7, 8] arising from the diagonalisation of the quark mass matrices. In the SM it is this very matrix that is responsible for all weak decays of hadrons as well as for CP non-conservation[1].

CP-violation was first observed in 1964 in kaon decay [9] and in 2003 for the first

[1] A different source of CP violation appears in QCD when including non-trivial topological effects due to the "$\Theta-$term" known as the strong CP problem.

time in the B meson system in the decay $B \to J/\psi K_S^0$ [10]. The CKM matrix plays a fundamental role in the description of weak decays. Theoretical prediction of weak hadron decays suffer generally from uncertainties due to non-perturbative strong interaction effects preventing a straightforward determination of the CKM matrix elements. An improved understanding of these decays is therefore mandatory in order to test the SM and to find eventually new physics effects.

B meson decays are promising candidates to provide these kind of insights. Remarkably the perturbatively calculable parton decay emerges as the leading contribution to physical observables whereas non perturbative corrections are suppressed by Λ_{QCD}^2/m_Q^2 with m_Q being the heavy quark mass.

Flavour changing neutral current (FCNC) B decays like $B \to X_s\gamma$ or $B \to X_s l^+ l^-$ are forbidden at the tree level and suppressed at the loop level by the GIM mechanism [11] and by the small quark-mixing matrix elements which involve the transitions between the third and the first two generations in the Cabibbo-Kobayashi-Maskawa (CKM) matrix. This mechanism seems to be confirmed by the present experimental data through the fact that the branching ration of FCNC are tiny. The "loop" suppresion of FCNC processes leads to a strong dependence on virtually exchanged particles, such as the top quark or the electroweak gauge bosons in the SM.

In many extensions of the SM, there are additional one-loop contributions in which non-SM particles propagate in the loop. If the new particles are not considerably heavier than those of the SM, the new contributions to these decays can be as large as those of the SM. As an illustration of the high sensitivity of these decays to new physics, we mention that the most stringent bound on the mass of the charged Higgs-boson in the type-II two-Higgs-doublet model comes from rare B-decays, viz $B \to X_s\gamma$, leading to $M_H > 380$ GeV [12, 13].

One should try to get information on the parameters in a given extension of the SM - the two-Higgs-doublet models (THDM) in this thesis - from all processes which allow both a clean theoretical prediction and an accurate measurement. This means that precision studies of the THDM contributions similar to those for $B \to X_s\gamma$ [14–18], where higher order QCD corrections are crucial, should also be done for the process $B \to X_s l^+ l^-$ [19].

We present the derivation of the analytic results for the one- and two-loop corrections to the Wilson coefficients $C_7(\mu_W)$, $C_9(\mu_W)$ and $C_{10}(\mu_W)$ in the SM and in type-I and type-II two-Higgs-doublet models at the matching scale μ_W. The two-loop corrections of $\mathcal{O}(\alpha_s)$ are important ingredients for next-to-next-to-leading logarithmic (NNLO) predictions of various observables related to the decays $B \to X_s l^+ l^-$ ($l = e, \mu$) in these models. We published the missing $\mathcal{O}(\alpha_s)$-corrections to the Wilson Coefficient C_9 in the THDMs for the first time [19]. For all other derived Wilson coefficients we confirm the published results.

Rare loop decays do not only have a potential to detect new physics in B-decays, but also in the decays of the the next-to lightest-supersymmetric-particle (NLSP) into axinos, a well motivated candidate for the lightest supersymmetric particle (LSP) as well as for cold dark matter. Axinos are predicted to exist in models involving low-energy supersymmetry (SUSY) and the Peccei-Quinn solution [20] to the strong CP problem. They are spin 1/2 supersymmetric partners of axions [21]. SUSY is widely considered as perhaps the most attractive framework in which the Fermi scale can be

naturally connected with physics around the Planck scale. The Peccei-Quinn (PQ) mechanism, which invokes a global, chiral $U(1)$ symmetry group spontaneously broken at some high energy scale $f_{\tilde{a}} \sim 10^{11}$ GeV remains the most compelling way of solving the strong CP problem. Of particular importance to both experimental searches and cosmology is the lightest supersymmetric particle (LSP). Axinos, being massive and electrically and color neutral are an interesting candidate for the LSP. One of the most important consequences of supersymmetry for cosmology in the presence of unbroken R-parity is the fact that the LSP is stable and may contribute substantially to the relic mass density in the universe [22]. If the contribution is of order the critical density, such a particle is considered an attractive dark matter (DM) candidate. In the minimal SUSY model (MSSM), the LSP is usually *assumed* to be the lightest of the four neutralinos. In this thesis we assume that the LSP is the axino, rather than the lightest neutralino. This assumption is justified by experimental bounds: Searches at LEP have now pushed the neutralino mass limit above about 28 GeV in the MSSM [22], whereas in the Constrained MSSM (CMSSM) [23], it is already around 42 GeV [24][2]. In contrast to the neutralino, the mass of the axino, $m_{\tilde{a}}$, remains not only virtually unconstrained experimentally but also theoretically one can easily imagine it in the few to tens of GeV range. Assuming a charged stau to be the NLSP we show that the NLSP decays of the stau into axinos can be used to probe an axino LSP scenario in supersymmetric KSVZ models [21, 26]. In KSVZ models additional heavy quarks and squarks are introduced. The KSVZ axino couples directly only to these additional heavy (s)quarks. Thus there is no tree-level decay of staus into axinos. The first possible decay channel is the threebody decay of the stau $\tilde{\tau} \to \tau\ \tilde{a}\ \gamma$, which arises first at one-loop level, whereas the two-body decay $\tilde{\tau} \to \tau\ \tilde{a}$ arises first at two-loop level. The total decay rates of these decay channels will be calculated with the help of the loop techniques derived for rare B-decays. For the charged slepton NLSP scenario considered in this thesis, there have been proposals which discuss how such NLSPs could be stopped and collected for an analysis of the decays in the LSP. It was found that up to $\mathcal{O}(10^3\text{-}10^4)$ and $\mathcal{O}(10^3\text{-}10^5)$ of charged NLSP can be trapped per year at the Large Hadron Collider (LHC) and the International Linear Collider (ILC), respectively, by placing 1-10 ktons of massive additional material around planned collider detectors [27, 28]. Thus the derived total decay rates can be used to test the axino LSP scenario at future colliders.

The following chapters are organized as follows:

- The chapters 2-5 give a short introduction into the underlying theoretical background of this thesis: In chapter 2 we give an overview of the particle content of the Standard Model (SM). The sensitivity of FCNC B decays to physics beyond the SM provides the possibility to find constraints on parameter spaces of new physics models. As an example of such a new physics modell, we will introduce in chapter 3 Two-Higgs-doublet models (THDM), which arise by extending the Higgs sector of the SM by introducing a second Higgs doublet. Chapter 4 is dedicated to the concepts of regularisation and renormalisation of Quantum Chromo Dynamics (QCD). Chapter 5 covers the subject of effective theories be-

[2]These bounds strongly depend on the assumption that the masses of the gauginos (the fermionic partners of the gauge bosons) are equal at a grand-unified scale. In the absence of this condition one recovers a model independent bound $m_\chi \gtrsim 3$ GeV [25].

ing a necessary tool for the evaluation of B decays. The theoretical framework of weak B processes is based on the different mass scales involved in the decay allowing for a systematical factorisation of high an low energy scale effects with the help of an operator product expansion (OPE). This results in an effective theory Lagrangian which describes the interaction of the light degrees of freedom (leptons and light quarks) in terms of effective interaction vertices – the so called operators. The effect of the decoupled heavy degrees of freedom is absorbed into the effective coupling constants – Wilson coefficients – which can be calculated reliably in perturbation theory.

- In chapters 6-8 we derive the analytic results for the two-loop corrections to the Wilson coefficients $C_7(\mu_W)$, $C_9(\mu_W)$ and $C_{10}(\mu_W)$ in the SM (chapters 6-7) and type-I and type-II two-Higgs-doublet models (chapter 8) at the matching scale μ_W up to $\mathcal{O}(\alpha_s)$-precision. All in chapters 6-8 derived Wilson coefficients are summarised in chapter 9. Additionally we quote all necessary matching conditions for all the operators that are relevant for the rare B-decay $\bar{B} \to X_s l^+ l^-$ in the SM and type-II THDM.

- In a scenario, where the NLSP is a charged stau and the LSP is an axino, we will derive in chapter 10 the threebody decay of the stau $\tilde{\tau} \to \tau\ \tilde{a}\ \gamma$ and the two-body decay $\tilde{\tau} \to \tau\ \tilde{a}$ in KSVZ models. The total decay rate of these channels can be used to test the axino LSP scenario at the LHC.

The appendices focus on the technical details of loop calculations. We present a software package which enables us to perform the basic steps of the one- and two-loop calculations (Dirac algebra, tensor reduction, partial fraction, reduction to master integrals with the help of recurrence relations) fully automatically. Finally we complete the theoretical background of this theses by giving e.g the used Feynman rules. The appendices are organised as follows:

- In appendix A the basic steps of the calculation of the integrals in the considered rare decays are shown. Furthermore, we introduce the program routines which enabled us to perform the calculation of the loop integrals appearing in the full SM and THDM side of the matching calculation as well as the decay into axinos fully automatically. These program routines are summarised in appendix C, where the written software is documented. In appendix B we display the analytical expressions of the recurrence relations, which enabled us to reduce arbitrary scalar two-loop integrals with up to three different masses and no dependence on external momenta to integrals where the highest power of all occurring propagators is one. These recurrence relations were coded and are part of the in appendix C documented software.

- Appendices E-G complement the theoretical background of this theses: Appendix E gives an introduction to Lie algebras needed to perform the colour algebra of the two-loop diagrams in rare b-decays. In appendix D we complete the operator basis of $\bar{B} \to X_s l^+ l^-$ decays with the so called evanescent and Equation-of-Motion (EOM) vanishing operators. Appendix F introduces the two-component fermion notation used to describe the super potential of axion and heavy quark

multiplets in chapter 10. Appendix G summarises all Feynman rules needed for the calculation of the rare b decays in the SM and THDM as well as the Feynman rules needed for the calculation of the rare decays of staus into axinos.

Chapter 2

The Standard Electroweak Model

2.1 Particles and Interactions

The Standard Model is a gauge field theory based on the gauge group G_{SM}

$$G_{SM} = SU(3)_C \otimes SU(2)_L \otimes U(1)_Y, \tag{2.1}$$

where $SU(3)_C$ corresponds to the strong interaction acting only on colour-charged particles (quarks and gluons) leaving all other particles untouched. The group $SU(2)_L$ only acts on left-handed fields, thus violating maximally parity. Finally, the group $U(1)_Y$ acts on particles with weak hypercharge. The electroweak interaction

$$G_{EW} = SU(2)_L \otimes U(1)_Y, \tag{2.2}$$

spontaneously breaks down to the group $U(1)_Q$, where Y and Q denote the weak hypercharge generator and the electric charge generator, respectively. Tables 2.1 and 2.2 summarise the fermionic and bosonic fields of the theory as well as their transformation properties.

Each quark flavour q ($q = u, d, s, c, t, b$) occurs in three different colours indicated by the additional colour index $\alpha = 1, 2, 3$ carried by quark fields (see table 2.1). The three colour versions of a quark are summarized in the vector:

$$q = \begin{pmatrix} q^1 \\ q^2 \\ q^3 \end{pmatrix}. \tag{2.3}$$

The fundamental constituents of any Dirac spinor ϕ are the Weyl fermions. In the chiral basis, the Dirac spinor can be written in the following way:

$$\psi = \begin{pmatrix} \xi \\ 0 \end{pmatrix} + \begin{pmatrix} 0 \\ \chi \end{pmatrix} \tag{2.4}$$

with ξ and χ being 2 component-Weyl spinors [1]. Introducing the two chiral projectors

$$P_L = \frac{1 - \gamma_5}{2}, \quad P_R = \frac{1 + \gamma_5}{2} \tag{2.5}$$

[1] Here we have omitted the upper and lower indices of the Weyl spinors. A more detailed introduction to Weyl spinors can be found in appendix F.

we can define left- and right-handed fields ψ_L and ψ_R

$$\psi_L = P_L\psi = \begin{pmatrix}\xi\\0\end{pmatrix}; \qquad \psi_R = P_R\psi = \begin{pmatrix}0\\\chi\end{pmatrix}. \tag{2.6}$$

	Generation 1	2	3	$SU(3)_C$ Rep.	$SU(2)_L$ T	T_3	Rep.	$U(1)_Y$ Y	$U(1)_Q$ Q
Quarks	u_L^α	c_L^α	t_L^α	**3**	1/2	1/2	**2**	1/6	2/3
	d_L^α	s_L^α	b_L^α		1/2	−1/2		1/6	−1/3
	u_R^α	c_R^α	t_R^α	**3**	0	0	**1**	2/3	2/3
	d_R^α	s_R^α	b_R^α		0	0		−1/3	−1/3
Leptons	$\begin{pmatrix}\nu_e\\e\end{pmatrix}_L$	$\begin{pmatrix}\nu_\mu\\\mu\end{pmatrix}_L$	$\begin{pmatrix}\nu_\tau\\\tau\end{pmatrix}_L$	**1**	1/2	1/2	**2**	−1/2	0
					1/2	−1/2		−1/2	−1
	e_R	μ_R	τ_R	**1**	0	0	**1**	-1	-1

Table 2.1: Fermionic content of the Standard Model and its transformation properties. The subscript L (R) corresponds to left-handed (right-handed) fields. The superscript α denotes the colour index. The connection between the quantum numbers of the weak hypercharge and the electromagnetic charge and the third component of the weak isospin is given by $Y = Q - T_3$, where $Q = q/e$ and q is the charge of the corresponding particle.

Boson	$SU(3)_C$ Rep.	$SU(2)_L$ Rep.	Y	Q	Function
W_μ	**1**	**3**			$SU(2)_L$ gauge bosons
B_μ	**1**	**1**			$U(1)_Y$ gauge bosons
G_μ^α	**8**	**1**	0	0	$SU(3)_C$ gauge bosons
$\phi = \begin{pmatrix}\phi^+\\\phi^0\end{pmatrix}$	**1**	**2**	1/2 1/2	1 0	Generation of mass

Table 2.2: Bosonic content (gauge fields, Higgs boson) of the Standard Model and its transformation properties. Again, the superscript α denotes the colour index.

The left-handed leptons and quarks are put in $SU(2)_L$ doublets [29]

$$\begin{pmatrix}\nu_e\\e^-\end{pmatrix}_L \qquad \begin{pmatrix}\nu_\mu\\\mu^-\end{pmatrix}_L \qquad \begin{pmatrix}\nu_\tau\\\tau^-\end{pmatrix}_L \tag{2.7}$$

$$\begin{pmatrix}u\\d'\end{pmatrix}_L \qquad \begin{pmatrix}c\\s'\end{pmatrix}_L \qquad \begin{pmatrix}t\\b'\end{pmatrix}_L \tag{2.8}$$

with the corresponding right-handed fields transforming as singlets under $SU(2)_L$. The primes are discussed below. The electroweak interactions of quarks and leptons are

mediated by the massive weak gauge bosons $W^{\pm}$ and Z^o and by the photon A. These interactions are summarized by the Lagrangian

$$\mathcal{L}_{int} = \mathcal{L}_{\rm CC} + \mathcal{L}_{\rm NC} \tag{2.9}$$

where

$$\mathcal{L}_{\rm CC} = \frac{g_2}{\sqrt{2}}(J^+_\mu W^{+\mu} + J^-_\mu W^{-\mu}) \tag{2.10}$$

describes the *charged current* interactions and

$$\mathcal{L}_{\rm NC} = eJ^{em}_\mu A^\mu + \frac{g_2}{2\cos\Theta_W} J^o_\mu Z^\mu \tag{2.11}$$

the *neutral current* interactions. Here e is the QED coupling constant, g_2 is the $SU(2)_L$ coupling constant and Θ_W is the Weinberg angle. The currents are given as follows

$$J^+_\mu = (\bar{u}\gamma_\mu P_L d') + (\bar{c}\gamma_\mu P_L s') + (\bar{t}\gamma_\mu P_L b') + (\bar{\nu}_e\gamma_\mu P_L e) + (\bar{\nu}_\mu\gamma_\mu P_L \mu) + (\bar{\nu}_\tau\gamma_\mu P_L \tau) \tag{2.12}$$

$$J^{em}_\mu = \sum_f Q_f \bar{f}\gamma_\mu f \tag{2.13}$$

$$J^o_\mu = \sum_f \bar{f}\gamma_\mu(v_f - a_f\gamma_5)f \tag{2.14}$$

$$v_f = T^f_3 - 2Q_f \sin^2\Theta_W \qquad a_f = T^f_3 \tag{2.15}$$

where Q_f and T^f_3 denote the charge and the third component of the weak isospin of the left-handed fermion f_L.

In our discussion of weak decays an important role is played by the Fermi constant:

$$\frac{G_F}{\sqrt{2}} = \frac{g_2^2}{8M_W^2} \tag{2.16}$$

which has the value

$$G_F = 1.16637(1)\cdot 10^{-5}\ \text{GeV}^{-2}, \tag{2.17}$$

where the 1 in the paranthesis indicates the one-standard deviation in the last digit. Other values of the relevant parameters will be collected in appendix H.

The interactions between the gauge bosons are standard and can be found in any textbook (e.g. [30]) on gauge theories.

The primes in (2.8) indicate that the weak eigenstates (d', s', b') are not equal to the corresponding mass eigenstates (d, s, b), but are rather linear combinations of the latter [29]. This is expressed through the relation

$$\begin{pmatrix} d' \\ s' \\ b' \end{pmatrix} = \begin{pmatrix} V_{ud} & V_{us} & V_{ub} \\ V_{cd} & V_{cs} & V_{cb} \\ V_{td} & V_{ts} & V_{tb} \end{pmatrix} \begin{pmatrix} d \\ s \\ b \end{pmatrix}, \tag{2.18}$$

where the unitary matrix connecting theses two sets of states is the Cabibbo-Kobayashi-Maskawa (CKM) matrix. Let us introduce the notation $c_{ij} = cos\theta_{ij}$ and $s_{ij} = sin\theta_{ij}$

with i and j being generation labels ($i, j = 1, 2, 3$). The standard parametrisation of the CKM-matrix is then given as follows [31]:

$$V = \begin{pmatrix} c_{12}c_{13} & s_{12}c_{13} & s_{13}e^{-i\delta} \\ -s_{12}c_{23} - c_{12}s_{23}s_{13}e^{i\delta} & c_{12}c_{23} - s_{12}s_{23}s_{13}e^{i\delta} & s_{23}c_{13} \\ s_{12}s_{23} - c_{12}c_{23}s_{13}e^{i\delta} & -s_{23}c_{12} - s_{12}c_{23}s_{13}e^{i\delta} & c_{23}c_{13} \end{pmatrix}, \tag{2.19}$$

where δ is the phase necessary for CP violation. c_{ij} and s_{ij} can all be chosen to be positive and δ may vary in the range $0 \leq \delta \leq 2\pi$. However the measurements of CP violation in K decays force δ to be in the range $0 \leq \delta \leq \pi$.

The extensive phenomenology of the last years has shown that s_{13} and s_{23} are small numbers: $\mathcal{O}(10^{-3})$ and $\mathcal{O}(10^{-2})$, respectively. Consequently to an excellent accuracy $c_{13} = c_{23} = 1$ and the four independent parameters are given as follows

$$s_{12} = |V_{us}|, \quad s_{13} = |V_{ub}|, \quad s_{23} = |V_{cb}|, \quad \delta \tag{2.20}$$

with the phase δ extracted from CP violating transitions or loop processes sensitive to $|V_{td}|$. The latter fact is based on the observation that for $0 \leq \delta \leq \pi$ there is a one-to-one correspondence between δ and $|V_{td}|$ given by:

$$|V_{td}| = \sqrt{a^2 + b^2 - 2ab\cos\delta}, \qquad a = |V_{cd}V_{cb}|, \qquad b = |V_{ud}V_{ub}|. \tag{2.21}$$

The unitarity of the CKM matrix provides us with several relations among

$$V_{ud}V_{ub}^* + V_{cd}V_{cb}^* + V_{td}V_{tb}^* = 0 \tag{2.22}$$

is the most useful. In the complex plane the relation (2.22) can be represented as a triangle, the so-called "unitarity-triangle". Phenomenologically, this triangle is very interesting as it involves simultaneously the elements V_{ub}, V_{cb} and V_{td} which are under extensive discussion at present. In the considered rare B-decays the following unitarity-relation will play an important role:

$$V_{us}^*V_{ub} + V_{cs}^*V_{cb} + V_{ts}^*V_{tb} = 0. \tag{2.23}$$

Summarising the particle content of the Standard Model, we find that it contains 45 Weyl fermions, 12 gauge bosons and one Higgs doublet [2]. There are 18 independent parameters in the model:

- 6 fermion masses: $m_u,\ m_d,\ m_c,\ m_s,\ m_t,\ m_b$;
- 3 lepton masses: $m_e,\ m_\mu,\ m_\tau$;
- 1 gauge boson mass: M_z.
  The mass of the electrically charged bosons $W^\pm$ is connected to M_z via the Weinberg angle:
  $$M_W = M_Z \cos\Theta_W; \tag{2.24}$$
- 1 Higgs boson mass;

[2] The various ghost fields present in the SM are not discussed.

- 3 couplings: the electromagnetic, the electroweak and the strong couplings e, g_2, g_s. The electromagnetic charge and electroweak couplings are connected via the the Weinberg angle
$$g_2 \sin \theta_W = e; \tag{2.25}$$
- 4 CKM matrix parameters.

Chapter 3

Two-Higgs-Doublet Models

The Standard Model with two Higgs doublets is a minimal extension of the Higgs sector of the SM. In the following we consider models with two complex $Y = 1$[1], $SU(2)_L$ scalar doublets:

$$\phi_1 = \begin{pmatrix} \phi_1^+ \\ \phi_1^0 \end{pmatrix} = \begin{pmatrix} \phi_1 + i\phi_2 \\ \phi_3 + i\phi_4 \end{pmatrix}, \quad \phi_2 = \begin{pmatrix} \phi_2^+ \\ \phi_2^0 \end{pmatrix} = \begin{pmatrix} \phi_5 + i\phi_6 \\ \phi_7 + i\phi_8 \end{pmatrix}. \tag{3.1}$$

The most general two-Higgs doublet scalar potential subject to gauge invariance and a discrete symmetry $\phi_1 \to -\phi_1$ only violated by dimension-two terms is given by [32,33]

$$\begin{aligned} V(\phi_1\phi_2) \;=\; & \lambda_1 \left(\phi_1^\dagger\phi_1 - v_1^2\right)^2 + \lambda_2 \left(\phi_2^\dagger\phi_2 - v_2^2\right)^2 + \lambda_3 \left[\left(\phi_1^\dagger\phi_1 - v_1^2\right) + \left(\phi_2^\dagger\phi_2 - v_1^2\right)\right]^2 + \\ & \lambda_4 \left[\left(\phi_1^\dagger\phi_1\right)\left(\phi_2^\dagger\phi_2\right) - \left(\phi_1^\dagger\phi_2\right)\left(\phi_2^\dagger\phi_1\right)\right] + \\ & \lambda_5 \left[\mathrm{Re}(\phi_1^\dagger\phi_2) - \mathrm{v_1 v_2}\cos\xi\right]^2 + \lambda_6 \left[\mathrm{Im}(\phi_1^\dagger\phi_2) - \mathrm{v_1 v_2}\sin\xi\right]^2 + \\ & \lambda_7 [\mathrm{Re}(\phi_1^\dagger\phi_2) - \mathrm{v_1 v_2}\cos\xi][\mathrm{Im}(\phi_1^\dagger\phi_2) - \mathrm{v_1 v_2}\sin\xi], \end{aligned} \tag{3.2}$$

where the λ_i are all real parameters (by hermicity). In the minimal supersymmetric model (MSSM) we have $\lambda_7 = 0$ at tree-level [33] [2].

The violation of the discrete symmetry $\phi_1 \to -\phi_1$ only by dimension-two terms ensures that flavour-changing neutral currents are not too large [34]. We are free to choose a Higgs fermion coupling which avoids tree-level FCNCs. It can be shown [34] that only the neutral Higgs bosons have a non vanishing vacuum expectation value (VEV). If all the λ_i are non-negative, then the minimum of the potential is manifestly

$$\langle\phi_1\rangle = \begin{pmatrix} 0 \\ v_1 \end{pmatrix}, \quad \langle\phi_2\rangle = \begin{pmatrix} 0 \\ v_2 e^{i\xi} \end{pmatrix}, \tag{3.3}$$

which breaks the $SU(2) \otimes U(1)_Y$ down to $U(1)_{EM}$. If $\sin\xi \neq 0$, there is CP violation in the Higgs sector.

In the following we do not focus on the most general two-Higgs doublet scalar potential eq. (3.2), but on that part of the potential which reproduces the Higgs sector of

[1] Note that in the MSSM the two Higgs doublet models have opposite hypercharge.

[2] In CP-violating two-Higgs doublet models, it is important to keep $\lambda_7 \neq 0$ if one wishes to retain the overall freedom to redefine th Higgs field phases.

the MSSM: Supersymmetry imposes the condition $\lambda_5 = \lambda_6$ [35]. Then the penultimate line of eq. (3.2) can be combined into a term proportional to $|\phi^\dagger\phi_2 - v_1 v_2 e^{i\xi}|^2$:

$$\begin{aligned}
&(\mathrm{Re}(\phi_1^\dagger\phi_2))^2 - 2\ \mathrm{v}_1\mathrm{v}_2\ \cos\xi\ \mathrm{Re}(\phi_1^\dagger\phi_2) + \mathrm{v}_1^2\mathrm{v}_2^2\ \cos^2\xi \\
&+(\mathrm{Im}(\phi_1^\dagger\phi_2))^2 - 2\ \mathrm{v}_1\mathrm{v}_2\ \sin\xi\ \mathrm{Im}(\phi_1^\dagger\phi_2) + \mathrm{v}_1^2\mathrm{v}_2^2\ \sin^2\xi \\
&= |\phi_1^\dagger\phi_2)|^2 - 2v_1v_2[\cos\xi\ \mathrm{Re}(\phi_1^\dagger\phi_2) + \sin\xi\ \mathrm{Im}(\phi_1^\dagger\phi_2)] + \mathrm{v}_1^2\mathrm{v}_2^2 \\
&= |\phi_1^\dagger\phi_2)|^2 - v_1v_2(e^{i\xi}\phi_1\phi_2^\dagger + e^{-i\xi}\phi_1^\dagger\phi_2) + v_1^2v_2^2 \\
&= (\phi_1^\dagger\phi_2 - v_1v_2e^{i\xi})(\phi_1\phi_2^\dagger - v_1v_2e^{-i\xi}) \\
&= |\phi_1^\dagger\phi_2 - v_1v_2e^{i\xi}|^2.
\end{aligned}$$

In the MSSM we have $\lambda_5 = \lambda_6$ and $\lambda_7 = 0$. Thus the phase ξ can be rotated away by a redefinition of the field ϕ_2 without affecting other terms in the potential:

$$\phi_2 \to e^{i\xi}\phi_2. \tag{3.4}$$

In this case, eq. (3.2) represents the most general CP-invariant potential. In the following we henceforth set $\xi = 0$. The vacuum expectation values of ϕ_1 and ϕ_2 can now be chosen to be real and positive. A key parameter of the model is the ratio for the vacuum expectation values

$$\tan\beta = \frac{v_2}{v_1}. \tag{3.5}$$

ϕ_1 and ϕ_2 have eight degrees of freedom. There are three Goldstone bosons to give mass to the $W^\pm$ and Z, thus five physical Higgs particles bosons remain. After spontaneous symmetry breaking the two doublets give rise to two charged ($H^\pm$), two neutral CP-even (H^0 and h^0) and one neutral CP-odd (A^0) Higgs fields [35]. In the following we will focus our attention to the charged Higgs states. They are given by

$$H^\pm = -\phi^\pm\sin\beta + \phi_2^\pm\sin\beta, \tag{3.6}$$

where $\phi^- \equiv (\phi^+)^*$. The mass is given by $m_{H^\pm}^2 = \lambda_4(v_1^2 + v_2^2)$. Requiring the absence of flavour changing neutral currents at the tree-level one obtains two possibilities: the type-I and the type-II THDM [36]. We denote by Model-I the case in which the quarks and leptons do not couple to the first Higgs doublet ϕ_1, but to the second Higgs doublet ϕ_2. In Model-II we assume that ϕ_1 only couples to down-type quarks and leptons and ϕ_2 only to up-type quarks and neutrinos. Model-II corresponds to the Higgs sector in the MSSM. The part of the Lagrangian relevant for our calculation is the Yukawa interaction between the charged physical Higgs bosons $H^\pm$ and the quarks (in its mass eigenstate basis):

$$\mathcal{L}_I = \frac{g}{\sqrt{2}}\left\{\left(\frac{m_{di}}{M_W}\right)X\,\overline{u}_{Lj}V_{ji}\,d_{Ri} + \left(\frac{m_{ui}}{M_W}\right)Y\,\overline{u}_{Ri}V_{ij}\,d_{Lj}\right\}H^+ + \mathrm{h.c.}\,. \tag{3.7}$$

The couplings X and Y are

$$\begin{array}{lllll}
X = -\cot\beta, & Y & = & \cot\beta & \text{(type-I)}, \\
X = \tan\beta, & Y & = & \cot\beta & \text{(type-II)},
\end{array}$$

where $\tan\beta = v_2/v_1$, with v_1 and v_2 being the vacuum expectation values of the Higgs doublets ϕ_1 and ϕ_2, respectively. In the following we will use the generic form (3.7) for the interaction between $H^\pm$ and the quarks.

Chapter 4

Dimensional Regularisation and Renormalisation

The perturbative expansion of Green functions in coupling constants is a well defined procedure which can be illustrated by Feynman graphs and the corresponding analytic expressions can be easily found by the application of the Feynman rules. When going beyond the tree-level approximation the analytic expressions of the Green functions contain integrations over virtual momenta which turn out to be infinite. To allow a proper treatment of the divergencies, a regularisation procedure is required. This equals to a modification of the theory such that the possibly divergent expressions become well defined and in a suitable limit the original (divergent) theory is recovered. For gauge theories it is convenient to use the method of dimensional regularisation [4] which guarantees gauge invariance of the regularised theory. This section collects basic facts about QCD-renormalisation following [37]. In particular we discuss the (naive) dimensional regularisation, the MS and $\overline{\rm MS}$ renormalization schemes.

4.1 Dimensional Regularisation

The Lagrangian density of QCD, omitting the ghosts and setting the gauge parameter to $\xi = 1$, is given by:

$$\begin{aligned}\mathcal{L}_{QCD} &= -\frac{1}{4}(\partial_\mu A^a_\nu - \partial_\nu A^a_\mu)(\partial^\mu A^{a\nu} - \partial^\nu A^{a\mu}) - \frac{1}{2}(\partial^\mu A^a_\mu)^2 \\ &\quad + \bar{q}_\alpha (i\ \partial\!\!\!/ - m_q) q_\alpha - g_s \bar{q}_\alpha T^a_{\alpha\beta} \gamma^\mu q_\beta A^a_\mu \\ &\quad + \frac{g_s}{2} f^{abc}(\partial_\mu A^a_\nu - \partial_\nu A^a_\mu) A^{b\mu} A^{c\nu} - \frac{g_s^2}{4} f^{abe} f^{cde} A^a_\mu A^b_\nu A^{c\mu} A^{d\nu}. \end{aligned} \tag{4.1}$$

Here A^a_μ are the gluon fields with $(a, b, c = 1, ..8)$ and $q = (q_1, q_2, q_3)$ is the color triplet of quark flavour q, ($q = u$, d, s, c, b, t). g_s is the QCD coupling so that

$$\alpha_s = \frac{g_s^2}{4\pi}. \tag{4.2}$$

T^a and f^{abc} are the generators and structure constants of $SU(3)_C$ (for more details about Lie Algebras and the fundamental representation of $SU(3)_C$ we refer to appendix E). From the Lagrangian (4.1) one can derive the Feynman rules for QCD.

All Feynman rules actually needed for our calculations are summarised in appendix G. In order to deal with divergences that appear in loop corrections to Green functions we have to regularise the theory in order to obtain an explicit parametrisation of the singularities. In this thesis we will employ *dimensional regularisation* (DR). It is the favourite regularisation in gauge theories as it preserves all symmetries of the theory. Feynman diagrams are evaluated in $D = 4-2\,\varepsilon$ space-time dimensions and singularities are extracted as poles for $\varepsilon \to 0$. Thus the results of one-loop or two-loop calculations have the following general structure:

$$\text{One Loop Result} = \frac{a_1}{\varepsilon} + b_1 \ , \tag{4.3}$$

$$\text{Two Loop Result} = \frac{a_2}{\varepsilon^2} + \frac{b_2}{\varepsilon} + c_2 \ , \tag{4.4}$$

where a_i, b_i and c_2 are finite. Let us consider the second term in the second line in eq. (4.1). The mass dimensions of q_i, A^a_μ and $\mathcal{L}$ are $(D-1)/2$, $(D-2)/2$ and D respectively. Thus the dimension of g_s in $D = 4-2\varepsilon$ dimensions is simply equal to ε. As it is more useful to work with a dimensionless coupling constant in arbitrary D dimensions we make to this end the replacement

$$g_s \quad \to \quad g_s \mu^\varepsilon, \tag{4.5}$$

where μ is an arbitrary parameter with the dimensions of mass and g_s on the r.h.s. is dimensionless.

4.1.1 Naive Dimensional Regularisation

The most commonly used scheme applying dimensional regularisation is the so called "naive dimensional regularisation" (NDR) scheme.

The D-dimensional metric tensor g is introduced satisfying

$$g_{\mu\nu} g^{\nu\mu} = g^\mu_\mu = D, \tag{4.6}$$

where $D = 4 - 2\epsilon$ in all kind of expressions containing Lorentz indices. The Dirac gamma matrices $\gamma^\mu = (\gamma^0, \gamma^i)$, where the Latin index i is employed to denote spatial indices 1,2,3, satisfy the anticommutation relations

$$\{\gamma^\mu, \gamma^\nu\} = 2g^{\mu\nu} \ = \ 2g_{\mu\nu}. \tag{4.7}$$

The γ_5 is defined by

$$\gamma^5 = \gamma_5 = i\gamma^0\gamma^1\gamma^2\gamma^3 \tag{4.8}$$

and anti-commutes with all γ^μ:

$$\{\gamma^5, \gamma^\mu\} = 0. \tag{4.9}$$

It has been emphasised in the literature that this rule leads to algebraic inconsistencies [38, 39]. Indeed, the NDR is inconsistent with

$$Tr(\gamma^\mu\gamma^\nu\gamma^\rho\gamma^\sigma\gamma_5) \neq 0 \tag{4.10}$$

for dimensions of space-time $D = 4 - 2\epsilon$, $\epsilon \neq 0$. However the latter condition is often considered to be necessary for an acceptable regularisation, since at $D = 4$ we must find

$$Tr(\gamma^\mu\gamma^\nu\gamma^\rho\gamma^\sigma\gamma_5) = 4\mathrm{i}\varepsilon^{\mu\nu\rho\sigma} \ . \tag{4.11}$$

Provided one can avoid the calculation of traces like (4.11), which contain γ_5 matrices, it has been demonstrated in many explicit calculations [40] that the NDR gives correct results consistent with schemes without the γ_5 problem. As in our calculations we have no closed fermion loops and thus no traces to perform, we can ignore the algebraic inconsistencies of the NDR and apply the NDR-scheme without any modifications.

4.2 Renormalization of QCD

In order to eliminate the divergences in Green functions the fields and parameters in the Lagrangian have to be renormalised through

$$\begin{array}{ll} A^a_{0\mu} = Z_3^{1/2} A^a_\mu & q_0 = Z_q^{1/2} q \\ g_{0,s} = Z_g g_s \mu^\varepsilon & m_0 = Z_m m, \end{array} \tag{4.12}$$

where the index "0" indicates unrenormalised quantities. A^a_μ and q are renormalised fields, g_s is the renormalised QCD coupling and m the renormalised quark mass. The factors Z_i $(i = 3, q, g, m)$ are the renormalisation constants. They are divergent quantities, chosen in such a manner that the divergences disappear once the Greens functions have been expressed in terms of renormalized quantities only. The unrenormalized parameters $g_{0,s}$ and m_0 are independent of the scale μ. This implies, in particular, that g_s must be μ-dependent. Since Z_i have a perturbative expansion in g_s (see below eq. (4.16) they must also depend on μ. Consequently the renormalized mass m is also μ-dependent.

4.2.1 The Counterterm Method

A straightforward way to implement renormalization is provided by the counterterm method. Thereby parameters and fields in the original Lagrangian, considered as unrenormalized (bare) quantities, are reexpressed through renormalized ones by means of (4.12). Thus

$$\mathcal{L}^0_{QCD} = \mathcal{L}_{QCD} + \mathcal{L}_C, \tag{4.13}$$

where $\mathcal{L}_{QCD}$ is given in (4.1). $\mathcal{L}^0_{QCD}$ is also given by (4.1) but with q replaced by q_0 and similarly for A^a_μ, g_s and m. $\mathcal{L}_C$ is the *counterterm* Lagrangian. It is simply defined by (4.13). For instance:

$$\mathcal{L}_q = \bar{q}_0 i \not{\partial} q_0 - m_0 \bar{q}_0 q_0 \equiv \bar{q} i \not{\partial} q - m\bar{q}q + (Z_q - 1)\bar{q} i \not{\partial} q - (Z_q Z_m - 1) m \bar{q} q \ . \tag{4.14}$$

$\mathcal{L}_{QCD}$ given entirely in terms of renormalized quantities leads to the usual Feynman rules given in appendix G. The counterterms ($\sim (Z-1)$) can be formally treated as new interaction terms that contribute to Green functions calculated in perturbation

theory. For these new interactions also Feynman rules can be derived. For instance, the Feynman rule for the counterterms in (4.14) reads (p is the quark momentum)

$$i\delta_{\alpha\beta}[(Z_q-1)\ \not{p}-(Z_qZ_m-1)m]\ . \tag{4.15}$$

The constants Z_i are determined such that the contributions from these new interactions cancel the divergences in the Green functions resulting from the calculations based on $\mathcal{L}_{QCD}$ in (4.13) only. There is some arbitrariness how this can be done because a given renormalization prescription can in general subtract not only the divergences but also finite parts. The subtractions of finite parts is, however, not uniquely defined. This leads to the *renormalization scheme dependence* of Z_i and of the renormalized fields and parameters.

4.2.2 MS and $\overline{\text{MS}}$ Renormalization Schemes

The simplest renormalization scheme is the *Minimal Subtraction Scheme*(MS) in which only divergences are subtracted. In this scheme, the renormalization constants are given by

$$Z_i=\frac{\alpha_s}{4\pi}\frac{a_{1i}}{\varepsilon}+\left(\frac{\alpha_s}{4\pi}\right)^2\left(\frac{a_{2i}}{\varepsilon^2}+\frac{b_{2i}}{\varepsilon}\right)+\mathcal{O}(\alpha_s^3) \tag{4.16}$$

where a_{ji} and b_{ji} are μ-independent constants. An important virtue of this scheme is that the renormalization constants do not have any explicit μ-dependence, but depend on μ only through g_s. Similarly, the renormalization constants Z_i do not depend on masses. The MS-scheme bellows thus to the class of mass independent renormalization schemes.

Starting with the MS scheme, one can construct a whole class of subtraction schemes which differ from MS by a different continuation of the renormalized coupling constant to D dimensions. For these MS-like schemes we have

$$g_{0,s}=Z_g^k g_s^k \mu_k^\varepsilon \qquad \text{where } \mu_k=\mu f_k \tag{4.17}$$

and f_k is an arbitrary number which defines the particular scheme "k". Since different schemes in this class differ from the MS scheme only by a shift in μ, the renormalization constants for these schemes can be obtained from (4.16) by replacing g_s by g_s^k characteristic for a given scheme. The constants a_{ji} and b_{ji}, being μ-independent, remain unchanged. Of particular interest is the so-called $\overline{\text{MS}}$ scheme in which

$$\mu_{\overline{MS}}=\frac{\mu e^{\gamma_E/2}}{\sqrt{(4\pi)}}. \tag{4.18}$$

Changing from the MS to the $\overline{\text{MS}}$-scheme we observe from eq. (A.26) that in the $\overline{\text{MS}}$-scheme the terms $-(\gamma_E-\ln(4\pi))$, the artefacts of DR, are absent in all integrals.

Chapter 5

Effective Theory

For processes taking place at energy scales much lower than M_W, the Standard Model can be replaced by an so called "effective theory". This theory is built out only of SM fields being much lighter then the W-boson.

5.1 Operator product expansion

The decay of a b-quark can be separated into two distinct parts: processes taking place at energy scales much lower than M_W, and processes taking place at energy scales higher than M_W. These parts are separated from each other conceptually and practically. The conceptual difference between both energy ranges will be illustrated in the following with the transition $b \to cd\bar{u}$. In the left frame of fig. 5.1 the dominant SM Feynman diagram of this process is shown. The amplitude of this tree-level process

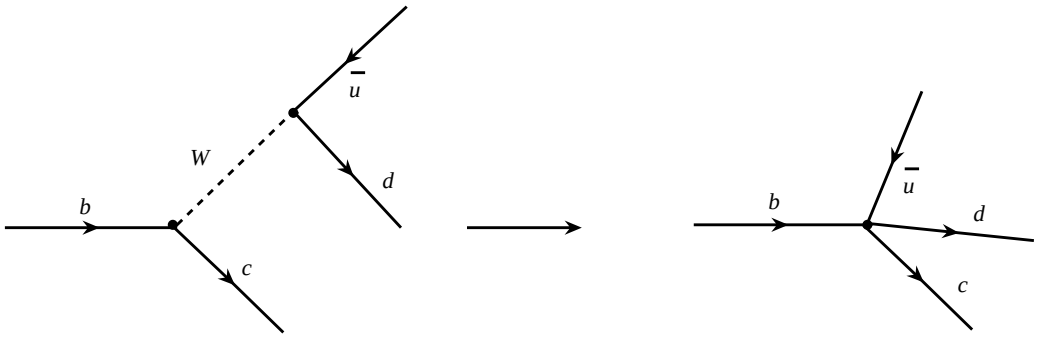

Figure 5.1: The process $b \to cd\bar{u}$ from a high-energy (left) and low-energy (right) point of view.

is given by (fig. 5.1 multiplied by i) [1]:

$$A_{full} = \frac{-g_2^2}{2} V_{cb} V_{ud}^* (\bar{d}\gamma_\mu P_L u) \frac{g^{\mu\nu}}{k^2 - M_W^2} (\bar{c}\gamma_\nu P_L b), \tag{5.1}$$

[1] We use the term "amplitude" in the meaning of an "amputated Green function" multiplied by i.

where k denotes the four-momentum flowing through the W propagator. The two energy scales involved in this process are the W-mass M_W (80 GeV) and the momentum k, which is of the order of the mass m_b ($\sim$ 4 GeV). Since $m_b \ll M_W$ and thus also $k \ll M_W$ it is justified to use the ratio k^2/M_W^2 as an expansion parameter. Expanding the amplitude (5.1) in $O(k^2/M_W^2)$ we get:

$$A_{full} = \frac{g_2^2}{2} V_{cb} V_{ud}^* \left(\left[\frac{1}{M_W^2} (\bar{d}\gamma_\mu P_L u)(\bar{c}\gamma^\mu P_L b) + \mathcal{O}(k^2/M_W^2) \right] \right., \tag{5.2}$$

Since k, the momentum transfer through the W propagator, is very small as compared to M_W, terms of the order $\mathcal{O}(k^2/M_W^2)$ can be safely neglected and the full amplitude A_{full} can be approximated by the first term on the r.h.s. of eq. (5.2). Now the result of (5.2) may be also obtained from

$$\mathcal{H}_{\text{eff}} = \frac{4G_F}{\sqrt{2}} V_{cb} V_{ud}^* (\underbrace{(\bar{d}\gamma_\mu P_L u)(\bar{c}\gamma^\mu P_L b)}_{\text{dimension 6 operator}} + \text{higher dimensional operators}), \tag{5.3}$$

where G_F is the Fermi constant

$$G_F = \frac{g_2^2}{4\sqrt{2} M_W^2}. \tag{5.4}$$

The higher dimensional operators correspond to the terms $\mathcal{O}(k^2/M_W^2)$ in eq.(5.2). Neglecting the latter terms corresponds to the neglect of higher dimensional operators. In the following we will always neglect higher dimensional operators keeping only operators of mass dimension 5 or 6. This simple example illustrates the basic idea of the operator product expansion (OPE): the product of two charged current operators is expanded into a series of local operators, whose contributions are weighted by effective coupling constants, the Wilson coefficients [41]. These Wilson coefficient C_i can be determined by the requirements that the amplitude A_{full} in the full theory is reproduced by the corresponding amplitude in the effective theory.

$$A_{full} = A_{eff} = \frac{4G_F}{\sqrt{2}} V_{cb} V_{ud}^* C\mathcal{O}, \tag{5.5}$$

where $\mathcal{O} = (\bar{d}\gamma_\mu P_L u)(\bar{c}\gamma^\mu P_L b)$. This procedure is called "the *matching* of the full theory onto the effective theory". The full theory is the one in which *all* particles appear as dynamical degrees of freedom, whereas the effective theory is constructed by integrating out the heavy fields, in our case the W. From eq. (5.5) we see that in our simple example the Wilson coefficient is equal to 1. Taking into consideration these QCD-effects, the effective Hamilton in eq. (5.3) changes to

$$\mathcal{H}_{\text{eff}} = \frac{4G_F}{\sqrt{2}} V_{cb} V_{ud}^* (C_1(\mu)\mathcal{O}_1 + C_2(\mu)\mathcal{O}_2), \tag{5.6}$$

where

$$\mathcal{O}_1 = (\bar{d}_\alpha \gamma_\mu P_L u_\beta)(\bar{c}_\beta \gamma^\mu P_L b_\alpha), \tag{5.7}$$

$$\mathcal{O}_2 = (\bar{d}_\alpha \gamma_\mu P_L u_\alpha)(\bar{c}_\alpha \gamma^\mu P_L b_\alpha) \tag{5.8}$$

with α and β being color indices. QCD effects lead to a new operator $\mathcal{O}_1$ differing from the already existing operator $\mathcal{O}_2$ only in its colour structure. Along with the new operator we have a new Wilson Coefficient C_1. The Wilson coefficients C_1 and C_2, the coupling constants for the interaction terms $\mathcal{O}_1$ and $\mathcal{O}_2$ become nontrivial functions of $\mathcal{O}(\alpha_s)$, M_W and the renormalisation scale μ. If QCD is neglected, we have $C_1 = 0$, $C_2 = 1$ and eq. (5.6) reduces to eq. (5.3).

The Wilson Coefficients $C_i(\mu)$, where $i = 1, 2$ in our simple example, depend on the separation scale μ: All physics above the scale μ (short distance effects) is contained in the Wilson coefficients, whereas low energy (long distance effects) are incorporated in matrix elements involving the operators. This separation of long- and short distance effects is the most important property of the OPE: The short-distance part (incorporated in the Wilson coefficients) is in general independent of any external state. Using a high renormalization scale $\mu = \mu_W$ of the order of the W-mass, the corresponding coupling constant $\alpha_s(\mu_W)$ is small. Thus the Wilson coefficients can be expanded in $\mathcal{O}(\alpha_s)$ and be calculated in fixed order perturbation theory. The expansion of the Wilson coefficient is given by

$$\begin{aligned} C_i(\mu_W) &= C_i^{(0)}(\mu_W) + \frac{\alpha_s}{(4\pi)} C_i^{(1)}(\mu_W) + \frac{\alpha_s^2}{(4\pi)^2} C_i^{(2)}(\mu_W) + \mathcal{O}(\alpha_s^3) \\ &= C_i^{(0)}(\mu_W) + \frac{g_s^2}{(4\pi)^2} C_i^{(1)}(\mu_W) + \frac{g_s^4}{(4\pi)^4} C_i^{(2)}(\mu_W) + \mathcal{O}(g_s^6). \end{aligned} \tag{5.9}$$

5.2 Effective Hamiltonian

We use the framework of an effective low energy theory with five quarks, obtained by integrating out the heavy degrees of freedom of masses $M_{\text{heavy}} \geq M_W$. These heavy masses are t-quark, the $W^{\pm}$ and Z mass as well as the charged Higgs bosons $H^{\pm}$, whose masses M_H are assumed to be of the same order of magnitude as M_W. We only take into account operators up to dimension six and set $m_s = 0$ (with $|\Delta B| = |\Delta S| = 1$). This is justified due to the strong suppression of higher dimension operators in the operator product expansion (see section 5.1).

The effective theory Lagrangian relevant to $b \to s+$(light particles) decays has the following form

$$\begin{aligned} \mathcal{L}_{eff} &= \mathcal{L}_{QCD\times QED}(u, d, s, c, b, e, \mu, \tau) \\ &\quad + \frac{4G_F}{\sqrt{2}} \left\{ \sum_{Q=u,c} \lambda_Q (C_1^c \mathcal{O}_1^Q + C_2^c \mathcal{O}_2^Q + C_{11}^c \mathcal{O}_{11}^Q) \right. \\ &\quad \left. + \sum_{i\epsilon A} [(\lambda_u + \lambda_c) C_i^c \; + \; \lambda_t C_i^t] \mathcal{O}_i \right\} \end{aligned} \tag{5.10}$$

with $A = \{3...10, 31...36, evanescent\}$ numbering the relevant operators $\mathcal{O}_i$. The corresponding Hamiltonian is given by $\mathcal{H}_{eff} = -\mathcal{L}_{eff}$.

The quantities

$$\lambda_q = V_{qs}^* V_{qb} \quad (q = u, c, t) \tag{5.11}$$

collect the dependence on the CKM matrix elements. From the unitarity of the CKM matrix

$$\lambda_u + \lambda_c + \lambda_t = 0, \tag{5.12}$$

we get with the approximation $|\lambda_u| \ll |\lambda_c|, |\lambda_t|$

$$\lambda_c = -\lambda_t, \tag{5.13}$$

which removes any CP violating effect from the Hamiltonian. Thus we will refrain in the following from using the unitarity of the CKM-matrix.

The first term in eq. (5.10) consists of kinetic terms of the light SM particles as well as their QCD and QED interactions. The remaining two terms consist of $\Delta B = -\Delta S = 1$ local operators of dimension ≤ 6, built out of those light fields:[2] Since both the u- and c-quarks are treated as massless in the present calculation, the Hamiltonian is symmetric under $u \leftrightarrow c$ exchange. This symmetry has already been taken into account in eq. (5.10), as the same Wilson coefficients C_i^c occur both in the u-quark and the c-quark sectors. The values of the Wilson coefficients are found in the matching procedure, which amounts to requiring equality of $b \to s+$(light particles) Green functions calculated in the effective theory and in the full model (SM or THDM), up to $\mathcal{O}[(\text{external momenta and light masses})^2/M_W^2]$. Contributions of order g_s^{2n} to each Wilson coefficient originate from n-loop SM diagrams, which follows from the particular convention for powers of gauge couplings in the normalisation of our operators.

The operators $\mathcal{O}_i$ entering the effective Lagrangian can be divided into two classes: physical operators $\mathcal{O}_1$-$\mathcal{O}_{10}$ and the non-physical operators. One has some freedom in the choice of the operator bases, we followed the conventions given in [42].

5.2.1 Physical Operators

The physical operators $\mathcal{O}_i$ consist of the current-current operators $\mathcal{O}_{1,2}^Q$ $(Q = \{u, c\})$, the QCD penguin operators $\mathcal{O}_{3,...,6}$ $(q = \{u, d, s, c, b\})$, the electro-magnetic moment type operator $\mathcal{O}_7$, the chromo-magnetic moment type operator $\mathcal{O}_8$ and finally the semileptonic operators $\mathcal{O}_{9,10}$. They are given by

$$\begin{aligned}
\mathcal{O}_1^Q &= (\bar{s}\gamma_\mu P_L \mathbf{T}^a Q)\,(\bar{Q}\gamma^\mu P_L \mathbf{T}^a b)\,, & \mathcal{O}_2^Q &= (\bar{s}\gamma_\mu P_L Q)\,(\bar{Q}\gamma^\mu P_L b)\,,\\
\mathcal{O}_3 &= (\bar{s}\gamma_\mu P_L b)\textstyle\sum_q (\bar{q}\gamma^\mu q)\,, & \mathcal{O}_4 &= (\bar{s}\gamma_\mu P_L \mathbf{T}^a b)\textstyle\sum_q (\bar{q}\gamma^\mu \mathbf{T}^a q)\,,\\
\mathcal{O}_5 &= (\bar{s}\gamma_\mu\gamma_\nu\gamma_\rho P_L b)\textstyle\sum_q (\bar{q}\gamma^\mu\gamma^\nu\gamma^\rho q)\,, & \mathcal{O}_6 &= (\bar{s}\gamma_\mu\gamma_\nu\gamma_\rho P_L \mathbf{T}^a b)\textstyle\sum_q (\bar{q}\gamma^\mu\gamma^\nu\gamma^\rho \mathbf{T}^a q)\,,\\
\mathcal{O}_7 &= \tfrac{e}{g_s^2} m_b (\bar{s}\sigma^{\mu\nu} P_L b) F_{\mu\nu}\,, & \mathcal{O}_8 &= \tfrac{1}{g_s} m_b (\bar{s}\sigma^{\mu\nu} P_L \mathbf{T}^a b) G^a_{\mu\nu}\,,\\
\mathcal{O}_9 &= \tfrac{e^2}{g_s^2} (\bar{s}\gamma_\mu P_L b)\textstyle\sum (\bar{l}\gamma^\mu l)\,, & \mathcal{O}_{10} &= \tfrac{e^2}{g_s^2} (\bar{s}\gamma_\mu P_L b)\textstyle\sum (\bar{l}\gamma^\mu\gamma_5 l),
\end{aligned} \tag{5.14}$$

where $\mathbf{T}^a$ $(a = 1, ..., 8)$ are the $SU(3)_C$ colour generators defined in Appendix E , and g_s and e are the strong and electromagnetic coupling constants q and l appearing in the sums run over the light quarks $(q = u, ..., b)$ and the charged leptons, respectively.

[2] The s-quark mass is neglected here, i.e. it is assumed to be negligibly small when compared to m_b. No such assumption is made concerning m_c or m_t.

We note that due to the particular conventions concerning the powers of the strong coupling constant g_s in the definition of our operators [43], the contributions of order g_s^{2n} to each Wilson coefficient originate from n-loop diagrams. It should be noted that the above basis of physical operators results from the SM, however in extensions of the SM other physical operators could become relevant, too. In this theses we consider THDM scenario for low values of $\tan\beta$. In this case the SM operator basis suffices.

5.2.2 Non-Physical Operators

In addition to the physical operators several non-physical operators have to be included in the matching procedure of full and effective theories. They can be divided in two classes: EOM-vanishing operators and evanescent operators.

EOM-vanishing operators

The *EOM-vanishing* operators vanish by the $QCD \otimes QED$ equation of motion (EOM) of the effective theory up to a total derivative. They appear in intermediate steps of the off-shell calculation of the processes $b \to s\gamma$ ($b \to sg$) and contribute to the final results of Wilson coefficients of physical operators when going beyond leading order matching.

Evanascent operators

Evanescent operators vanish algebraically in four dimensions, however in $D \neq 4$ dimensions they are indispensable and contribute to Wilson coefficients of physical operators. The name "evanescent" originates from the fact that such operators vanish in 4 dimensions due to the identity

$$\gamma_{\alpha_1}\gamma_{\alpha_2}\gamma_{\alpha_3} = g_{\alpha_1\alpha_2}\gamma_{\alpha_3} - g_{\alpha_1\alpha_3}\gamma_{\alpha_2} + g_{\alpha_2\alpha_3}\gamma_{\alpha_1} + i\varepsilon_{\beta\alpha_1\alpha_2\alpha_3}\gamma^{\beta}\gamma_5. \tag{5.15}$$

This identity cannot be analytically extended to D dimensions. Thus diagrams containing triple products of Dirac matrices cannot be reduced to anything simpler in D-dimensions.

All non-physical operators appearing in our calculation are summarized in appendix D, as far as the evanescent operators are concerned, only $\mathcal{O}_{11}^{Q}$ and $\mathcal{O}_{1}^{E,Q}$ from the section D.2 are needed for the matching calculation.

Naive dimensional regularisation with fully anticommuting γ_5 has been used in our matching computation. Using this simple scheme could not cause any difficulties, because the choice of the four-quark operator basis given in eq. (5.14) allowed us to avoid the appearance of Dirac traces containing γ_5 in the effective theory diagrams. No such traces were present in the SM and THDM diagrams, either (for details see chapter 4).

Chapter 6

Matching for Photonic $\Delta B = -\Delta S = 1$ Penguins in the SM

The goal of this chapter is to find two-loop QCD contributions to Wilson coefficients of operators in the effective theory giving leading electroweak contributions to the $\Delta B = -\Delta S = 1$ transitions accompanied by either a real photon or a lepton pair emission in the SM. In the latter case we will restrict ourselves to processes mediated by a virtual photon. i.e. we do not consider SM diagrams where the W or Z boson couple directly to the lepton line. This processes will be discussed in chapter 7

The techniques derived for the SM contributions will be applied in chapter 8 to photonic and Z–penguins in the THDM. To describe the matching calculations for photonic penguins we follow the very nice and clear introduction to the techniques of matching calculations given in [42].

6.1 Preliminaries

Photonic $\Delta B = -\Delta S = 1$ transitions accompanied by a real photon give contributions to the Wilson Coefficients C_7, decays accompanied by an off-shell photon decaying into a lepton pair give contributions to the "photonic" part of C_9 (C_9 gets also contributions from W-boxes and Z-penguins). The simplest way to find the Wilson coefficients up to $\mathcal{O}(\alpha_s)$is to require equality of the off-shell 1PI amputated Green functions calculated in the full SM and in the effective theory. In order to derive C_7 up to $\mathcal{O}(\alpha_s)$as well as the contribution deriving from photonic penguins to C_9 the following functions have to be considered:

Up to one loop, we need to consider the $b \to s\gamma$, $b \to s\ g$ and $b \to sc\bar{c}$ functions. At two loops, only the $b \to s\gamma$ function is necessary. In the cases of $b \to s\gamma$ and $b \to s\ g$, we work at the leading order in α_{em} and up to $\mathcal{O}[(\text{external momenta})^2/M_W^2]$. In the $b \to sc\bar{c}$ case, external momenta can be neglected.

We set all the light particle masses to zero in the whole calculation. An exception is the b-quark mass, which is being included up to linear order. This means that we maintain m_b only in Yukawa couplings and in the b-quark propagator numerators. The terms of order m_b^2 are neglected. One can justify this procedure by formally treating the b-quark mass term as an interaction with an external scalar field.

The Feynman integrands for the one- and two-loop Feynman diagrams are generated with the help of the program *FeynArts* [44].

A priori the integrals of rare B-decays are quite complicated, as we have to deal with two heavy masses: on the one hand the top-mass and on the other hand the W-mass (SM) or the charged Higgs mass (THDM), as well as a complicated structure of the momenta in the denominator. A typical propagator structure is given by

$$I = \frac{1}{(q_1^2 - m_1^2)^{n_1}(q_1^2 - m_2^2)^{n_2}(q_2 + k_1)^2 - m_2^2)^{n_3}((q_1 + q_2 + k_2) - m_2^2)_4^n}, \tag{6.1}$$

where q_1 and q_2 are the loop momenta, k_1 and k_1 the external momenta, $n_j \geq 0$ and $\sum_j n_j = 6$. At the moment exact results for diagrams with more than one mass scale do not exist beyond one-loop, as the exact calculation of two-loop graphs with two mass scales is technically very demanding. Therefore we use the Heavy Mass Expansion (HME) [45].

6.1.1 Heavy Mass Expansion

The HME is an asymptotic expansion in small momenta and masses. The basic idea is to use the hierarchy of mass scales and momenta to reduce complicated two-loop calculations to simpler ones. The following assumptions are made:

1. all the masses of a given Feynman diagram Γ can be divided into a set of large $\underline{M} = \{M_1, M_2, \ldots\}$ and small $\underline{m} = \{m_1, m_2, \ldots\}$ masses,
2. all external momenta $\underline{k} = \{k_1, k_2, \ldots\}$ are small compared to the scale of the large masses $\underline{M}$.

The ansatz is that the dimensionally regularised (unrenormalised) Feynman integral F_Γ associated with the Feynman diagram Γ can be written as

$$F_\Gamma \overset{M\to\infty}{\sim} \sum_\gamma F_{\Gamma/\gamma} \circ \mathcal{T}_{\underline{k}^\gamma, \underline{m}^\gamma} F_\gamma(\underline{k}^\gamma, \underline{m}^\gamma, \underline{M}), \tag{6.2}$$

where the sum is performed over all subgraphs γ of Γ which fulfil the following two conditions simultaneously:

- γ contains all lines with heavy masses ($\underline{M}$),
- γ consists of connected[1] components that are one-particle-irreducible with respect to the lines with small masses ($\underline{m}$).

The operator $\mathcal{T}$ performs a Taylor expansion in the variables k_i^2/M_j^2 and m_l^2/M_j^2, where k_i belongs to $\underline{k}^\gamma$, the set of external momenta with respect to the subgraph γ. m_l belongs to the set of light masses $\underline{m}^\gamma$ of γ. M_j is the heavy mass of the propagator to which the light mass or the external momenta belong to.

In our special case the only diagram contributing in the HME is the Taylor expansion of the full diagram Γ, as all subdiagrams vanish in DR (see fig. 6.1).

[1] A graph is called connected when it can not be separated into two or more distinct pieces without cutting any line.

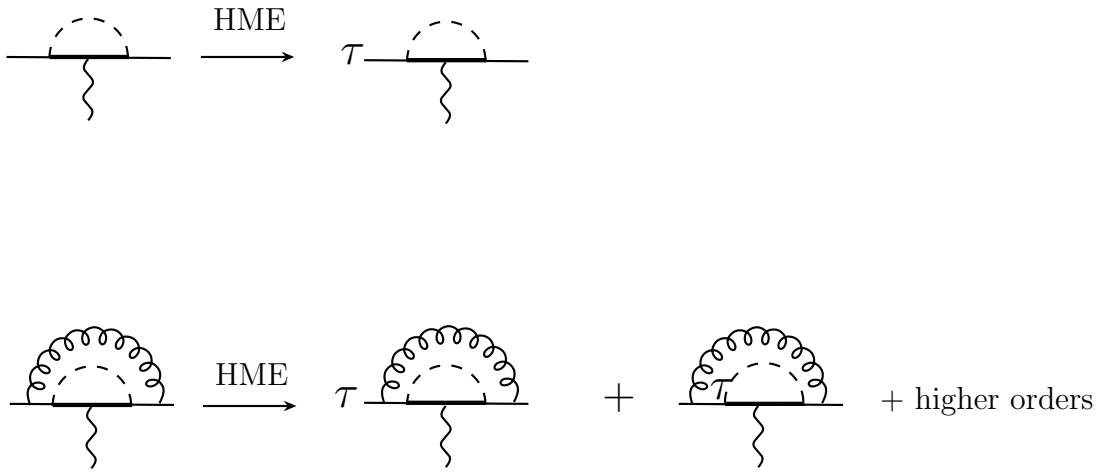

Figure 6.1: Expansion of the full theory in the HME for the example process $b \to \gamma$. τ symbolises the Taylor expansion in small masses and momenta as described in eq. (6.2). Thick lines stand for heavy quarks (in our example the top mass), dashed lines heavy bosons like the $W^{\pm}, \pi^{\pm}$ in the SM or the charged Higgs in the THDM. In line two we show the two subdiagrams needed to be evaluated in the HME for the two-loop diagrams.

After Taylor expansion of the two-loop integrals we deal with the calculation of a large number of rather simple integrals. Matching these results with effective low energy theories we find out to which mass power we must expand the Taylor series in the HME. In our case we have to match to an effective theory with operators of mass dimension six[2]. Therefore it is sufficient to expand the full side up to second order in external momenta and m_b (neglecting m_b^2 though). Expansion up to higher order in the external momenta would correspond to Wilson coefficients of operators of higher mass dimensions and can therefore be safely neglected. The Taylor expansion of the Feynman integrands in external momenta, as well as setting all the light masses to zero, creates *spurious infrared divergences* that we regularise dimensionally. As we shall see, all these divergences cancel out in the matching conditions relating the full and the effective theory Green functions, the spurious IR-divergencies get cancelled by the UV-divergencies on the effective theory side.

6.1.2 Partial Fraction and Tensor Reduction

After Taylor expansion in external momenta and factorising them out, the integrals remain dependend only on loop momenta and two heavy masses: M_W and m_t. Subsequent application of partial fraction decomposition allows a reduction of all the integrals to those in which a single mass parameter occurs in the propagator denominators together with a given loop momentum. Finally, after reducing tensor integrals to scalar ones, the non-vanishing integrals obtained at one and two loops are respectively as

[2]Note that the Fermi constant has mass dimension m^{-2} leading to the correct mass dimension of the effective Lagrangian of m^4.

follows:

$$\begin{aligned} &\mu^{2\epsilon} \int \frac{d^D\, q}{(2\pi)^D} \frac{1}{(q^2 - m^2)^n}, \\ &\mu^{4\epsilon} \int \frac{d^D q_1\; d^D q_2}{(2\pi)^{2D} (q_1^2 - m_1^2)^{n_1} (q_2^2 - m_2^2)^{n_2} [(q_1 - q_2)^2]^{n_3}}, \end{aligned} \tag{6.3}$$

which are known explicitly [46,47]. Explicit formulae for Taylor expansion, partial fraction and tensor reduction as well as analytical results for all occurring scalar one- and two-loop integrals are given in appendix A. In appendix C we introduce furthermore all written routines performing these steps automatically.

6.2 The Full Side in the Standard Model

In this section we will show the basic steps in the derivation of the one- and two-loop functions of the process $b \to s\gamma$, as well as the $b \to s\ gluon$ and $b \to sc\bar{c}$ up to one-loop precision. The latter are needed to recover one-loop contributions to certain Wilson coefficients which take part in the two-loop $b \to s\gamma$ matching condition (see section 6.5). In the following section we will give the basic steps of the calculation of the $b \to s\gamma$ function up to two loops. As there is no tree-level contribution to this function, the first contributions arise at one-loop.

6.2.1 $b \to s\gamma$ at One-Loop Precision

The four 1PI diagrams arising at one-loop are presented in fig. 6.2.

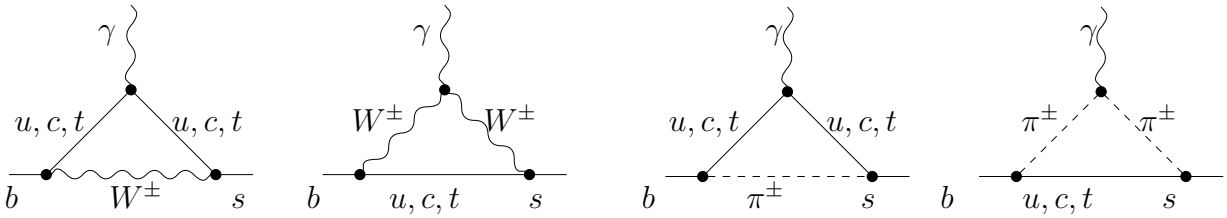

Figure 6.2: One-loop 1PI diagrams for $b \to s\gamma$ in the SM. The charged would-be Goldstone boson is denoted by $\pi^\pm$. There is no $W^\pm \pi^\mp \gamma$ coupling in the background-field gauge.

We calculate the corresponding unrenormalized amputated Green function off shell, in the background-field version of the 't Hooft-Feynman gauge. The Feynman integrands are expanded up to the second order in external momenta and m_b (neglecting m_b^2 though). We refrain from using unitarity of the CKM matrix. The result can be written in the following form:

$$i \frac{4G_F}{\sqrt{2}} \frac{eP_R}{(4\pi)^2} N_\epsilon^{(1)}(M_W) \left\{ (V_{us}^* V_{ub} + V_{cs}^* V_{cb}) \sum_{j=1}^{13} h_j^{(1)} S_j \;\; + \;\; V_{ts}^* V_{tb} \sum_{j=1}^{13} f_j^{(1)}(x) S_j \right\} + \mathcal{O}(\epsilon^2), \tag{6.4}$$

where $P_R = \frac{1}{2}(1+\gamma_5)$, $N_\epsilon^{(1)}(M_W) = 1 - \epsilon\kappa(M_W) + \epsilon^2(\frac{1}{12}\pi^2 + \frac{1}{2}\kappa^2(M_W))$, $\kappa(M_W) = \gamma_E - \ln(4\pi) + \ln(M_W^2/\mu_W^2)$. S_k stands for Dirac structures depending on the incoming b-quark momentum p and on the outgoing photon momentum k

$$\begin{aligned} S_j &= \big(\gamma_\mu \not{p}\not{k},\ \gamma_\mu\,(p\cdot k),\ \gamma_\mu p^2,\ \gamma_\mu k^2,\ \not{p}k_\mu,\ \not{p}p_\mu,\ \not{k}p_\mu,\ \not{k}k_\mu, \\ &\qquad m_b\not{k}\gamma_\mu,\ m_b\gamma_\mu\not{k},\ m_b\not{p}\gamma_\mu,\ m_b\gamma_\mu\not{p},\ M_W^2\gamma_\mu\big)_j\,. \end{aligned} \tag{6.5}$$

We will see in the matching procedure (see section 6.5) that explicit results are needed only for the coefficients at the structures S_2, S_8 and S_{10}:

$$\begin{aligned} h_2^{(1)} &= \tfrac{23}{9} + \tfrac{145}{54}\epsilon, \qquad h_8^{(1)} = -\tfrac{4}{9\epsilon} + \tfrac{7}{54} + \tfrac{59}{324}\epsilon, \qquad h_{10}^{(1)} = 0, \\ f_2^{(1)}(x) &= \tfrac{15x^3-16x^2+4x}{3(x-1)^4}\ln x + \tfrac{-8x^3-105x^2+141x-46}{18(x-1)^3} \\ &\quad +\epsilon\left\{\tfrac{-15x^3+16x^2-4x}{6(x-1)^4}\ln^2 x + \tfrac{8x^4+115x^3-150x^2+48x}{18(x-1)^4}\ln x + \tfrac{-76x^3-645x^2+885x-290}{108(x-1)^3}\right\}, \\ f_8^{(1)}(x) &= \tfrac{-3x^4-15x^3-6x^2+20x-8}{18(x-1)^4}\ln x + \tfrac{71x^3+78x^2-111x+34}{108(x-1)^3} + \epsilon\left\{\tfrac{3x^4+15x^3+6x^2-20x+8}{36(x-1)^4}\ln^2 x\right. \\ &\quad \left. +\tfrac{-71x^4-79x^3+162x^2-144x+48}{108(x-1)^4}\ln x + \tfrac{529x^3-102x^2+195x-118}{648(x-1)^3}\right\}, \\ f_{10}^{(1)}(x) &= \tfrac{-3x^2+2x}{6(x-1)^3}\ln x + \tfrac{5x^2-3x}{12(1-x)^2} + \epsilon\left\{\tfrac{3x^2-2x}{12(x-1)^3}\ln^2 x + \tfrac{-5x^3+2x^2}{12(x-1)^3}\ln x + \tfrac{11x^2-5x}{24(x-1)^2}\right\} \end{aligned} \tag{6.6}$$

with $x = m_t^2/M_W^2$.

6.2.2 $b \to s\gamma$ at Two-Loop Precision

Let us now proceed to an evaluation of the first QCD correction to the considered Green function. The corresponding two-loop diagrams are shown in fig. 9.1.

In analogy to eq. (6.4), we write the unrenormalized two-loop result as

$$i\frac{4G_F}{\sqrt{2}}\frac{e g_s^2 P_R}{(4\pi)^4} N_\epsilon^{(2)}(M_W)\left\{(V_{us}^*V_{ub} + V_{cs}^*V_{cb})\sum_{j=1}^{13} h_j^{(2)} S_j \;+\; V_{ts}^*V_{tb}\sum_{j=1}^{13} f_j^{(2)}(x) S_j\right\} + \mathcal{O}(\epsilon), \tag{6.7}$$

where g_s is the QCD gauge coupling and $N_\epsilon^{(2)}(M_W) = 1 - 2\epsilon\kappa(M_W) + \epsilon^2(\frac{1}{6}\pi^2 + 2\kappa^2(M_W))$. The two-loop analogues of the coefficients given in eq. (6.6) are found to have the following form:

$$\begin{aligned} h_2^{(2)} &= -\tfrac{272}{81\epsilon} - \tfrac{3740}{243}, \qquad h_8^{(2)} = -\tfrac{128}{81\epsilon^2} - \tfrac{1088}{243\epsilon} - \tfrac{314}{729} - \tfrac{128\pi^2}{243}, \qquad h_{10}^{(2)} = \tfrac{20}{9\epsilon} + \tfrac{92}{27}, \\ f_2^{(2)}(x) &= \tfrac{1}{\epsilon}\left\{\tfrac{8x(-45x^3-34x^2+53x-10)}{9(x-1)^5}\ln x + \tfrac{4(x^4+641x^3-501x^2+83x-8)}{27(x-1)^4}\right\} \\ &\quad +\tfrac{8x(7x^3-69x^2+61x-14)}{9(x-1)^4} Li_2\left(1-\tfrac{1}{x}\right) + \tfrac{4x(45x^3+34x^2-53x+10)}{3(x-1)^5}\ln^2 x \\ &\quad +\tfrac{4(-6x^5-4497x^4+2622x^3+811x^2-638x+88)}{81(x-1)^5}\ln x + \tfrac{2(-719x^4+35822x^3-35073x^2+11492x-1802)}{243(x-1)^4}, \end{aligned}$$

$$
\begin{aligned}
f_8^{(2)}(x) &= \tfrac{1}{\epsilon}\left\{\tfrac{4(243x^4+486x^3-419x^2+130x-8)}{81(x-1)^5}\ln x + \tfrac{2(-185x^4-3313x^3+369x^2+905x-368)}{243(x-1)^4}\right\} \\
&+ \tfrac{4(32x^4+283x^3-135x^2-70x+64)}{81(x-1)^4} Li_2\left(1-\tfrac{1}{x}\right) + \tfrac{2(-243x^4-486x^3+419x^2-130x+8)}{27(x-1)^5}\ln^2 x \\
&+ \tfrac{2(370x^5+7933x^4-1370x^3-683x^2+238x-8)}{243(x-1)^5}\ln x + \tfrac{2(-3301x^4-20714x^3+4182x^2+202x+191)}{729(x-1)^4}, \\
f_{10}^{(2)}(x) &= \tfrac{1}{\epsilon}\left\{\tfrac{2x(36x^2+x-10)}{9(x-1)^4}\ln x + \tfrac{11x^3-169x^2+132x-28}{9(x-1)^3}\right\} + \tfrac{2x(-15x^3+8x^2-21x+10)}{9(x-1)^4} Li_2\left(1-\tfrac{1}{x}\right) \\
&+ \tfrac{x(-36x^2-x+10)}{3(x-1)^4}\ln^2 x + \tfrac{-22x^4+396x^3-377x^2+142x-16}{9(x-1)^4}\ln x + \tfrac{31x^3-1071x^2+630x-112}{54(x-1)^3}.
\end{aligned}
\tag{6.8}
$$

The last two elements we need to know on the SM side are the $b \to s\, g$ and $b \to sc\bar{c}$ functions up to one-loop. They are used to recover one-loop contributions to certain Wilson coefficients which take part in the two-loop $b \to s\gamma$ matching condition.

6.2.3 $b \to s\, g$ at One-Loop Precision

Similarly to the $b \to s\gamma$ case, there is no tree-level contribution to the $b \to s\, g$ Green function in the SM. The one-loop contribution is given by the diagrams presented in fig. 6.3.

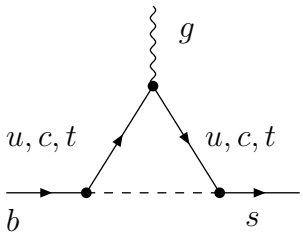

Figure 6.3: One-loop 1PI diagrams for $b \to sg$. The dashed lines is $W^\pm$ or $\pi^\pm$ in the SM and $H^\pm$ in the THDM. The off-shell part of this contributions contributes to $b \to sq\bar{q}$.

In analogy to eq. (6.4), the result can be written as

$$
i\frac{4G_F}{\sqrt{2}}\frac{g_s P_R T^a}{(4\pi)^2} N_\epsilon^{(1)}(M_W)\left\{(V_{us}^* V_{ub} + V_{cs}^* V_{cb})\sum_{j=1}^{13} u_j^{(1)} S_j \;+\; V_{ts}^* V_{tb}\sum_{j=1}^{13} v_j^{(1)}(x) S_j\right\} + \mathcal{O}(\epsilon^2),
\tag{6.9}
$$

where T^a denotes the SU(3) generator corresponding to the outgoing gluon. The coefficients at the structures S_2, S_8 and S_{10} read

$$
u_2^{(1)} = \tfrac{4}{3} + \tfrac{22}{9}\epsilon, \qquad u_8^{(1)} = -\tfrac{2}{3\epsilon} + \tfrac{1}{9} + \tfrac{11}{54}\epsilon, \qquad u_{10}^{(1)} = 0,
\tag{6.10}
$$

$$
\begin{aligned}
v_2^{(1)}(x) &= \tfrac{-5x^2+2x}{(x-1)^4}\ln x + \tfrac{-x^3+15x^2+12x-8}{6(x-1)^3} \\
&\quad +\epsilon\left\{\tfrac{5x^2-2x}{2(x-1)^4}\ln^2 x + \tfrac{x^4-16x^3-30x^2+24x}{6(x-1)^4}\ln x + \tfrac{-5x^3+159x^2+60x-88}{36(x-1)^3}\right\}, \\
v_8^{(1)}(x) &= \tfrac{3x^2+5x-2}{3(x-1)^4}\ln x + \tfrac{5x^3-12x^2-39x+10}{18(x-1)^3} \\
&\quad +\epsilon\left\{\tfrac{-3x^2-5x+2}{6(x-1)^4}\ln^2 x + \tfrac{-5x^4+17x^3+54x^2-36x+12}{18(x-1)^4}\ln x + \tfrac{19x^3-192x^2-57x-22}{108(x-1)^3}\right\}, \\
v_{10}^{(1)}(x) &= \tfrac{x}{2(x-1)^3}\ln x + \tfrac{x^2-3x}{4(x-1)^2} + \epsilon\left\{\tfrac{-x}{4(x-1)^3}\ln^2 x + \tfrac{-x^3+4x^2}{4(x-1)^3}\ln x + \tfrac{x^2-7x}{8(x-1)^2}\right\}.
\end{aligned}
\tag{6.11}
$$

6.2.4 $b \to sc\bar{c}$ up to One-Loop Precision

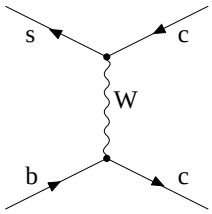

Figure 6.4: Tree-level $b \to sc\bar{c}$ diagram on the SM side.

Contrary to the functions considered so far, the $b \to sc\bar{c}$ function does acquire a tree-level contribution in the SM. It is given by the diagram shown in fig. 6.4. For vanishing external momenta, it gives[3]:

$$-i\frac{4G_F}{\sqrt{2}}V_{cs}^*V_{cb}(\gamma_\mu P_L)\otimes(\gamma^\mu P_L). \tag{6.12}$$

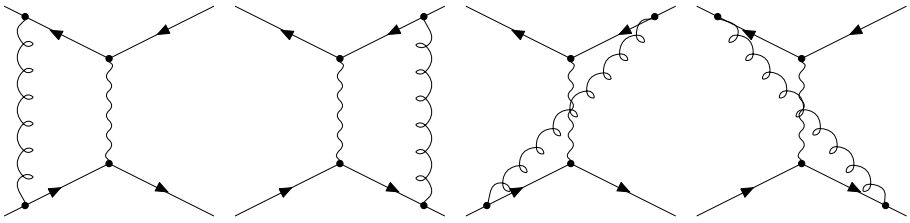

Figure 6.5: One-loop $b \to sc\bar{c}$ diagrams on the SM side, which do not vanish in dimensional regularisation when all the light particle masses are set to zero.

The non-vanishing one-loop diagrams for the $b \to sc\bar{c}$ functions are shown in fig. 6.5. When the external momenta are set to zero, we find the following result for the corre-

[3]The tensor product symbol $\Gamma \otimes \Gamma'$ is used here to denote the tree-level $(\bar{s}\Gamma c)(\bar{c}\Gamma' b)$ amputated Green function.

sponding amputated Green function:

$$i\tfrac{4G_F}{\sqrt{2}}\tfrac{g_s^2}{(4\pi)^2}V_{cs}^*V_{cb}N_\epsilon^{(1)}(M_W)\left\{\left(-\tfrac{6}{\epsilon}-15-\tfrac{39}{2}\epsilon\right)(\gamma_\mu P_L T^a)\otimes(\gamma^\mu P_L T^a)\right.$$
$$\left.+\left(-\tfrac{1}{\epsilon}-\tfrac{3}{2}+\mathcal{O}(\epsilon)\right)\left[(\gamma_\mu\gamma_\nu\gamma_\rho P_L T^a)\otimes(\gamma^\mu\gamma^\nu\gamma^\rho P_L T^a)-16(\gamma_\mu P_L T^a)\otimes(\gamma^\mu P_L T^a)\right]\right\}+\mathcal{O}(\epsilon^2). \tag{6.13}$$

The Dirac structure in the last line of the above equation vanishes in four dimensions. However, there is no way to express it as $\epsilon\times$(simpler structure). The coefficient at this structure will give us the Wilson coefficient of an evanescent operator in the effective theory [40, 48, 49]. The necessity of recovering this coefficient (as well as keeping $\mathcal{O}(\epsilon)$ parts of other one-loop coefficients) is a price we have to pay for regularising infrared divergences dimensionally. The above result is the last one we need to know on the SM side in order to recover SM-contribution deriving from photonic penguins to the Wilson coefficients C_7^i, C_9^i $(i = 1, 2)$. The results for the functions $h_j^i, f_j^i, u_j^i, v_j^i$ for $i = 1, 2$ and $j = 2, 8, 10$ have been derived with the help of the *Mathematica* packages *Fermions* and *Integrals* described in detail in appendix A. They are in agreement with the results published in [42]. In section 6.5 we shall study the same Green functions in the effective theory framework.

6.3 QCD-Renormalisation of the Effective Lagrangian

The Lagrangian of the effective theory has been given in eq. (5.10). It is written in terms of bare fields and parameters. In order to express it in terms of the QCD-renormalized quantities, we replace the QCD gauge coupling, b-quark mass, quark fields and the Wilson coefficients (see section 4.1.1) with

$$g_s \to Z_{g_s} g_s \mu^\varepsilon, \qquad m_b \to Z_m m_b, \qquad q \to Z_q^{1/2} q, \qquad C_i^Q \to \sum_j C_j^Q Z_{ji}. \tag{6.14}$$

After QCD renormalisation, the structure of the effective Lagrangian is the same as in eq. (5.10), but only the photonic penguin contribution to the Wilson coefficients C_i^Q [4] are replaced by some other constants that we denote here by A_i^Q. Below, we shall need

$$\begin{aligned}
A_j^Q &= Z_q^2 \sum_i C_i^Q Z_{ij} \qquad\qquad \text{for } j = 1, 2, 4, 11,\\
A_7^Q &= Z_q Z_{g_s}^{-2}\left[Z_m \sum_i C_i^Q Z_{i7} \;+\; (Z_m - 1)\sum_i C_i^Q Z_{i(35)}\right],\\
A_8^Q &= Z_q Z_{g_s}^{-2}\left[Z_m \sum_i C_i^Q Z_{i8} \;+\; (Z_m - 1)\sum_i C_i^Q Z_{i(34)}\right],\\
A_9^Q &= Z_q Z_{g_s}^{-2} \sum_i C_i^Q Z_{i9}.
\end{aligned} \tag{6.15}$$

[4] Note that in this chapter C_i^Q does not stand for the full Wilson-coefficient (which can get additional SM-contributions from Z-penguins and W-boxes as well as contritutions from models beyond the SM as the THDM), but **only** for contributions arising from photonic penguins in the SM. In chapter 9 C_7^t will be called $-\frac{1}{2}[A_7]_W$ and C_9^t will appear as $[C_9]_W$.

For simplicity, we shall use the MS scheme in the present section. The $\overline{MS}$ results for the Wilson coefficients can be obtained from the MS ones by simply setting $\gamma_E - \ln(4\pi)$ to zero, i.e. replacing $\kappa(M_W)$ by $\ln(M_W^2/\mu_W^2)$.

In the MS scheme, the renormalisation constants read [29, 50]

$$\begin{aligned}
Z_{g_s} &= 1 + \tfrac{g_s^2}{(4\pi)^2\epsilon}\left(-\tfrac{1}{2}\beta_0\right) + \mathcal{O}(g_s^4) && \text{with } \beta_0 = \tfrac{11N-2f}{3} = \tfrac{23}{3} \text{ for f=5 active flavours,}\\
Z_q &= 1 + \tfrac{g_s^2}{(4\pi)^2\epsilon}\left(-\gamma_q^{(0)}\right) + \mathcal{O}(g_s^4) && \text{with } \gamma_q^{(0)} = C_F = \tfrac{N^2-1}{2N} = \tfrac{4}{3},\\
Z_m &= 1 + \tfrac{g_s^2}{(4\pi)^2\epsilon}\left(-\tfrac{1}{2}\gamma_m^{(0)}\right) + \mathcal{O}(g_s^4) && \text{with } \gamma_m^{(0)} = 6\, C_F = 8,\\
Z_{ij} &= \delta_{ij} + \tfrac{g_s^2}{(4\pi)^2}\left[a_{ij}^{01} + \tfrac{1}{\epsilon}a_{ij}^{11}\right] + \tfrac{g_s^4}{(4\pi)^4}\left[a_{ij}^{02} + \tfrac{1}{\epsilon}a_{ij}^{12} + \tfrac{1}{\epsilon^2}a_{ij}^{22}\right] + \mathcal{O}(g^6),
\end{aligned}$$

where $N = 3$ is the number of colours, f is the number of quark flavours and C_F is the quadratic Casimir operator in the fundamental representation (see section E.5). The finite terms a_{ij}^{0k} can be different from zero, if and only if, P_i is an evanescent operator and P_j not.

Our off-shell operator basis is chosen in such a manner that as many operators as possible are EOM-vanishing. This means that no linear combination of the remaining operators is EOM-vanishing. In such a case, the EOM-vanishing operators do not mix into the remaining ones, i.e. $Z_{ij} = 0$ when P_i is EOM-vanishing and P_j not. In consequence, we only need to know explicitly the mixing among the physical and evanescent operators.

The powers of coupling constants in front of our operators eq. (5.14, D.1, D.6) have been chosen in such a way that terms of order g^{2n} in the renormalisation constants originate from n-loop diagrams in the effective theory. As one can see, the sum of powers of gauge coupling constants in front of a given operator is always equal to "(number of fields in this operator)-4". In the original QCD and QED Lagrangians, the powers of coupling constants are equal to "(number of fields)-2". Here, two powers are traded for G_F that normalises the effective Lagrangian. All the renormalisation constants in the effective theory up to two loops are known from former anomalous dimension computations [43,51–54] (although some of them need to be transformed into our operator basis (5.14)). Here, we shall need the one-loop renormalisation constant matrix $\hat{a}^{11}$ for $\{\mathcal{O}_1, \mathcal{O}_2, \mathcal{O}_4, \mathcal{O}_7, \mathcal{O}_8, \mathcal{O}_9, \mathcal{O}_{11}\}$ only. According to [42, 55] it reads

$$\hat{a}^{11} = \begin{array}{c|ccccccc|c}
 & \mathcal{O}_1 & \mathcal{O}_2 & \mathcal{O}_4 & \mathcal{O}_7 & \mathcal{O}_8 & \mathcal{O}_9 & \mathcal{O}_{11} & \\
\hline
 & -2 & \frac{4}{3} & -\frac{1}{9} & 0 & 0 & -\frac{16}{27} & * & \mathcal{O}_1\\
 & 6 & 0 & \frac{2}{3} & 0 & 0 & -\frac{4}{9} & 1 & \mathcal{O}_2\\
 & 0 & 0 & -\frac{50}{9} & 0 & 0 & \frac{16}{27} & 0 & \mathcal{O}_4\\
 & 0 & 0 & 0 & \frac{16}{3} - \beta_0 & 0 & 0 & 0 & \mathcal{O}_7\\
 & 0 & 0 & 0 & -\frac{16}{9} & \frac{14}{3} & 0 & 0 & \mathcal{O}_8\\
 & 0 & 0 & 0 & 0 & 0 & -\beta_0 & 0 & \mathcal{O}_9\\
 & 0 & 0 & 0 & 0 & 0 & 0 & * & \mathcal{O}_{11}
\end{array} , \tag{6.16}$$

where the stars denote entries not needed in this special matching calculation. In addition, for the two-loop matching of photonic penguins in the charm sector, we need the following entries from the matrices $\hat{a}^{12}$ and $\hat{a}^{22}$:

$$\begin{aligned}
a_{27}^{12} &= \tfrac{116}{81}, & a_{27}^{22} &= 0, & a_{(11)7}^{01} &= 0,\\
a_{29}^{12} &= \tfrac{776}{243}, & a_{29}^{22} &= \tfrac{148}{81}, & a_{(11)9}^{01} &= \tfrac{64}{27}.
\end{aligned} \tag{6.17}$$

6.4 The Effective Theory Side

At this point, we are ready to calculate all the necessary 1PI Green functions on the effective theory side. This turns out to be very simple, as all the particles in the effective theory are massless in our approach.[5] Consequently, all the loop diagrams vanish in dimensional regularisation due to the cancellation between ultraviolet and infrared divergences. In effect, we need to know only the tree-level matrix element of the effective Lagrangian. The ultraviolet counterterms present in this matrix element reproduce precisely the infrared divergences in the effective theory, which have to be equal to the infrared divergences on the SM side. As we shall see in section 6.5, all the $1/\epsilon^n$ poles will indeed cancel in the matching condition.

External gluons in the Green functions considered on the Standard Model side have been the background ones. Therefore, we can maintain only the background gluon field in $\mathcal{L}_{eff}$, since only tree-level diagrams are non-vanishing on the effective theory side. This is why we could omit EOM-vanishing operators proportional to quantum gluons in our operator basis, even though the calculation is performed off-shell. For the purpose of the present section, it is convenient to redefine $\mathcal{O}_9$ so that it contains a sum over all the light charged fermions f weighted by their electric charges Q_f

$$\mathcal{O}_9 = -\frac{e^2}{g^2}(\bar{s}_L\gamma_\mu b_L)\sum_f Q_f(\bar{f}\gamma^\mu f). \tag{6.18}$$

This redefinition will be only used for the matching of photonic penguins in the SM (THDM) and will thus not be valid for the matching of Z-penguin in chapters 7 and 8.

We now write down the effective theory counterparts of the Green functions considered in section 6.3. Their structure follows directly from tree-level Feynman rules for the operators given in eqs. (5.14) and (D.1).

6.4.1 $b \to s\,\gamma$

First we will give the $b \to s\,\gamma$ function (cf. eq. (6.4)):

$$i\frac{4G_F}{\sqrt{2}}\frac{eP_R}{g_s^2}\left\{(V_{us}^*V_{ub}+V_{cs}^*V_{cb})\sum_{j=1}^{12}\tilde{h}_jS_j \quad + \quad V_{ts}^*V_{tb}\sum_{j=1}^{12}\tilde{f}_jS_j\right\} \tag{6.19}$$

with the coefficients at the structures S_2, S_8 and S_{10} given by

$$\begin{aligned}
\tilde{h}_2 &= -4A_{35}^c, & \tilde{h}_8 &= 2A_{35}^c - A_{36}^c, & \tilde{h}_{10} &= A_7^c + A_{35}^c,\\
\tilde{f}_2 &= -4A_{35}^t, & \tilde{f}_8 &= 2A_{35}^t - A_{36}^t, & \tilde{f}_{10} &= A_7^t + A_{35}^t
\end{aligned} \tag{6.20}$$

to all orders in QCD. The above coefficients follow from the tree-level "$b \to s\ \gamma$-Feynman rules generated by the operators.

[5] The b-quark mass is formally treated as a perturbative interaction with an external scalar field, and we include only terms that are linear in this interaction.

6.4.2 $b \to s\ g$

Similarly, for $b \to s\ g$ we get:

$$i\frac{4G_F}{\sqrt{2}}\frac{P_R T^a}{g_s}\left\{(V_{us}^* V_{ub} + V_{cs}^* V_{cb})\sum_{j=1}^{12}\tilde{u}_j S_j \;+\; V_{ts}^* V_{tb}\sum_{j=1}^{12}\tilde{v}_j S_j\right\} \tag{6.21}$$

with

$$\begin{array}{lllllllll} \tilde{u}_2 &=& -4A_{34}^c, & \tilde{u}_8 &=& 2A_{34}^c - A_{31}^c, & \tilde{u}_{10} &=& A_8^c + A_{34}^c, \\ \tilde{v}_2 &=& -4A_{34}^t, & \tilde{v}_8 &=& 2A_{34}^t - A_{31}^t, & \tilde{v}_{10} &=& A_8^t + A_{34}^t. \end{array} \tag{6.22}$$

In both the $b \to s\gamma$ and $b \to s\ g$ cases, the coefficients at other structures depend on A_{32}^Q and A_{33}^Q, too. In each of these two cases, coefficients at 12 independent Dirac structures S_j [6] are given by linear combinations of only 6 independent quantities. It is just a consequence of QCD×QED gauge invariance of our effective Lagrangian. Therefore, the coefficients at the structures S_k must satisfy $12-6=6$ linear constraints. This must be also the case for the SM Green functions, because they must match the effective theory ones. These linear constraints of the SM Greens functions are

$$\begin{array}{lllllllll} s_2^{(i)} - s_7^{(i)} &=& 0 & s_6^{(i)} - 2s_3^{(i)} &=& 0 & s_5^{(i)} + s_6^{(i)} + s_7^{(i)} &=& 0 \\ s_4^{(i)} + s_8^{(i)} - s_3^{(i)} &=& 0 & s_{11}^{(i)} + s_{12}^{(i)} &=& 0 & s_9^{(i)} + s_{10}^{(i)} + s_{11}^{(i)} &=& 0, \end{array} \tag{6.23}$$

where $s_k^{(i)}$ $(s = (h, j, u, v),\ i = (1, 2))$ is the coefficient of the S_k-Dirac structure of the considered process. These gauge constraints are only fullfilled after proper renormalisation. Checking these constraints on the SM side has been an important cross-check in our calculation.

6.4.3 $b \to sc\bar{c}$

$b \to sc\bar{c}$ function is the last function to be considered on the effective theory side. It takes the form

$$\begin{aligned} & i\frac{4G_F}{\sqrt{2}}V_{cs}^* V_{cb}\,\{A_1^c(\gamma_\mu P_L T^a)\otimes(\gamma^\mu P_L T^a) \;+\; A_2^c(\gamma_\mu P_L)\otimes(\gamma^\mu P_L) \\ & \;+\; A_{11}^c\,[(\gamma_\mu\gamma_\nu\gamma_\rho P_L T^a)\otimes(\gamma^\mu\gamma^\nu\gamma^\rho P_L T^a) - 16(\gamma_\mu P_L T^a)\otimes(\gamma^\mu P_L T^a)]\} \\ & + [\text{terms proportional to } (A_{31}^Q + A_4^Q)]. \end{aligned} \tag{6.24}$$

6.5 Matching

The perturbative expansion of the Wilson coefficients is given in eq. (5.9). We shall first recover the Wilson coefficients at all the EOM-non-vanishing operators up to one-loop. Then, two-loop contributions to the coefficients at P_7 and P_9 will be found.

[6] The 13. Dirac structure $M_W^2\gamma_\mu$ gets completely renormalized away by the electroweak counterterm.

6.5.1 QCD Renormalisation of the Full Side

It might be surprising that we can actually start the matching without having considered diagrams with UV counterterms on the SM side. Apart from the electroweak counterterm proportional to $\bar{s}\not{D}b$, we should include the QCD renormalisation of the quark wave functions and masses.

The electroweak counterterm proportional to $\bar{s}\not{D}b$ is taken in the MOM scheme, at $q^2 = 0$ for the $\bar{s}\not{\partial}b$ term, and at vanishing external momenta for the terms containing gauge bosons. It is achieved by an appropriate flavour-off-diagonal renormalisation of the quark wave functions. The only effect of such a renormalisation in the present case is that the coefficients at the structure S_{13} in eqs. (6.4), (6.7) and (6.9) are completely renormalized away. This is welcome, because the structure S_{13} was absent from the effective theory counterparts of these equations (eqs. (6.19) and (6.21)).

As far as the QCD renormalisation of the quark wave functions in internal lines and in vertices is concerned, it combines to an overall factor, which could be obtained by renormalising only those terms in the vertices that correspond to external fields in a given Green function. However, one-loop external quark field renormalisation is the same on the full and effective theory sides. Consequently, we can omit counterterms with Z_q on the SM side and simultaneously set Z_q to unity on the effective theory side.

The same refers to the renormalisation of the b-quark mass, since m_b is actually treated as an external scalar field. We omit the corresponding counterterms on the full theory side and simultaneously set Z_m to unity on the effective theory side. This is how we get rid of terms proportional to $(Z_m - 1)$ in eq. (6.15).

As far as the renormalisation of the QCD gauge coupling is concerned, no such counterterms occur on the full theory side in our particular calculation. On the effective theory side, we maintain all the necessary factors of Z_{g_s}.

The last relevant quantity that acquires QCD renormalisation on the full theory side is the top quark mass. However, contributions from the corresponding counterterm diagrams can be obtained by differentiating lower order results with respect to m_t (see below).

6.5.2 $b \to sc\bar{c}$ Matching

Let us first match the $b \to sc\bar{c}$ Green function up to one loop. The first thing to notice is that terms proportional to $A_{31}^Q + A_4^Q$ in the last line of eq. (6.24) are not important at the considered order, because

$$A_4^Q = -A_{31}^Q + \mathcal{O}(g_s^4). \tag{6.25}$$

The reason for this relation is that the $b \to sd\bar{d}$ 1PI Green function acquires its leading contribution only at two loops in the SM. Lower-order tree-level contributions to this function must vanish in the effective theory, which implies the above relation.

Similarly, from the fact that the $b \to se^+e^-$ 1PI function vanishes at one-loop, we find

$$A_9^Q = +A_{36}^Q + \mathcal{O}(g_s^4), \tag{6.26}$$

so long as the W-boson boxes and Z-boson penguins are not taken into account on the SM side.

Returning to the $b \to sc\bar{c}$ function, we compare eqs. (6.12), (6.13) and (6.24), and immediately find

$$\begin{aligned} A_1^c &= \frac{g_s^2}{(4\pi)^2} N_\epsilon^{(1)}(M_W) \left(-\frac{6}{\epsilon} - 15 - \frac{39}{2}\epsilon \right) + \mathcal{O}(g_s^4, \epsilon^2), \\ A_2^c &= -1 + \mathcal{O}(g_s^4), \\ A_{11}^c &= \frac{g_s^2}{(4\pi)^2} (1 - \epsilon\kappa(M_W)) \left(-\frac{1}{\epsilon} - \frac{3}{2} \right) + \mathcal{O}(g_s^4, \epsilon), \end{aligned} \tag{6.27}$$

which implies that (cf. eqs. (6.15)-(6.16) with Z_q set to unity)

$$C_1^{c(0)} = 0, \qquad C_2^{c(0)} = -1, \qquad C_{11}^{c(0)} = 0, \tag{6.28}$$

and

$$\begin{aligned} C_1^{c(1)} &= N_\epsilon^{(1)}(M_W) \left(-\frac{6}{\epsilon} - 15 - \frac{39}{2}\epsilon \right) - \frac{1}{\epsilon} C_2^{c(0)} a_{21}^{11} + \mathcal{O}(\epsilon^2) \\ &= -15 + 6\kappa(M_W) + \epsilon \left(-\frac{39}{2} + 15\kappa(M_W) - 3\kappa(M_W)^2 - \frac{1}{2}\pi^2 \right) + \mathcal{O}(\epsilon^2), \end{aligned} \tag{6.29}$$

$$C_2^{c(1)} = 0, \tag{6.30}$$

$$\begin{aligned} C_{11}^{c(1)} &= (1 - \epsilon\kappa(M_W)) \left(-\frac{1}{\epsilon} - \frac{3}{2} \right) - \frac{1}{\epsilon} C_2^{c(0)} a_{2(11)}^{11} + \mathcal{O}(\epsilon) \\ &= -\frac{3}{2} + \kappa(M_W) + \mathcal{O}(\epsilon). \end{aligned} \tag{6.31}$$

Indeed, all the $1/\epsilon$ poles have cancelled in the final results for the one-loop Wilson coefficients.

The coefficient C_2^c is the only one that acquires a tree-level contribution in our calculation. For all the other coefficients considered below, we have $C_i^{Q(0)} = 0$.

6.5.3 $b \to s\ g$ Matching

Let us now turn to the $b \to s\ g$ matching. Solving the set of linear equations {(6.22),(6.25)}, one finds

$$\begin{aligned} A_4^c &= \left(\frac{1}{2}\tilde{u}_2 + \tilde{u}_8 \right), \\ A_8^c &= \left(\frac{1}{4}\tilde{u}_2 + \tilde{u}_{10} \right). \end{aligned} \tag{6.32}$$

to all orders in QCD. Comparing the one-loop contributions on the full side eqs. (6.9)[7] with the effective Lagrangian (6.21), one finds

$$\begin{aligned} A_4^c &= \frac{g_s^2}{(4\pi)^2} N_\epsilon^{(1)}(M_W) \left(\frac{1}{2} u_2^{(1)} + u_8^{(1)}\right) + \mathcal{O}(g_s^4, \epsilon^2), \\ A_8^c &= \frac{g_s^2}{(4\pi)^2} (1 - \epsilon\kappa(M_W)) \left(\frac{1}{4} u_2^{(1)} + u_{10}^{(1)}\right) + \mathcal{O}(g_s^4, \epsilon^2), \end{aligned} \tag{6.33}$$

which implies that (cf. eqs. (6.15)-(6.16) with Z_q and Z_m set to unity)

$$\begin{aligned} C_4^{c(1)} &= N_\epsilon^{(1)}(M_W) \left(\frac{1}{2} u_2^{(1)} + u_8^{(1)}\right) - \frac{1}{\epsilon} a_{24}^{11} C_2^{c(0)} + \mathcal{O}(\epsilon^2), \\ &= \frac{7}{9} + \frac{2}{3}\kappa(M_W) + \epsilon \left(\frac{77}{54} - \frac{7}{9}\kappa(M_W) - \frac{1}{3}\kappa(M_W)^2 - \frac{1}{18}\pi^2\right) + \mathcal{O}(\epsilon^2), \\ C_8^{c(1)} &= (1 - \epsilon\kappa(M_W)) \left(\frac{1}{4} u_2^{(1)} + u_{10}^{(1)}\right) + \mathcal{O}(\epsilon^2). \end{aligned} \tag{6.34}$$

Similarly,

$$\begin{aligned} C_4^{t(1)} &= (1 - \epsilon\kappa(M_W)) \left(\frac{1}{2} v_2^{(1)}(x) + v_8^{(1)}(x)\right) + \mathcal{O}(\epsilon^2), \\ C_8^{t(1)} &= (1 - \epsilon\kappa(M_W)) \left(\frac{1}{4} v_2^{(1)}(x) + v_{10}^{(1)}(x)\right) + \mathcal{O}(\epsilon^2). \end{aligned} \tag{6.35}$$

6.5.4 $b \to s\gamma$ Matching

Finally, we perform the $b \to s\gamma$ matching. Solving the trivial set of linear equations {(6.20),(6.26)}, one finds

$$\begin{aligned} A_7^c &= \left(\frac{1}{4}\tilde{h}_2 + \tilde{h}_{10}\right), \\ A_9^c &= \left(\frac{1}{2}\tilde{h}_2 - \tilde{h}_8\right) \end{aligned} \tag{6.36}$$

to all orders in QCD. Comparing eqs. (6.4), (6.7) and (6.19) we get

$$\begin{aligned} A_7^c &= \frac{g_s^2}{(4\pi)^2} \left[(1 - \epsilon\kappa(M_W)) \left(\frac{1}{4} h_2^{(1)} + h_{10}^{(1)}\right) + \mathcal{O}(\epsilon^2)\right] \\ &+ \frac{g_s^4}{(4\pi)^4} \left[(1 - 2\epsilon\kappa(M_W)) \left(\frac{1}{4} h_2^{(2)} + h_{10}^{(2)}\right) + \mathcal{O}(\epsilon)\right] + \mathcal{O}(g^6), \\ A_9^c &= \frac{g_s^2}{(4\pi)^2} \left[N_\epsilon^{(1)}(M_W) \left(-\frac{1}{2} h_2^{(1)} - h_8^{(1)}\right) + \mathcal{O}(\epsilon^2)\right] \\ &+ \frac{g_s^4}{(4\pi)^4} \left[N_\epsilon^{(2)}(M_W) \left(-\frac{1}{2} h_2^{(2)} - h_8^{(2)}\right) + \mathcal{O}(\epsilon)\right] + \mathcal{O}(g^6), \end{aligned} \tag{6.37}$$

[7] Without S_{13}, since it has been renormalized away by the electroweak counterterm mentioned in section 6.3 subsection.

which implies that (cf. eqs. (6.15)-(6.17) with Z_q and Z_m set to unity)

$$\begin{aligned}
C_7^{c(1)} &= (1-\epsilon\kappa(M_W))\left(\frac{1}{4}h_2^{(1)}+h_{10}^{(1)}\right)+\mathcal{O}(\epsilon^2),\\
&= \frac{23}{36}+\epsilon\left(\frac{145}{216}-\frac{23}{36}\kappa(M_W)\right)+\mathcal{O}(\epsilon^2),\\
C_9^{c(1)} &= N_\epsilon^{(1)}(M_W)\left(-\frac{1}{2}h_2^{(1)}-h_8^{(1)}\right)-\frac{1}{\epsilon}a_{29}^{11}C_2^{c(0)}+\mathcal{O}(\epsilon^2)\\
&= -\frac{38}{27}-\frac{4}{9}\kappa(M_W)+\epsilon\left(-\frac{247}{162}+\frac{38}{27}\kappa(M_W)+\frac{2}{9}\kappa(M_W)^2+\frac{1}{27}\pi^2\right)+\mathcal{O}(\epsilon^2)
\end{aligned} \tag{6.38}$$

and

$$\begin{aligned}
C_7^{c(2)} &= (1-2\epsilon\kappa(M_W))\left(\frac{1}{4}h_2^{(2)}+h_{10}^{(2)}\right)-\frac{1}{\epsilon}\left[a_{27}^{12}C_2^{c(0)}+(a_{77}^{11}+\beta_0)C_7^{c(1)}+a_{87}^{11}C_8^{c(1)}\right]+\mathcal{O}(\epsilon)\\
&= -\frac{713}{243}+\frac{4}{81}\kappa(M_W)+\mathcal{O}(\epsilon),\\
C_9^{c(2)} &= N_\epsilon^{(2)}(M_W)\left(-\frac{1}{2}h_2^{(2)}-h_8^{(2)}\right)-\frac{1}{\epsilon^2}\left(a_{29}^{22}+\beta_0 a_{29}^{11}\right)C_2^{c(0)}\\
&\quad -\frac{1}{\epsilon}\left[a_{29}^{12}C_2^{c(0)}+a_{19}^{11}C_1^{c(1)}+a_{49}^{11}C_4^{c(1)}\right]-a_{(11)9}^{01}C_{11}^{c(1)}+\mathcal{O}(\epsilon)\\
&= -\frac{524}{729}-\frac{16}{3}\kappa(M_W)+\frac{128}{81}\kappa(M_W)^2+\frac{128}{243}\pi^2+\mathcal{O}(\epsilon).
\end{aligned} \tag{6.39}$$

Similarly, in the top sector we find

$$\begin{aligned}
C_7^{t(1)} &= (1-\epsilon\kappa(M_W))\left[\frac{1}{4}f_2^{(1)}(x)+f_{10}^{(1)}(x)\right]+\mathcal{O}(\epsilon^2)\\
&= \tfrac{3x^3-2x^2}{4(1-x)^4}\ln x+\tfrac{46-205x+312x^2-145x^3}{72(-1+x)^4}\\
&+ \epsilon\left[\kappa(M_W)\left(\tfrac{46-159x+153x^2-22x^3}{72(-1+x)^3}-\tfrac{\left(-2x^2+3x^3\right)\ln(x)}{4(-1+x)^4}\right)\right.\\
&+ \left.\tfrac{-290+975x-933x^2+122x^3}{432(-1+x)^3}-\tfrac{x\left(-48+162x-157x^2+22x^3\right)\ln(x)}{72(-1+x)^4}-\tfrac{x^2(-2+3x)\ln(x)^2}{8(-1+x)^4}\right]+\mathcal{O}(\epsilon^2),\\
C_9^{t(1)} &= (1-\epsilon\kappa(M_W))\left[-\frac{1}{2}f_2^{(1)}(x)-f_8^{(1)}(x)\right]+\mathcal{O}(\epsilon^2)\\
&= \tfrac{+3x^4-30x^3+54x^2-32x+8}{18(1-x)^4}\ln x+\tfrac{47x^3-237x^2+312x-104}{108(1-x)^3}\\
&+ \epsilon\left[\kappa(M_W)\left(\tfrac{-104+312x-237x^2+47x^3}{108(-1+x)^3}-\tfrac{\left(8-32x+54x^2-30x^3+3x^4\right)\ln(x)}{18(-1+x)^4}\right)\right.\\
&+ \left.\tfrac{988-2850x+2037x^2-301x^3}{648(-1+x)^3}+\tfrac{\left(-48+288x^2-266x^3+47x^4\right)\ln(x)}{108(-1+x)^4}-\tfrac{\left(8-32x+54x^2-30x^3+3x^4\right)\ln(x)^2}{36(-1+x)^4}\right]+\mathcal{O}(\epsilon^2),
\end{aligned} \tag{6.40}$$

$$\begin{aligned} C_7^{t(2)} &= (1-2\epsilon\kappa(M_W))\left[\frac{1}{4}f_2^{(2)}(x)+f_{10}^{(2)}(x)\right]-\frac{1}{\epsilon}\gamma_m^{(0)}x\frac{\partial}{\partial x}C_7^{t(1)} \\ &- \frac{1}{\epsilon}\left[(a_{77}^{11}+\beta_0)C_7^{t(1)}+a_{87}^{11}C_8^{t(1)}\right]+\mathcal{O}(\epsilon), \\ C_9^{t(2)} &= (1-2\epsilon\kappa(M_W))\left[-\frac{1}{2}f_2^{(2)}(x)-f_8^{(2)}(x)\right]-\frac{1}{\epsilon}\gamma_m^{(0)}x\frac{\partial}{\partial x}C_9^{t(1)}-\frac{1}{\epsilon}a_{49}^{11}C_4^{t(1)}+\mathcal{O}(\epsilon). \end{aligned} \tag{6.41}$$

Here, the x-derivative terms stand for contributions from the top-quark mass renormalisation on the full theory side. Instead of including these terms, we could just calculate the corresponding one-loop SM diagrams with counterterm insertions. However, derivatives give us the same results much faster.

Plugging in the functions $f_2^{(2)},\ f_8^{(2)},\ f_{10}^{(2)}$ it is easy to see that all the $1/\epsilon$ poles indeed cancel in $C_7^{t(2)}$ and $C_9^{t(2)}$. As usual, the $\mathcal{O}(\epsilon)$ parts of the one-loop Wilson coefficients have affected the results of the two-loop matching.

The results for $C_2^{c(0)}$, $C_1^{c(1)}$, $C_2^{c(1)}$, $C_4^{Q(1)}$, $C_7^{Q(1)}$, $C_9^{Q(1)}$, $C_7^{Q(2)}$ and $C_9^{Q(2)}$ obtained in the present chapter are summarised in chapter 9 after passing to the $\overline{MS}$ scheme. In the $\overline{MS}$ we have

$$\kappa(M_W) = \ln(M_W^2/\mu_W^2) = -\ln(\mu_W^2/m_t^2) - \ln x \tag{6.42}$$

and get for the top contributions

$$\begin{aligned} C_7^{t(1)} &= [A_7]_W^0(x)+\mathcal{O}(\epsilon), \\ C_7^{t(2)} &= [A_7]_W^1(x)+\mathcal{O}(\epsilon), \\ C_9^{t(1)} &= [C_9^{l\bar{l}}]_W^0(x)+\mathcal{O}(\epsilon), \\ C_9^{t(2)} &= [C_9^{l\bar{l}}]_W^1(x)+\mathcal{O}(\epsilon) \end{aligned} \tag{6.43}$$

with the functions $[A_7]_W^0(x), [A_7]_W^1(x), [C_9^{l\bar{l}}]_W^0(x), [C_9^{l\bar{l}}]_W^1(x)$ given in table 9.1.

All the other matching conditions summarised there have been found in an analogous manner. In the two-loop Z-penguin contributions to C_9^Q and C_{10}^Q, the effect of renormalising the $\bar{s}\not{d}b$ term on the SM side is less trivial than in the photonic penguin case and will be explained in detail in section 7.2. In the two-loop matching for $\mathcal{O}_1^c$ and $\mathcal{O}_2^c$ scalar integrals with three non-vanishing masses are necessary [46]. These integrals are given in section A.12.5. Nevertheless, the basic algorithm remains the same as in the $\mathcal{O}_7$ and $\mathcal{O}_9$ cases.

Chapter 7

Matching for $\Delta B = -\Delta S = 1$ Z-penguins and boxes in the SM

In order to complete calculation of all $\mathcal{O}(\alpha_s)$-contributions to C_7 and C_9 we will calculate in this chapter contributions from Z-penguins. Furthermore we will give a short overview of the matching calculation for W-boxes in the SM, the last ingredient needed to complete the matching calculation in the SM for C_9 up to $\mathcal{O}(\alpha_s)$. In order to perform the complete two-loop matching for to C_7 and C_9 up to $\mathcal{O}(\alpha_s)$ we also have to consider contributions deriving from Z-penguins and boxes.

7.1 $\Delta B = -\Delta S = 1$ Z-Penguins

The one-loop contribution are given by the diagrams in fig. 7.1.

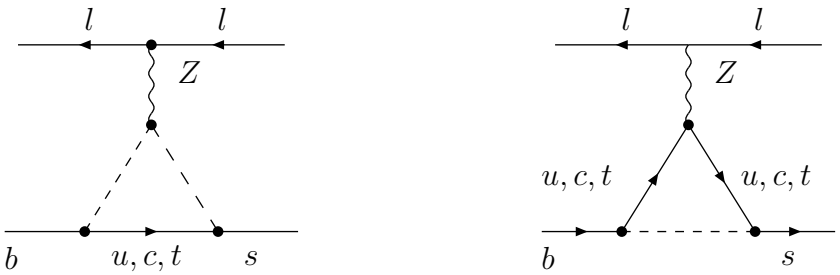

Figure 7.1: One-loop diagrams for $b \to s l^+ l^-$. The dashed lines are $W^\pm/\pi^\pm$ in the SM resp. $H^\pm$ in the THDM.

The unrenormalised one-loop result Green function can be written as

$$i\frac{4G_F}{\sqrt{2}}\frac{e^2}{(4\pi)^2}\left(\frac{c_W s_W}{4}\right) N_\epsilon^{(1)}(M_i)$$
$$\left\{ t_i^{(1)} \;\; \lambda_t \left(\frac{1-4s_W^2}{s_W^2}\bar{s}\gamma_\mu P_L b \sum(\bar{l}\gamma^\mu l) - \frac{1}{s_W^2}\bar{s}\gamma_\mu P_L b) \sum(\bar{l}\gamma^\mu\gamma_5 l) \right) \right\} \; + \; \mathcal{O}(\epsilon^2), \quad (7.1)$$

where the index $i = W$ stands for the SM contributions, the index $i = H$ for contributions deriving from Z-penguins in the THDM which will be discussed in in chapter

8. We have again neglected contributions deriving from up quark loops, as $\lambda_u \ll \lambda_c$. Furthermore we neglect contributions from charm quark loops, as their contributions are suppressed by $\frac{m_c^2}{M_W^2}$. We introduced the abbreviations

$$c_W = \cos\,\theta_W, \quad s_W = \sin\,\theta_W. \tag{7.2}$$

The coefficient derives $t_W^{(1)}$ from Z-penguins with top quarks in the loop and is given by:

$$\begin{aligned} t_W^{(1)} &= \frac{1}{c_W s_W}\left[\frac{\left(-3+2s_W^2\right)(2+x)}{12\epsilon} + \frac{3\left(-2-25x+x^2\right)+2s_W^2\left(2+x+3x^2\right)}{24(-1+x)}\right. \\ &+ \frac{x\left(-12-24x+4s_W^2 x-3x^2+2s_W^2 x^2\right)\ln(x)}{12(-1+x)^2} \\ &+ \epsilon\left(\frac{3\left(-2-33x+x^2\right)+2s_W^2\left(2+x+7x^2\right)}{48(-1+x)} + \frac{-\left(x\left(24-78x+4s_W^2 x+3x^2+6s_W^2 x^2\right)\right)}{24(-1+x)^2}\right. \\ &+ \left.\left.\frac{x\left(-12-24x+4s_W^2 x-3x^2+2s_W^2 x^2\right)}{24(-1+x)^2}\right)\right]. \end{aligned} \tag{7.3}$$

Let us now turn to the two-loop QCD corrections to the Z-penguins. The corresponding Feynman diagrams are given in fig. 9.1. The unrenormalised two-loop Green function can be written as

$$i\frac{4G_F}{\sqrt{2}}\frac{e^2 g_s^2}{(4\pi)^4}\left(\frac{c_W s_W}{4}\right) N_\epsilon^{(2)}(M_i)$$
$$\left\{t_i^{(2)}\ \lambda_t\left(\frac{1-4s_W^2}{s_W^2}\bar{s}\gamma_\mu P_L b\sum(\bar{l}\gamma^\mu l) - \frac{1}{s_W^2}\bar{s}\gamma_\mu P_L b)\sum(\bar{l}\gamma^\mu\gamma_5 l)\right)\right\} + \mathcal{O}(\epsilon^2), \tag{7.4}$$

where $t_W^{(2)}$ is given by

$$\begin{aligned} t_W^{(2)} &= \tfrac{1}{\epsilon^2}\frac{\left(-3+2{s_W}^2\right)x}{3c_W s_W} \\ &+ \frac{(-1+x)\left(9+303x+123x^2+33x^3+2{s_W}^2\left(-3-5x-29x^2+x^3\right)\right)-6x\left(12+\left(60-8{s_W}^2\right)x+\left(9-6{s_W}^2\right)x^2+\left(-3+2{s_W}^2\right)x^3\right)\ln(x)}{\epsilon\ 9c_W s_W(-1+x)^3} \\ &+ \tfrac{1}{18c_W s_W(-1+x)^3}\left[(-1+x)\left(-21+963x+855x^2+63x^3+2{s_W}^2\left(7-41x-133x^2+11x^3\right)\right)\right. \\ &- 4x\left(-78+\left(402-20{s_W}^2\right)x-12\left(-9+5{s_W}^2\right)x^2+\left(33+2{s_W}^2\right)x^3\right)\ln(x) \\ &+ 6x\left(33+189x+18x^2-6x^3+2{s_W}^2\left(1-15x-6x^2+2x^3\right)\right)\ln(x)^2 \\ &- \left.12(-1+x)\,x\left({s_W}^2(2-8x)+3\left(7+4x+2x^2\right)\right)\mathrm{Li}_2(\frac{-1+\mathrm{x}}{\mathrm{x}})\right]. \end{aligned} \tag{7.5}$$

Whereas in the case of photonic penguins the only effect of the electroweak renormalisation was to renormalise away completely the coefficients of S_{13} (and had thus no further influence on the final Wilson coefficient), the influence of the electroweak renormalisation in the Z-penguins is less trivial. In the following section we will therefore give details of the electroweak renormalisation.

7.2 Electroweak Renormalisation

In this section we derive the electroweak counterterm for the $\bar{s}bZ$-vertex. We start from the kinetic term for the b and s quarks in the unrenormalised Lagrangian:

$$\mathcal{L}_{\rm kin} = \bar{b}^0_L(i\ \partial\!\!\!/)b^0_L + \bar{s}^0_L(i\ \partial\!\!\!/)s^0_L, \tag{7.6}$$

where $b^0_L = P_L d^0$. Introducing field renormalisation allowing off-diagonal pieces in b-s-sector we get

$$\begin{aligned} b^0_L &= Z_{11}b_L + Z_{12}s_L, \\ s^0_L &= Z_{21}b_L + Z_{22}s_L. \end{aligned} \tag{7.7}$$

Inserting in (7.6) we find:

$$\begin{aligned} \mathcal{L}_{\rm kin} &= (Z_{11}\bar{b}_L + Z_{12}\bar{s}_L)i\ \partial\!\!\!/(Z_{11}b_L + Z_{12}s_L) + \\ &\quad (Z_{21}\bar{b}_L + Z_{22}\bar{s}_L)i\ \partial\!\!\!/(Z_{21}b_L + Z_{22}s_L) \\ &= \underbrace{\mathcal{L}^{\rm diagonal}_{\rm kin}}_{\text{in terms of renormalised fields}} + \mathcal{L}^{\rm non-diagonal}_{\rm kin}. \end{aligned} \tag{7.8}$$

The requirement that flavour non-diagonal propagation must be absent for the renormalised fields if we work in a mass (field) eigenbasis uniquely determines the electroweak counterterm of a given regularisation prescription. Therefore we find the counter term Lagrangian in the bottom-type quark sector by keeping only non-diagonal pieces in eq.(7.8) :

$$\begin{aligned} \mathcal{L}^{\rm non-diagonal}_{\rm kin,sb} &= \bar{s}_L i\ \partial\!\!\!/ d_L(Z_{12}Z_{11} + Z_{22}Z_{21}) \\ &= \kappa'\bar{s}i\ \partial\!\!\!/ P_L d, \end{aligned} \tag{7.9}$$

where

$$\kappa' = Z_{12}Z_{11} + Z_{22}Z_{21}. \tag{7.10}$$

Now κ' is determined just from the requirements that such non–diagonal propagation must be absent in the $b-s$-sector.

Next, considering the corresponding unrenormalised neutral current Lagrangian for bottom quarks we obtain:

$$\mathcal{L}_{\rm NC} = -\frac{g_2}{2\cos\theta_W}\left(1 - \frac{2}{3}\sin^2\theta_W\right)(\bar{b}_0\gamma_\mu P_L b_0) + \bar{s}_0\gamma_\mu P_L s_0)\cdot Z^\mu. \tag{7.11}$$

Due to the above non-diagonal field renormalisation the Lagrangian will also contain the term:

$$\Delta\mathcal{L}_{NC} = \mathcal{L}^{\rm non-diagonal}_{\rm NC} = -\kappa'\frac{g_2}{2\cos\theta_W}\left(1 - \frac{2}{3}\sin^2\theta_W\right)\bar{s}\gamma_\mu P_L b\cdot Z^\mu, \tag{7.12}$$

which is obtained from eq. (7.11) by using the relations (7.7) and keeping only flavour non–diagonal pieces. Eq. (7.12) yields the electroweak counter term contribution for

the $\bar{s}Zb$ vertex function once κ' has been determined [56]. In the above derivation we omitted right-handed fields which do not contribute at one-loop level to the Z-vertex. In order to derive κ' recall that the usual counter term in the Lagrangian

$$\mathcal{L}_{\text{counter}} = (Z_q - 1)\bar{q} i \not{\partial} q \tag{7.13}$$

gives the counter-term rule

$$i(Z_q - 1)\not{p} \tag{7.14}$$

at the level of diagrams (eq. (4.15)). Thus

$$\mathcal{L}_{\text{counter}} = \kappa' \bar{s} i \not{\partial} P_L b \tag{7.15}$$

gives the Feynman rule

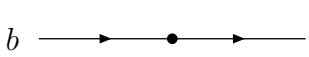

$$i\kappa' \not{p} P_L.$$

κ' can be derived by a simple one-loop calculation

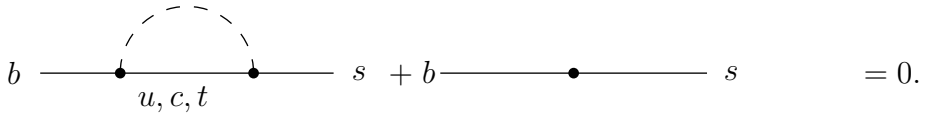

With

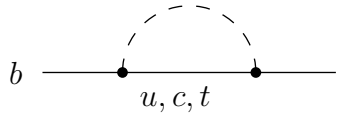

$$= iA\bar{s}\not{k} P_L b \Rightarrow \kappa' = -A,$$

we get for the contributions deriving from top quark loops in the SM:

$$\kappa'^{SM}_{t,1} = -A_t = -\frac{4G_F}{\sqrt{2}} \frac{e}{4\pi^2} V^*_{ts} V_{tb} N^{(1)}_\epsilon(M_W) k^{(1)}_{t,W}, \tag{7.16}$$

where

$$\begin{aligned} k^{(1)}_{t,W} &= \frac{1}{\epsilon}\frac{(2+x)}{2} - \frac{2 - x + 2x^2 - 3x^3 + 2x^2\,(2+x)\ln(x)}{4(-1+x)^2} \\ &+ \epsilon \frac{\left(-2 + x - 6x^2 + 7x^3 - 2x^2\,(2+3x)\ln(x) + 2x^2\,(2+x)\ln(x)^2\right)}{8(-1+x)^2} + \mathcal{O}(\epsilon^2). \end{aligned} \tag{7.17}$$

For the two-loop matching we have to evaluate to evaluate the electroweak-counterterm up to $\mathcal{O}(g_2^2\alpha_s)$. Thus the following two-loop self energy diagrams have to evaluated:

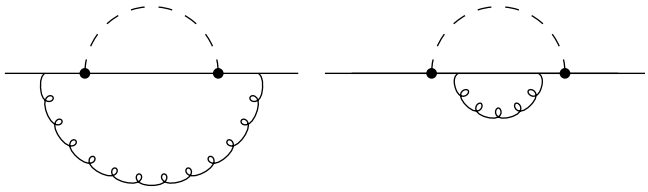

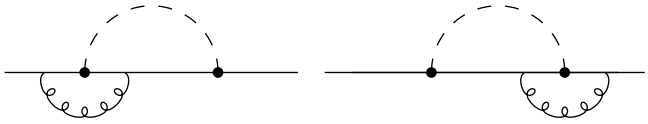

The dashed lines are again $W^{\pm}/\pi^{\pm}$ in the SM and $H^{\pm}$ in the later discussed THDM case. Performing the above two-loop integrals we obtain

$$\kappa_{t,2}^{\prime\, SM} \;=\; -A_t = -\frac{4G_F}{\sqrt{2}}\frac{eg_s^2}{(4\pi)^4}V_{ts}^*V_{tb}N_\epsilon^{(2)}(M_W)k_{t,W}^{(2)}, \tag{7.18}$$

where

$$\begin{aligned} k_{t,W}^{(2)} &= \frac{2x}{\epsilon^2} + \frac{2\left(3+2x+24x^2-30x^3+x^4-6x^2\left(-4-3x+x^2\right)\ln(x)\right)}{3(-1+x)^3\epsilon} \\ &+ \frac{1}{3\left(-1+x\right)^3}\Big[(-1+x)\left(7-41x-133x^2+11x^3\right)-4x^2\left(-10-30x+x^2\right)\ln(x) \\ &+ 6x\left(1-15x-6x^2+2x^3\right)\ln(x)^2+12\left(-1+x\right)x\left(-1+4x\right)\mathrm{Li}_2(\frac{-1+\mathrm{x}}{\mathrm{x}})\Big]. \end{aligned} \tag{7.19}$$

After adding the electroweak counterterm Lagrangian the electroweak renormalised Greens function can be obtained by making the following replacements in eq. (7.1) and eq. (7.4):

$$t_i^{(1)} \;\rightarrow\; t_i^{(1)} + ew\; k_{t,i}^{(1)}, \qquad t_i^{(2)} \;\rightarrow\; t_i^{(2)} + ew\; k_{t,i}^{(2)}, \tag{7.20}$$

where the factor

$$ew = \frac{1}{2\cos\theta_W \sin\theta_W}\left(1-\frac{2}{3}\sin^2\theta_W\right) \tag{7.21}$$

derives from the Z-lepton pair vertex. Let us now summarise the strategy needed for electroweak renormalisation:

- We know that weak interactions produce non-diagonal propagation in the (sb)-sector.
- Similarly to the quark wave renormalisation in QCD (eq. (4.12)) we use the field renormalisation as given in eq. (7.7).
- This produces a counter term in the kinetic terms which translates into the counter term rule $ik'\;\not{\partial}P_L$ (where k' is found from the equity of the counterterm and the corresponding one-loop (two-loop) correction), so that non-diagonal propagation is not present in the renormalised theory.
- We have to express the rest of the Lagrangian through renormalised fields. This produces in addition to the usual vertex $Zb\bar{b}$ and $Z\bar{s}s$ a non diagonal vertex which is represented by $\Delta\mathcal{L}_{\mathrm{NC}}$. This has to be added to the other diagrams. The rest of $\mathcal{L}$ is the same, thus no other parts of the calculation are effected by this electroweak renormalisation.

- Last but not least we want to give the connection to a more standard notation for electroweak counter terms: Bare and renormalised fields are connected via

$$q_0 = \sqrt{Z}q = \sqrt{1+\delta Z}q \simeq \left(1 + \frac{1}{2}\delta Z\right) q = q + \frac{1}{2}\delta Z q. \tag{7.22}$$

Thus

$$\begin{pmatrix} b_L^0 \\ s_L^0 \end{pmatrix} = \left(1 + \frac{1}{2}\delta Z^L\right) \begin{pmatrix} b_L \\ s_L \end{pmatrix} \tag{7.23}$$

and corresponding terms with $L \to R$ which where not needed in our matching calculation. Thus we get for the counterterm:

$$\frac{i}{2}(\delta Z^L_{sb})\not{p} = ik' \not{p} P_L \Rightarrow k' P_L = \frac{1}{2}\delta Z^L_{sb}.$$

7.3 The Effective Side and Matching

The Z-contributions to the $b \to s l^+ l^-$ Greens function on the effective side are given by (cf. eq. (7.1)):

$$\begin{aligned} & i\tfrac{4G_F}{\sqrt{2}}\lambda_t(C^t_{9,Z,i}\mathcal{O}_9 \ + \ C^t_{10,Z,i}\mathcal{O}_{10}) \\ = & \quad \tfrac{4G_F}{\sqrt{2}}\left(\tfrac{g_s^2}{(4\pi)^2}C^{t(1)}_{9,Z,i} + \tfrac{g_s^4}{(4\pi)^4}C^{t(2)}_{9,Z,i}\right)\tfrac{e^2}{g_s^2}(\bar{s}\gamma_\mu P_L b)\sum(\bar{l}\gamma^\mu l) \\ + & \quad \tfrac{4G_F}{\sqrt{2}}\left(\tfrac{g_s^2}{(4\pi)^2}C^{t(1)}_{10,Z,i} + \tfrac{g_s^4}{(4\pi)^4}C^{t(2)}_{10,Z,i}\right)\tfrac{e^2}{g_s^2}(\bar{s}\gamma_\mu P_L b)\sum(\bar{l}\gamma^\mu\gamma_5 l) + \mathcal{O}(\alpha_s^2). \end{aligned} \tag{7.24}$$

where $i = W$ denotes SM Z-penguin contributions, whereas $i = H$ denotes the THDM Z-penguin contribution to the Wilson-coefficients, which will be discussed in section 8.3. We could avoid explicit QCD renormalisation by setting Z_q to unity on both the full and effective side.

Comparing eq. (7.24) and eq. (7.1,7.4) with (7.20) we finally obtain for the SM Z-penguin contribution to C_9 and C_{10}:

$$\begin{aligned} C^{t(1)}_{(9,Z,W)} &= \tfrac{1-4s_W^2}{s_W^2}(1-\epsilon\kappa)\tfrac{c_W s_W}{4}(t_W^{(1)} + ew\ k^{(1)}_{t,W}) + \ \mathcal{O}(\epsilon^2) \\ &= \tfrac{1-4s_W^2}{s_W^2}\left[[C_9^{l\bar{l}}]^1_W + \tfrac{(-4+x)x}{8(-1+x)} - \tfrac{x\left(2-6x+x^2\right)\ln(x)}{8(-1+x)^2} - \tfrac{x(2+3x)\ln(x)^2}{16(-1+x)^2}\right] + \mathcal{O}(\epsilon^2), \\ C^{t(1)}_{(10,Z,W)} &= -\tfrac{1}{s_W^2}\left[[C_9^{l\bar{l}}]^1_W + \tfrac{(-4+x)x}{8(-1+x)} - \tfrac{x\left(2-6x+x^2\right)\ln(x)}{8(-1+x)^2} - \tfrac{x(2+3x)\ln(x)^2}{16(-1+x)^2}\right] + \mathcal{O}(\epsilon^2), \\ C^{t(2)}_{(9,Z,W)} &= \tfrac{1-4s_W^2}{s_W^2}(1-2\epsilon\kappa)\tfrac{c_W s_W}{4}(t_W^{(2)} + ew\ k^{(2)}_{t,W}) - \tfrac{1}{\epsilon}\gamma_m^{(0)} x\tfrac{\partial}{\partial x}C^{t(1)}_{(9,Z,W)} + \ \mathcal{O}(\epsilon) \\ &= \frac{1-4s_W^2}{s_W^2}[C_9^{l\bar{l}}]^2_W \ + \ \mathcal{O}(\epsilon), \\ C^{t(2)}_{(10,Z,W)} &= -\frac{1}{s_W^2}[C_9^{l\bar{l}}]^2_W \ + \ \mathcal{O}(\epsilon), \end{aligned} \tag{7.25}$$

where $[C_9^{l\bar{l}}]_W^1$ and $[C_9^{l\bar{l}}]_W^2$ are given in table 9.1. $[C_9^{l\bar{l}}]_W^1$ was first calculated in [57], $[C_9^{l\bar{l}}]_W^2$ in [56]. As before stands the x derivate for contributions from the top-quark mass renormalisation on the full theory side.

7.4 Box Diagrams

The last piece missing in order to complete the calculation of the SM contributions to C_7 and C_9 are the contributions deriving from box diagrams. In fig. (7.2) we show the one-loop box diagram contributing to $b \to sl^+l^-$, in fig. (9.2) the corresponding two-loop diagrams.

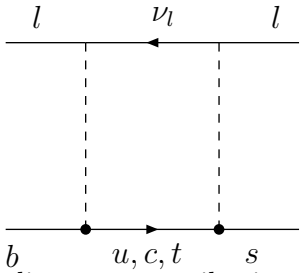

Figure 7.2: One-loop box diagrams contributing to $b \to sl^+l^-$. The dashed lines are $W^\pm$ and/or Would-be-Goldstone-Bosons.

In order to calculate the full SM side the main routine for the calculation of the one- and two-loop diagrams had to be slightly modified in order to be able to deal with two fermion lines.

Furthermore, the evanescent operator

$$\begin{aligned} \mathcal{O}_1^E &= \frac{e^2}{g_s^2}\left((\bar{s}\gamma_{\mu_1}\gamma_{\mu_2}\gamma_{\mu_3}P_L b)(l\gamma^{\mu_1}\gamma^{\mu_2}\gamma^{\mu_3}P_L l)) - 4(\bar{s}\gamma_{\mu_1}P_L b)(\bar{l}\gamma^{\mu}P_L l)\right) \\ &= \frac{e^2}{g_s^2}\left((\bar{s}\gamma_{\mu_1}\gamma_{\mu_2}\gamma_{\mu_3}P_L b)(l\gamma^{\mu_1}\gamma^{\mu_2}\gamma^{\mu_3}P_L l) - 2(\mathcal{O}_9 - \mathcal{O}_{10})\right) \end{aligned} \tag{7.26}$$

arises due to our D-dimensional matching calculation. This operator would vanish in 4 dimensions (see section D.2). Details of this matching calculation can be found in [58]. All published results have been confirmed. The corresponding Wilson coefficients can be find in chapter 9.

Chapter 8

Matching for $\Delta B = -\Delta S = 1$ penguins in the THDM

In this chapter we present the derivation of the analytic results for the two-loop corrections to the Wilson coefficients $C_9(\mu_W)$ and $C_{10}(\mu_W)$ in type-I and type-II two-Higgs-doublet models at the matching scale μ_W. They are important ingredients for next-to-next-to-leading logarithmic predictions of various observables related to the decays $B \to X_s l^+ l^-$ $(l = e, \mu)$ in these models. Additionally we rederived the already known two-loop correction to the Wilson coefficient $C_7(\mu_W)$ which is related to the decay $B \to X_s\gamma$. While these extra pieces are known for the coefficients C_7 [14–18] and C_{10} [59] for quite some time, the two-loop THDM contributions to C_9 have been first calculated in [60] and first published in [19]. We neglect diagrams with neutral Higgs-boson exchange. This omission is justified in the type-II model, if the coupling parameters $(m_l/M_W)\tan\beta$ and $m_l/(M_W\cos\beta)$ are sufficiently smaller than one. In this case the operator basis is the same as in the SM. Only the matching calculation for the Wilson coefficients gets changed by adding the contributions where the flavour transition is mediated by the exchange of the physical charged Higgs boson instead of W/Would-be Goldstone bosons. While these extra pieces are known for the coefficients C_7, C_8 and C_{10} to two-loop precision for quite some time [14–18, 59] the corresponding results for C_9 were first published by [19]. In order to calculate the $\mathcal{O}(\alpha_s)$ THDM-contributions to C_7, C_9 and C_{10} the photonic and Z-penguin diagrams given in fig. 9.1, where the dashed lines are now the charged Higgs-bosons, have to be calculated. Note that only the contributions from the internal top quarks have to be taken into account in these diagrams, as the charm contributions, which come with a relative suppression factor of $m_b m_c/m_t^2$ or m_c^2/m_t^2, only induce dimension 8 operators which are neglected in our treatment. The different contributions to the Wilson coefficients will be denoted as follows:

We write the one- and two-loop charged Higgs induced contributions to $C_9(\mu_W)$ and $C_{10}(\mu_W)$ in the form

$$\begin{aligned} C_{9,\mathrm{H}}^{(n)}(\mu_W) &= C_{(9,\gamma,H)}^{(t(n))}(\mu_W) + C_{(9,Z,H)}^{(t(n))}(\mu_W) \\ &= [D_9]_H^{(n-1)} + \frac{1-4s_W^2}{s_W^2}[C_9^{l\bar{l}}]_H^{(n-1)}, \\ C_{10,\mathrm{H}}^{(n)}(\mu_W) &= C_{(10,Z,H)}^{(t(n))}(\mu_W) = -[D_9]_H^{(n-1)}, \end{aligned} \tag{8.1}$$

where $s_W = \sin\theta_W$. Terms proportional to $Z^{(n)}$ ($\Gamma^{(n)}$) account for contribution the n-loop Z^0- (photon-) penguin diagrams. In eq. (8.1) we have additionally introduced the functions

$[C_9^{l\bar{l}}]_H^{(n-1)}$: $b \to s l^+ l^-$ mediated by n-loop Z-penguins in the THDM,
$[D_9]_H^{(n-1)}$: off-shell part of n-loop 1PI $b \to s\,\gamma$ in the THDM, contributing to $b \to s l^+ l^-$.

8.1 $b \to s\ g$

Let us now start with the calculation of Wilson coefficients deriving from gluonic one-loop penguins with charged Higgs bosons. They will be needed to perform the two-loop matching calculation of photonic penguin contributions to $C_{7,H}$ and $C_{9,H}$. In analogy to eq. (6.9) the corresponding Greens function can be written as

$$i\frac{4G_F}{\sqrt{2}}\frac{g_s P_R T^a}{(4\pi)^2} N_\epsilon^{(1)}(M_H)\left\{V_{ts}^* V_{tb}\sum_{j=1}^{13} v_j^{(1,H)}(y) S_j\right\} + \mathcal{O}(\epsilon^2), \tag{8.2}$$

where

$$y = \frac{m_t^2}{M_H^2}. \tag{8.3}$$

The THDM Wilson coefficients deriving from gluonic one-loop penguins (see fig. (6.3)) are given by

$$\begin{aligned} C_4^{t(1),H} &= (1-\epsilon\kappa(M_H))\left(\frac{1}{2}v_2^{(1,H)}(y) + v_8^{(1,H)}(y)\right) + \mathcal{O}(\epsilon^2), \\ C_8^{t(1),H} &= (1-\epsilon\kappa(M_H))\left(\frac{1}{4}v_2^{(1,H)}(y) + v_{10}^{(1,H)}(y)\right) + \mathcal{O}(\epsilon^2). \end{aligned} \tag{8.4}$$

The derivation of eq. (8.4) is in analogy to the derivation of (6.35). With

$$\begin{aligned} v_2^{(1,H)}(y) &= Y^2\left[\frac{-\left(y\left(2+3y-6y^2+y^3\right)\right)}{6(-1+y)^4} - \frac{y^2\ln(y)}{(-1+y)^4}\right. \\ &\quad \left. +\epsilon\left(\frac{y\left(-22-27y+54y^2-5y^3\right)}{36(-1+y)^4} + \frac{y^2\left(-6-6y+y^2\right)\ln(y)}{6(-1+y)^4} + \frac{y^2\ln(y)^2}{2(-1+y)^4}\right)\right], \\ v_8^{(1,H)}(y) &= Y^2\left[\frac{y\left(5-22y+5y^2\right)}{18(-1+y)^3} + \frac{y(-1+3y)\ln(y)}{3(-1+y)^4}\right. \\ &\quad \left. +\epsilon\left(\frac{y\left(19-170y+19y^2\right)}{108(-1+y)^3} - \frac{y^3(-27+5y)\ln(y)}{18(-1+y)^4} - \frac{y(-1+3y)\ln(y)^2}{6(-1+y)^4}\right)\right], \\ v_{10}^{(1,H)}(y) &= XY\left[\frac{-((-3+y)y)}{4(-1+y)^2} - \frac{y\ln(y)}{2(-1+y)^3} + \epsilon\left(\frac{-((-7+y)y)}{8(-1+y)^2} + \frac{(-4+y)y^2\ln(y)}{4(-1+y)^3} + \frac{y\ln(y)^2}{4(-1+y)^3}\right)\right] \end{aligned} \tag{8.5}$$

we get

$$\begin{aligned}
C_4^{t(1),H} &= Y^2 \left[\tfrac{3y^2-2y}{6(y-1)^4} \ln y + \tfrac{7y^3-29y^2+16y}{36(y-1)^3} \right. \\
&\quad + \epsilon \left(\tfrac{y\left(104-193y+23y^2\right)}{216(-1+y)^3} - \tfrac{\left(y^2\left(18-36y+7y^2\right)\ln(y)\right)}{36(-1+y)^4} - \tfrac{\left(y(-2+3y)\ln(y)^2\right)}{12(-1+y)^4} \right. \\
&\quad \left. \left. + \tfrac{-\left(y\left(-16+45y-36y^2+7y^3\right)\ln\left(\frac{{M_H}^2}{{\mu_W}^2}\right)\right)}{36(-1+y)^4} - \tfrac{y(-2+3y)\ln\left(\frac{{M_H}^2}{{\mu_W}^2}\right)\ln(y)}{6(-1+y)^4} \right) \right] + \mathcal{O}(\epsilon^2) \\
&= [E_4]_H^0 + \mathcal{O}(\epsilon), \\
C_8^{t(1),H} &= XY \left(-\tfrac{y}{2(y-1)^3} \ln y - \tfrac{y^2-3y}{4(y-1)^2} \right) - Y^2 \left[\tfrac{y^2}{4(y-1)^4} \ln y + \tfrac{y^3-5y^2-2y}{24(y-1)^3} \right] \\
&\quad + \epsilon \left(XY \tfrac{y\left(-7+8y-y^2+2(-4+y)y\ln(y)+2\ln(y)^2\right)}{8(-1+y)^3} \right. \\
&\quad + Y^2 \tfrac{y\left(-22-27y+54y^2-5y^3+6y\left(-6-6y+y^2\right)\ln(y)+18y\ln(y)^2\right)}{144(-1+y)^4} \\
&\quad \left. - \ln \tfrac{M_H^2}{\mu_W^2} \left(XY \tfrac{x\left(-6+8x-2x^2-4\ln(x)\right)}{8(-1+x)^3} + Y^2 \tfrac{x\left(-12-18x+36x^2-6x^3-36x\ln(x)\right)}{144(-1+x)^4} \right) \right) + \mathcal{O}(\epsilon^2).
\end{aligned} \tag{8.6}$$

After passing to the $\overline{\text{MS}}$-scheme, we replaced $\kappa(M_H)$ by $\ln \frac{M_H^2}{\mu_W^2}$ in the above Wilson-coefficients. In type-II models we have

$$C_8^{t(1),H} = -\frac{1}{2}[F_8]_H^{(0)} + \mathcal{O}(\epsilon). \tag{8.7}$$

$[E_4]_H^{(0)}$ and $[F_8]_H^{(0)}$ are given in the summary table 9.2.

8.2 $b \to s\gamma$

Let us now start with the matching for photonic penguins in the THDM. The corresponding one-loop diagrams are given in fig. 8.1.

Figure 8.1: One-loop 1PI diagram for $b \to s\gamma$ in the THDM. The off-shell part of this diagram contributes to $b \to s l^+ l^-$.

The result of the calculation of the corresponding unrenormalised amputated Green

function can be written as

$$i\frac{4G_F}{\sqrt{2}}\frac{eP_R}{(4\pi)^2}N_\epsilon^{(1)}(M_H)V_{ts}^*V_{tb}\sum_{j=1}^{13}f_j^{(1,H)}(x)S_j \;+\; \mathcal{O}(\epsilon^2), \tag{8.8}$$

The one-loop photonic contributions to C_7 and C_9 are given by

$$\begin{aligned} C_7^{t(1,H)} &= (1-\epsilon\kappa(M_H))\left[\frac{1}{4}f_2^{(1,H)}(y)+f_{10}^{(1,H)}(y)\right]+\mathcal{O}(\epsilon^2),\\ [D_9]_H^0 &= (1-\epsilon\kappa(M_H))\left[-\frac{1}{2}f_2^{(1,H)}(y)-f_8^{(1,H)}(y)\right]+\mathcal{O}(\epsilon^2). \end{aligned} \tag{8.9}$$

With

$$\begin{aligned} f_2^{(1,H)} &= Y^2\left[\frac{-\left(y\left(-7+5y+8y^2\right)\right)}{18(-1+y)^3}+\frac{y^2(-2+3y)\ln(y)}{3(-1+y)^4}\right.\\ &\quad\left.+\epsilon\left(\frac{-\left(y\left(-59+49y+76y^2\right)\right)}{108(-1+y)^3}+\frac{y^2\left(-12+15y+8y^2\right)\ln(y)}{18(-1+y)^4}-\frac{y^2(-2+3y)\ln(y)^2}{6(-1+y)^4}\right)\right],\\ f_8^{(1,H)} &= Y^2\left[\frac{y\left(17-64y+71y^2\right)}{108(-1+y)^3}-\frac{y\left(4-12y+9y^2+3y^3\right)\ln(y)}{18(-1+y)^4}\right.\\ &\quad\left.+\epsilon\left(\frac{y\left(43-308y+529y^2\right)}{648(-1+y)^3}-\frac{y^3(-27+71y)\ln(y)}{108(-1+y)^4}+\frac{y\left(4-12y+9y^2+3y^3\right)\ln(y)^2}{36(-1+y)^4}\right)\right],\\ f_{10}^{(1,H)} &= X\,Y\left[\frac{-(y(-3+5y))}{12(-1+y)^2}+\frac{y(-2+3y)\ln(y)}{6(-1+y)^3}\right.\\ &\quad\left.+\epsilon\left(\frac{-(y(-5+11y))}{24(-1+y)^2}+\frac{y^2(-2+5y)\ln(y)}{12(-1+y)^3}-\frac{y(-2+3y)\ln(y)^2}{12(-1+y)^3}\right)\right] \end{aligned} \tag{8.10}$$

we get

$$\begin{aligned} C_7^{t(1,H)} &= XY\left(\frac{-\left(y\left(3-8y+5y^2\right)\right)}{12(-1+y)^3}-\frac{(4-6y)y\ln(y)}{12(-1+y)^3}\right)\\ &\quad+Y^2\left(\frac{y\left(-42+72y+18y^2-48y^3-72y\ln(y)+108y^2\ln(y)\right)}{432(-1+y)^4}\right)\\ &\quad+\epsilon\left[Y^2\left(\frac{-\left(y\left(-59+49y+76y^2+6L_t\left(-7+5y+8y^2\right)\right)Y^2\right)}{432(-1+y)^3}\right.\right.\\ &\quad\left.+\frac{y\left(-7+18y^2+6L_ty(-2+3y)\right)Y^2\ln(y)}{72(-1+y)^4}+\frac{y^2(-2+3y)Y^2\ln(y)^2}{24(-1+y)^4}\right)\\ &\quad XY\left(\frac{-(y(-5+11y+2L_t(-3+5y)))}{24(-1+y)^2}+\frac{y(-3+6y+L_t(-4+6y))\ln(y)}{12(-1+y)^3}\right.\\ &\quad\left.\left.+\frac{y(-2+3y)\ln(y)^2}{12(-1+y)^3}\right)\right]+\mathcal{O}(\epsilon^2) \end{aligned} \tag{8.11}$$

In type-II THDM models we have $X=\tan\beta, Y=\cot\beta$. Thus we can write

$$C_7^{t(1,H)} \;=\; = [A_7]_H^{(0)}+\mathcal{O}(\epsilon), \tag{8.12}$$

where $[A_7]_H^{(0)}$ is given in table 9.2. For the contribution from the off-shell part of $b \to s\gamma$ we get

$$\begin{aligned}[D_9]_H^0 &= Y^2 \left(\Gamma^1 + \epsilon \left[\frac{-\left(y\left(220-455y+301y^2+6L_t\left(38-79y+47y^2\right)\right)\right)}{648(-1+y)^3} \right.\right. \\ &\left.\left. + \frac{y\left(38-81y+54y^2+6L_t\left(4-6y+3y^3\right)\right)\ln(y)}{108(-1+y)^4} + \frac{y\left(4-6y+3y^3\right)\ln(y)^2}{36(-1+y)^4} \right] \right) + \mathcal{O}(\epsilon^2)\end{aligned} \tag{8.13}$$

$\Gamma^{(1)}$ reads [61]

$$\Gamma^{(1)} = \frac{-\left(38-79y+47y^2\right)y}{108(y-1)^3} + \frac{\left(4-6y+3y^3\right)y}{18(y-1)^4}\ln y. \tag{8.14}$$

The $\mathcal{O}(\epsilon)$-pieces of the Wilson coefficients $C_4^{t(1),H}$, $C_8^{t(1),H}$, $C_7^{t(1),H}$ and $[D_9]_0^H$, which were not published before, will be needed in the two-loop matching calculation.
Let us now proceed the corresponding two-loop contributions. The two-loop photonic contributions to C_7 and C_9 are given by

$$\begin{aligned}C_7^{t(2),H} &= (1-2\epsilon\kappa(M_H))\left[\tfrac{1}{4}f_2^{(2,H)}(y) + f_{10}^{(2,H)}(y)\right] - \tfrac{1}{\epsilon}\gamma_m^{(0)} y\tfrac{\partial}{\partial y}C_7^{t(1,H)} \\ &\quad -\tfrac{1}{\epsilon}\left[(a_{77}^{11}+\beta_0)C_7^{t(1,H)} + a_{87}^{11}C_8^{t(1,H)}\right] + \mathcal{O}(\epsilon), \\ [D_9]_H^1 &= (1-2\epsilon\kappa(M_H))\left[-\tfrac{1}{2}f_2^{(2,H)}(y) - f_8^{(2,H)}(y)\right] - \tfrac{1}{\epsilon}\gamma_m^{(0)} y\tfrac{\partial}{\partial y}[D_9]_H^0 - \tfrac{1}{\epsilon}a_{49}^{11}C_4^{t(1,H)} + \mathcal{O}(\epsilon).\end{aligned} \tag{8.15}$$

With

$$\begin{aligned}f_2^{(2,H)}(y) &= Y^2\left(\tfrac{1}{\epsilon}\left[\frac{4y\left(-19-45y+135y^2+y^3\right)}{27(-1+y)^4} - \frac{8y^2\left(-11+14y+9y^2\right)\ln(y)}{9(-1+y)^5}\right]\right. \\ &- \frac{2y\left(622+3591y-9036y^2+719y^3\right)}{243(-1+y)^4} + \frac{8y^2\left(11-23y+7y^2\right)\mathrm{Li}_2(\frac{-1+y}{y})}{9(-1+y)^4} \\ &\left. - \frac{4y\left(28-385y+114y^2+921y^3+6y^4\right)\ln(y)}{81(-1+y)^5} + \frac{4y^2\left(-11+14y+9y^2\right)\ln(y)^2}{3(-1+y)^5}\right),\end{aligned}$$

$$
\begin{aligned}
f_8^{(2,H)}(y) &= Y^2\left(\frac{1}{\epsilon}\left[\frac{-2\left(355y-1377y^2+1701y^3+185y^4\right)}{243(-1+y)^4}+\frac{4\left(32y-89y^2+12y^3+189y^4\right)\ln(y)}{81(-1+y)^5}\right]\right.\\
&+ \frac{2y\left(335-4604y+13110y^2-5540y^3-3301y^4\right)}{729(-1+y)^5}+\frac{2y\left(-352+1591y-3636y^2+4763y^3+370y^4\right)\ln(y)}{243(-1+y)^5}\\
&- \left.\frac{2y\left(32-89y+12y^2+189y^3\right)\ln(y)^2}{27(-1+y)^5}+\frac{4y\left(32-81y+75y^2+32y^3\right)\mathrm{Li}_2(\frac{-1+y}{y})}{81(-1+y)^4}\right),\\
f_{10}^{(2,H)}(y) &= \frac{1}{\epsilon}\left[\frac{-2XY\left(21y-47y^2+8y^3\right)}{9(-1+y)^3}-\frac{\left(Y^2y\left(-4+5y+5y^2\right)\right)}{9(-1+y)^3}\right]\\
&+ \frac{\left(-570y+1266y^2-84Xy^3\right)XY}{54(-1+y)^3}+\frac{\left(-74y+133y^2-53y^3\right)Y^2}{54(-1+y)^3}\\
&+ Y^2\left(\frac{y\left(8-21y+14y^2+10y^3\right)\ln(y)}{9(-1+y)^4}+\frac{(1-2y)y^2\ln(y)^2}{(-1+y)^4}+\frac{2y^2\left(7-14y+y^2\right)\mathrm{Li}_2\left(\frac{-1+y}{y}\right)}{9(-1+y)^4}\right)\\
&+ XY\left(\frac{2\left(42y^2-109y^3+16y^4\right)\ln(y)}{9(-1+y)^4}+\frac{2\left(-8y+14y^2+3y^3\right)\ln(y)^2}{3(-1+y)^4}+\frac{16y\left(3-7y+2y^2\right)\mathrm{Li}_2\left(\frac{-1+y}{y}\right)}{9(-1+y)^3}\right)
\end{aligned}
\tag{8.16}
$$

we get for $C_7^{t(2,H)}$

$$
\begin{aligned}
C_7^{t(2,H)} &= X\,Y\left(\frac{16y\left(3-7y+2y^2\right)\mathrm{Li}_2\left(\frac{-1+y}{y}\right)}{9(-1+y)^3}+\frac{-4y\left(7-13y+2y^2\right)}{3(-1+y)^3}+\frac{2y\left(33-64y+7y^2\right)\ln(y)}{9(-1+y)^4}\right.\\
&+ \left.L_t\left(\frac{-2y\left(21-47y+8y^2\right)}{9(-1+y)^3}-\frac{4y\left(-8+14y+3y^2\right)\ln(y)}{9(-1+y)^4}\right)\right)\\
&+ Y^2\left(\frac{2y^2\left(18-37y+8y^2\right)\mathrm{Li}_2\left(\frac{-1+y}{y}\right)}{9(-1+y)^4}+\left(\frac{-\left(y\left(31+18y-135y^2+14y^3\right)\right)}{27(-1+y)^4}-\frac{2y^2\left(-14+23y+3y^2\right)\ln(y)}{9(-1+y)^5}\right)L_t\right.\\
&- \left.\frac{\left(y\left(-797+5436y-7569y^2+1202y^3\right)\right)}{486(-1+y)^4}+\frac{y\left(-7+463y-807y^2+63y^3\right)\ln(y)}{81(-1+y)^5}\right).
\end{aligned}
\tag{8.17}
$$

In type-II THDM models we obtain

$$
C_7^{t(2,H)} = -\frac{1}{2}[A_7]_H^{(1)}+\mathcal{O}(\epsilon) \tag{8.18}
$$

with $[A_7]_H^{(1)}$ given in table 9.2. For the photonic contribution to C_9 we get

$$
[D_9]_H^1 = Y^2\Gamma^{(2)}, \tag{8.19}
$$

where

$$
\begin{aligned}
\Gamma^{(2)} &= -\frac{380y^4-528y^3+72y^2+128y}{81(y-1)^4}\mathrm{Li}_2\left(1-\frac{1}{y}\right)+\frac{596y^4-672y^3+64y^2+204y}{81(y-1)^5}\ln y\\
&+ \frac{-6175y^4+9138y^3-3927y^2-764y}{729(y-1)^4}\\
&+ \left[\frac{432y^4-456y^3+40y^2+128y}{81(y-1)^5}\ln y+\frac{-352y^4-972y^3+1944y^2-1052y}{243(y-1)^4}\right]L_t.
\end{aligned}
\tag{8.20}
$$

Note that the $\Gamma^{(n)}$ depend via y on the renormalisation scheme for the t-quark mass.

8.3 $b \to sZ$

In this section we will give the matching equations for one-loop (fig. 7.1) and two-loop Z-penguins (fig. 9.1) in the THDM. The corresponding unrenormalised one- and two-loop Greens function are given in eq. (7.1-7.4) with $i = H$.

Comparing eq. (7.24) and eq. (7.1,7.4) with (7.20) we finally obtain for the THDM Z-penguin contribution to C_9 and C_{10}:

$$\begin{aligned}
C^{(t(1))}_{(9,Z,H)} &= \tfrac{1-4s_W^2}{s_W^2}(1-\epsilon\kappa)\tfrac{c_W s_W}{4}(t_H^{(1)} + ew\ k_{t,H}^{(1)}) + \ \mathcal{O}(\epsilon^2) \\
&= \tfrac{1-4s_W^2}{s_W^2}\left[[C_9^{l\bar{l}}]_H^1 + \ \epsilon Y^2 \tfrac{xy}{8}\left(\tfrac{1+L_t}{-1+y} - \tfrac{(1+L_t)\ln(y)}{(-1+y)^2} - \tfrac{\ln(y)^2}{2(-1+y)^2}\right)\right] + \mathcal{O}(\epsilon^2), \\
C^{(t(1))}_{(10,Z,H)} &= -\tfrac{1}{s_W^2}\left[[C_9^{l\bar{l}}]_H^1 + \ \epsilon Y^2 \tfrac{xy}{8}\left(\tfrac{1+L_t}{-1+y} - \tfrac{(1+L_t)\ln(y)}{(-1+y)^2} - \tfrac{\ln(y)^2}{2(-1+y)^2}\right)\right] + \ \mathcal{O}(\epsilon^2), \\
C^{(t(2))}_{(9,Z,H)} &= \tfrac{1-4s_W^2}{s_W^2}(1-2\epsilon\kappa)\tfrac{c_W s_W}{4}(t_H^{(2)} + ew\ k_{t,H}^{(2)}) - \tfrac{1}{\epsilon}\gamma_m^{(0)} x\tfrac{\partial}{\partial x}C^{(t(1))}_{(9,Z,H)} - \tfrac{1}{\epsilon}\gamma_m^{(0)} y\tfrac{\partial}{\partial y}C^{(t(1))}_{(9,Z,H)} + \ \mathcal{O}(\epsilon) \\
&= \tfrac{1-4s_W^2}{s_W^2}[C_9^{l\bar{l}}]_H^2 \ + \ \mathcal{O}(\epsilon), \\
C^{(t(2))}_{(10,Z,H)} &= -\tfrac{1}{s_W^2}[C_9^{l\bar{l}}]_H^2 \ + \ \mathcal{O}(\epsilon),
\end{aligned} \tag{8.21}$$

where $[C_9^{l\bar{l}}]_H^1$ and $[C_9^{l\bar{l}}]_H^2$ with $Y^2 = \cot^2\beta$ are given in table 9.2. The x- and y-derivatives derive from top quark mass renormalisation on the full side. The function $t_H^{(1)}$ ($t_H^{(2)}$) deriving from one- (two-)loop Z-penguins as well as the function $k_{t,1}^{(1)}$ ($k_{t,2}^{(2)}$) deriving from one- (two-)loop self energy diagrams are given as follows:

$$\begin{aligned}
t_H^{(1)} &= \tfrac{x}{y}Y^2\left[\tfrac{\left(-3+2{s_W}^2\right)y}{12c_W\epsilon s_W} - \tfrac{y\left(3-2{s_W}^2+8{s_W}^2y-3y^2-6{s_W}^2y^2+12y\ln(y)-6y^2\ln(y)+4{s_W}^2y^2\ln(y)\right)}{24c_W s_W(-1+y)^2}\right. \\
&+ \left.\epsilon\left(\tfrac{y\left(3(1+y)+2{s_W}^2(-1+7y)\right)}{48c_W s_W(-1+y)} - \tfrac{\left(1+2{s_W}^2\right)y^3\ln(y)}{8c_W s_W(-1+y)^2} + \tfrac{y^2\left(6+\left(-3+2{s_W}^2\right)y\right)\ln(y)^2}{24c_W s_W(-1+y)^2}\right)\right], \\
k_{t,H}^{(1)} &= \tfrac{x}{y}Y^2\left[\tfrac{1}{\epsilon}\,\tfrac{y}{2} - \tfrac{y\left(-1+4y-3y^2+2y^2\ln(y)\right)}{4(-1+y)^2} + \epsilon\,\tfrac{y\left(1-8y+7y^2-6y^2\ln(y)+2y^2\ln(y)^2\right)}{8(-1+y)^2}\right], \\
t_H^{(2)} &= \tfrac{x}{y}Y^2\left[\tfrac{1}{\epsilon^2}\tfrac{\left(-3+2{s_W}^2\right)y}{3c_W s_W}\right. \\
&+ \tfrac{1}{\epsilon}\left(\tfrac{y\left(-3+2{s_W}^2-66y-28{s_W}^2y+33y^2+2{s_W}^2y^2\right)}{9c_W s_W(-1+y)^2} - \tfrac{2y^2\left(-12+9y-6{s_W}^2y-3y^2+2{s_W}^2y^2\right)\ln(y)}{3c_W s_W(-1+y)^3}\right) \\
&- \tfrac{2y^2\left(15-6{s_W}^2-81y-30{s_W}^2y+33y^2+2{s_W}^2y^2\right)\ln(y)}{9c_W s_W(-1+y)^3} \\
&+ \tfrac{y\left(-3+2{s_W}^2-27y-6{s_W}^2y+18y^2-12{s_W}^2y^2-6y^3+4{s_W}^2y^3\right)\ln(y)^2}{3c_W s_W(-1+y)^3} \\
&+ \left.\tfrac{y\left(2{s_W}^2\left(5-84y+11y^2\right)+3\left(-5-60y+21y^2\right)+12\left(3+6y-6y^2+{s_W}^2(-2+4y)\right)\mathrm{Li}_2(\frac{-1+y}{y})\right)}{18c_W s_W(-1+y)^2}\right],
\end{aligned}$$

$$k_{t,H}^{(2)} = \frac{x}{y}Y^2\left[\frac{2y}{\epsilon^2} - \frac{2\left(y-15y^2+15y^3-y^4-18y^3\ln(y)+6y^4\ln(y)\right)}{3\epsilon(-1+y)^3}\right.$$
$$\left. + \frac{y\left(-5+89y-95y^2+11y^3-4y\left(-3-15y+y^2\right)\ln(y)+6\left(1-3y-6y^2+2y^3\right)\ln(y)^2+12\left(1-3y+2y^2\right)\mathrm{Li}_2(\frac{-1+y}{y})\right)}{3(-1+y)^3}\right]. \quad (8.22)$$

8.4 $C_{9,H}$ and $C_{10,H}$ in the Pole Mass Scheme

In this section we illustrate the dependence on the chosen renormalization scheme (pole mass versus $\overline{\rm MS}$-scheme) on the THDM-contributions to C_9 and C_{10} [19]. The relation between the mass definitions in the $\overline{\rm MS}$- and pole mass scheme is given by

$$\overline{m}_t(\mu_W) = m_t^{\rm pole}\left(1 + \frac{2\alpha_S(\mu_W)}{\pi}\ln\frac{m_t^{\rm pole}}{\mu_W} - \frac{4}{3}\frac{\alpha_S(\mu_W)}{\pi}\right) + \mathcal{O}(\alpha_s^2), \quad (8.23)$$

where $\overline{m}_t(\mu_W)$ and $m_t^{\rm pole}$ are the top quark mass in the $\overline{\rm MS}$-scheme and pole mass scheme, respectively.

All one-loop contributions $[X^0]$ depend only via x (SM) resp. x and y (THDM) on the chosen renormalization scheme for the top mass. The corresponding contributions in the pole mass scheme can thus be simply obtained by replacing the top mass in the $\overline{\rm MS}$ scheme by the top mass in the pole scheme in the definitions of x and y in eq. (9.1). The two-loop contributions depend explicitly on the top-mass and thus gain additional new terms by changing the renormalization scheme. In the pole mass scheme we get

$$[C_9^{l\bar{l}}]_H^{1,\rm pole} = = [C_9^{l\bar{l}}]_H^1 - Y^2\left(L_t + \frac{4}{3}\right)T_\Gamma, \quad (8.24)$$
$$[D_9]_H^{1,\rm pole} = = [D_9]_H^1 - Y^2\left(L_t + \frac{4}{3}\right)T_Z, \quad (8.25)$$

where

$$T_\Gamma = \frac{4\left(31-59y+31y^2+9y^3\right)y}{27(y-1)^4} - \frac{16\left(1-3y^2+3y^3\right)y}{9(y-1)^5}\ln y, \quad (8.26)$$
$$T_Z = \frac{(3-4y+y^2)xy}{(y-1)^3} + \frac{2xy}{(y-1)^3}\ln y, \quad (8.27)$$

$$x = \left(\frac{m_t^{\rm pole}}{M_W}\right)^2, \qquad y = \left(\frac{m_t^{\rm pole}}{M_H}\right)^2, \qquad L_t = \ln\frac{\mu_W^2}{(m_t^{\rm pole})^2}. \quad (8.28)$$

Note that in $[C_9^{l\bar{l}}]_H^1$ and $[D_9^{l\bar{l}}]_H^1$ of eq. (8.24-8.25) the pole mass expressions for x and y have to be used.

8.5 Impact of the Two-Loop Contributions on $C_{10,\mathrm{H}}$

In this section we briefly illustrate the impact of the two-loop correction on $C_{10,\mathrm{H}}(\mu)^{(n)}$, the THDM contribution to the full Wilson-Coefficients $C_{10}(\mu)$. We introduce a rescaled Wilson coefficient (see eq. (5.9))

$$\begin{aligned}\hat{C}_{10,\mathrm{H}}(\mu_W) &\doteq \frac{1}{Y^2}\frac{4\pi}{\alpha_s(\mu_W)}C_{10,\mathrm{H}}(\mu_W) \\ &= \frac{1}{Y^2}\left(C^{(1)}_{10,\mathrm{H}}(\mu_W) + \frac{\alpha_s(\mu_W)}{4\pi}C^{(2)}_{10,\mathrm{H}}(\mu_W)\right) + \mathcal{O}(\alpha_s^2), \end{aligned} \tag{8.29}$$

where $Y^2 = \cot^2\beta$ both in type-I and type-II THDM models (see eq. (3.8)). In fig. 8.2 we plot the quantities

$$\frac{1}{Y^2}C^{(1)}_{10,\mathrm{H}}(\mu_W) \quad \text{and} \quad \frac{1}{Y^2}\left(C^{(1)}_{10,\mathrm{H}}(\mu_W) + \frac{\alpha_s(\mu_W)}{4\pi}C^{(2)}_{10,\mathrm{H}}(\mu_W)\right), \tag{8.30}$$

i.e. two approximations of $\hat{C}_{10,\mathrm{H}}$ as a function of the charged Higgs boson mass M_H for the $\overline{\mathrm{MS}}$- and for the pole mass scheme of the t-quark mass. As input parameters we use $\alpha_s(M_Z) = 0.119$, $m_t^{\mathrm{pole}} = 178.0$ GeV, $M_W = 80.4$ GeV and $s_W^2 = 0.231$ [31, 62]. The upper frame shows these quantities at the relatively low matching scale $\mu_W = M_W$. In this case m_t^{pole} and $\overline{m}_t(\mu_W)$ are numerically almost identical, the one-loop approximations (dotted and dashed lines) are close to each other. The inclusion of the two-loop corrections, however, considerably lowers the (absolute) size of the coefficient for all considered values of M_H. In the lower frame a higher matching scale of $\mu_W = 300$ GeV is chosen. As in this case m_t^{pole} and $\overline{m}_t(\mu_W)$ differ considerably, the renormalization scheme dependence of the one-loop results is rather large. When taking into account the two-loop corrections (solid and dash-dotted lines), the scheme dependence is drastically reduced.

Looking at the renormalization group equation (RGE) [63] for $\hat{C}_{10,\mathrm{H}}$, one finds that $\hat{C}_{10,\mathrm{H}}$ does not run, i.e.

$$\hat{C}_{10,\mathrm{H}}(\mu_b) = \hat{C}_{10,\mathrm{H}}(\mu_W), \tag{8.31}$$

where the low scale μ_b is of the order of m_b. In fig. 8.3 we show the dependence of $\hat{C}_{10,\mathrm{H}}(\mu_b)$ on the matching scale μ_W for $M_H = 300$ GeV (upper frame) and $M_H = 600$ GeV (lower frame). It can be clearly seen that the inclusion of the two-loop contributions drastically lowers the dependence on μ_W for both chosen Higgs masses. For both masses $\hat{C}_{10,\mathrm{H}}(\mu_b)$ at two-loop precision is nearly μ_W-independent for $\mu_W > 250$ GeV. For μ_W between M_W and 250 GeV the two-loop Wilson coefficient varies about $\pm 4\%$ for a Higgs mass of 300 GeV ($\pm 6\%$ for a Higgs mass of 600 GeV), whereas the corresponding one-loop coefficient varies about $\pm 11\%$ ($\pm 12\%$).

Finally we illustrate the dependence of the Wilson coefficient $C_{10,\mathrm{H}}(\mu_b)$ on the coupling constant $Y^2 = \cot^2\beta$. In fig. 8.4 we plot the relation between the SM contributions and the sum of SM and THDM contributions to C_{10}. We have chosen a matching scale of $\mu_W = M_W$ and a Higgs mass of 300 GeV and varied $Y^2 = \cot^2\beta$ between 1/100 and 1 corresponding to $\tan\beta$ values between 1 and 10. We neglect contributions from up quarks and use the unitarity of the CKM-matrix (eq. (2.23)) The inclusion of the

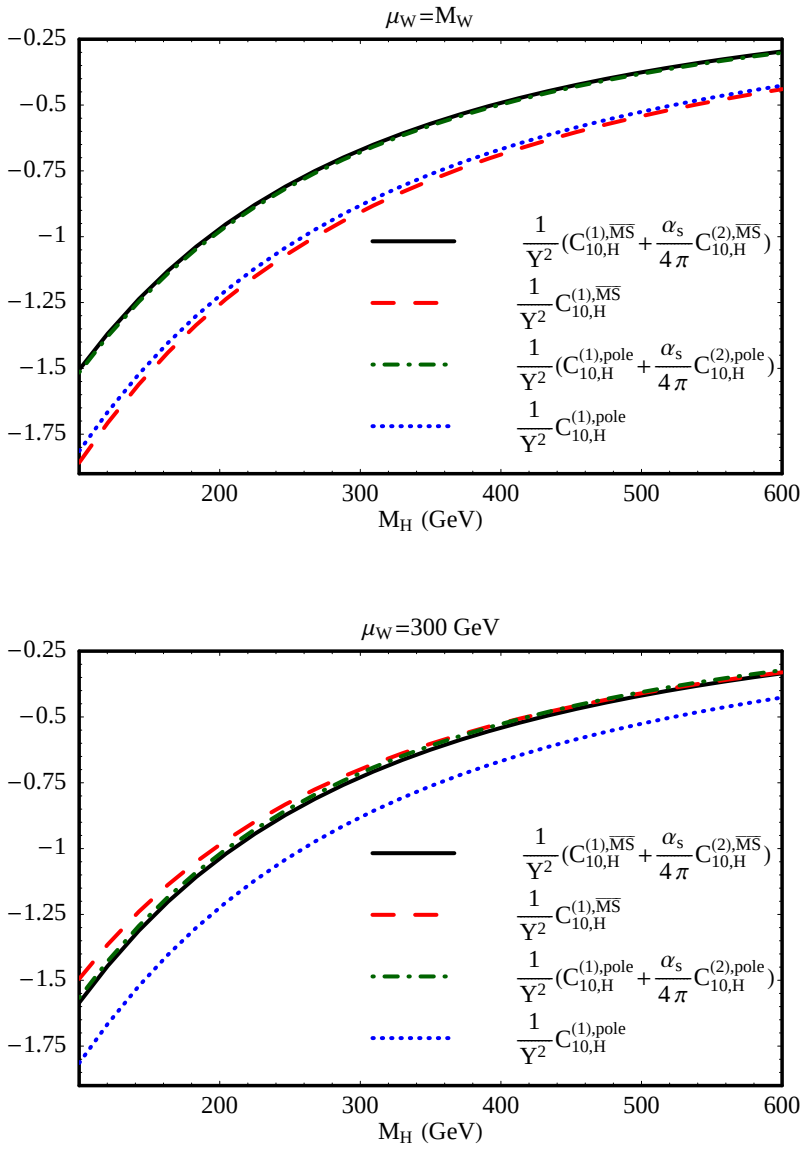

Figure 8.2: Dependence of the rescaled Wilson coefficient $\hat{C}_{10,\mathrm{H}}(\mu_W)$ (see eq. (8.29)) on the charged Higgs boson mass M_H at the matching scale $\mu_W = M_W$ (upper frame) and $\mu_W = 300$ GeV (lower frame). The dashed (dotted) line is the one-loop contribution expressed in $\overline{\mathrm{MS}}$ scheme (pole mass scheme) of the t-quark mass, while the solid (dash-dotted) line includes the two-loop corrections in the respective scheme.

THDM contribution lowers the value of $C_{10}(\mu_b)$, the higher the chosen value of Y^2 is, the stronger is this effect. For a value of $\cot\beta = \tan\beta = 1$ the Wilson coefficient gets lowered by 15 % by the inclusion of the THDM contributions (considering only one-loop contributions the Wilson coefficients gets lowered by 19 %).

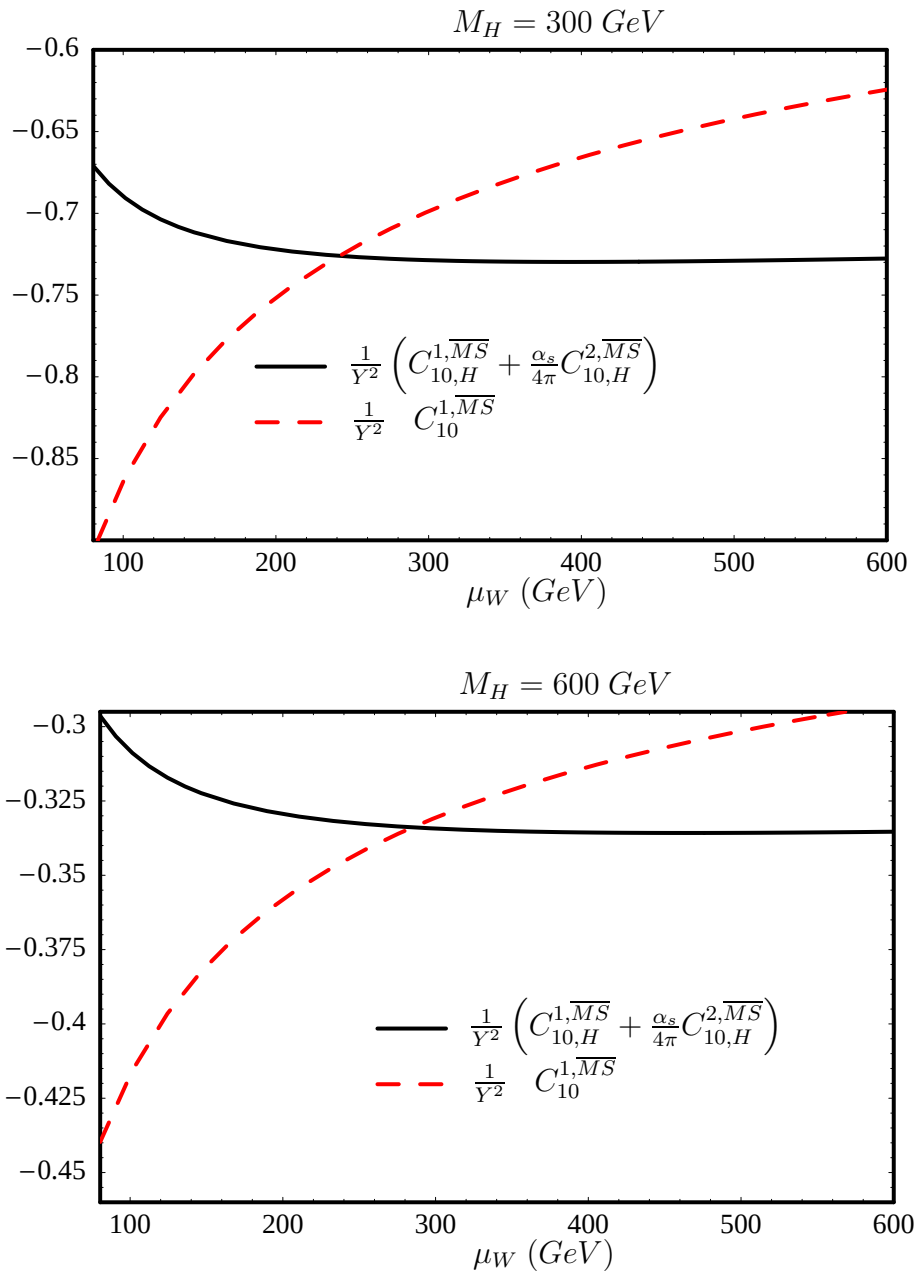

Figure 8.3: Dependence of the rescaled Wilson coefficient $\hat{C}_{10,\mathrm{H}}(\mu_b)$ on the matching scale μ_W (see eq. (8.29)) for $M_H = 300$ GeV (upper frame) and $M_H = 600$ GeV (lower frame). The dashed line shows the one-loop contribution expressed in $\overline{\mathrm{MS}}$ scheme for the t-quark mass, while the solid line includes the two-loop corrections in the same scheme.

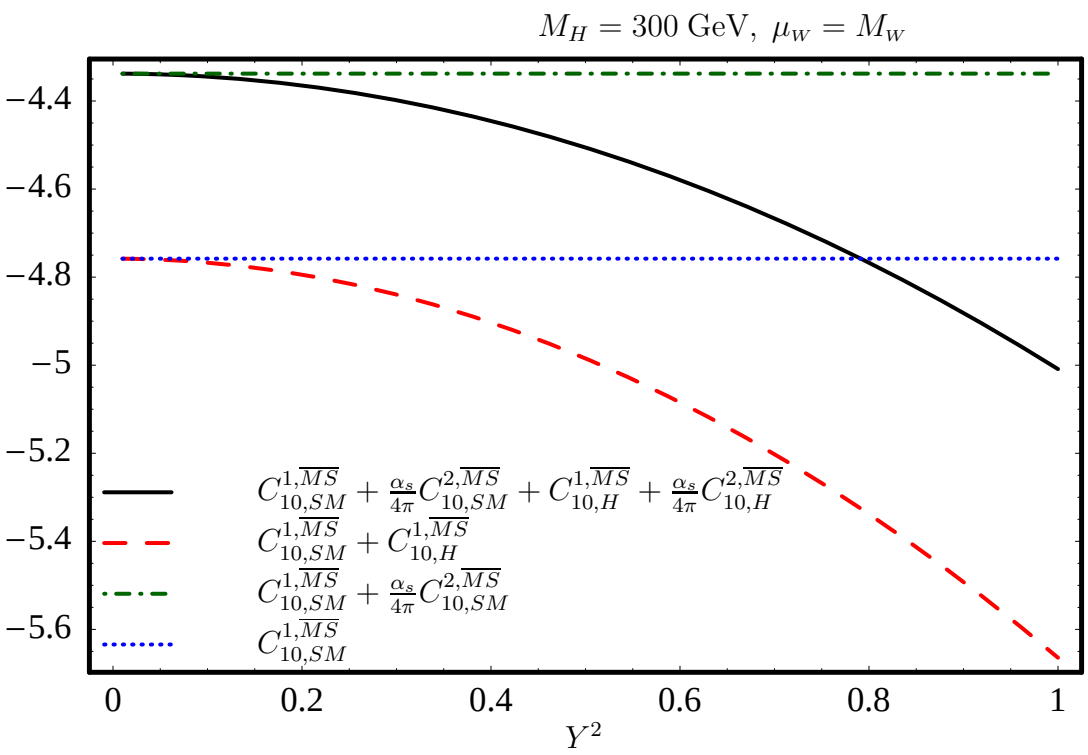

Figure 8.4: Dependence of the Wilson coefficient $C_{10,\mathrm{H}}(\mu_b)$ on the coupling constant $Y^2 = \cot^2\beta$. The solid line includes one - and two-loop contributions from the SM and the THDM, whereas the dashed lines includes only one-loop contributions from both the SM and the THDM. The dashed-dotted line shows the one-loop and two-loop contribution from the SM, whereas the dotted line shows only SM one-loop contributions.

Chapter 9

Wilson Coefficients

In chapters 6-8 we derived all necessary pieces to calculate the Wilson coefficients $C_7(\mu_W)$, $C_9(\mu_W)$ and $C_{10}(\mu_W)$ in the SM and THDM up to $\mathcal{O}(\alpha_s)$-precision. The $\mathcal{O}(\alpha_s)$-corrections are important ingredients for next-to-next-to-leading logarithmic predictions of various observables related to the decays $\bar{B} \to X_s l^+ l^-$ in these models. But these observables do not only depend on the Wilson coefficients $C_7(\mu_b), C_9(\mu_b)$ and $C_{10}(\mu_b)$ at the low-energy scale $\mu_b \backsim m_b$, but also on the Wilson coefficients $C_1(\mu_b)$-$C_6(\mu_b)$ as well as $C_8(\mu_b)$[1]. Therefore we will display in this chapter all relevant matching results for $\bar{B} \to X_s l\bar{l}$ in the SM and the THDM.

Most of Wilson coefficients given below have been approved by myself with the help of the program routines *Fermions* and *Integrals* described in appendix A. The rederivation of already published results was used to check thoroughly the written software and to get a deeper insight in the complicated calculation of two-loop contributions to Wilson Coefficients. We confirmed in all cases the published values. In section 9.3 we list explicitly all (re)derived results.

Before giving the Wilson coefficients we want to summarise the used abbreviations:

$$x = \left(\frac{m_t^{\overline{\rm MS}}(\mu_W)}{M_W}\right)^2, \qquad y = \left(\frac{m_t^{\overline{\rm MS}}(\mu_W)}{M_H}\right)^2, \tag{9.1}$$

$$L_t = \ln\frac{\mu_W^2}{m_t^{\overline{\rm MS}}}, \qquad L = \ln\frac{\mu_W^2}{m_W^2}, \qquad s_W = \sin\theta_W. \tag{9.2}$$

In these equations $m_t^{\overline{\rm MS}}$ denotes the top quark mass in the $\overline{\rm MS}$ scheme, M_W the W boson mass and M_H the charged Higgs mass. The integral representations for the functions $\mathrm{Li}_2(z)$ and $\mathrm{Cl}_2(x)$ are given in section A.13.2.

The calculation was performed in the background field formalism [30] in the t'Hooft-Feynman gauge. It allowed us to perform the matching without making use of the CKM-matrix unitarity (see eq. (2.23)). The usage of the unitarity would remove any CP-violating effects from the Hamiltonian (see also eq. (2.23)).

[1]The Wilson coefficients at the low energy scale can be obtained from the Wilson coefficients at the matching scale $\mu_W \backsim M_W$ by solving the Renormalization Group equation (RGE) [42].

9.1 Charm Sector

9.1.1 Charm Sector in the SM

The one- and two-loop matching conditions for diagrams in the charm sector can be summarized as follows [50]:

$$
\begin{aligned}
C_1^{c(1)} &= -15-6L, & C_1^{c(2)} &= T(x)-\tfrac{7987}{72}-\tfrac{17}{3}\pi^2-\tfrac{475}{6}L-17L^2,\\
C_2^{c(1)} &= 0, & C_2^{c(2)} &= -\tfrac{127}{18}-\tfrac{4}{3}\pi^2-\tfrac{46}{3}L-4L^2,\\
C_3^{c(1)} &= 0, & C_3^{c(2)} &= \tfrac{680}{243}+\tfrac{20}{81}\pi^2+\tfrac{68}{81}L+\tfrac{20}{27}L^2,\\
C_4^{c(1)} &= \tfrac{7}{9}-\tfrac{2}{3}L, & C_4^{c(2)} &= -\tfrac{950}{243}-\tfrac{10}{81}\pi^2-\tfrac{124}{27}L-\tfrac{10}{27}L^2,\\
C_5^{c(1)} &= 0, & C_5^{c(2)} &= -\tfrac{68}{243}-\tfrac{2}{81}\pi^2-\tfrac{14}{81}L-\tfrac{2}{27}L^2,\\
C_6^{c(1)} &= 0, & C_6^{c(2)} &= -\tfrac{85}{162}-\tfrac{5}{108}\pi^2-\tfrac{35}{108}L-\tfrac{5}{36}L^2,\\
C_7^{c(1)} &= \tfrac{23}{36}, & C_7^{c(2)} &= -\tfrac{713}{243}-\tfrac{4}{81}L,\\
C_8^{c(1)} &= \tfrac{1}{3}, & C_8^{c(2)} &= -\tfrac{91}{324}+\tfrac{4}{27}L,\\
C_9^{c(1)} &= -\tfrac{1}{s_w^2}[B_9^{l\bar{l}}]_c^0+[D_9]_c^0 & C_9^{c(2)} &= -\tfrac{1}{s_w^2}[B_9^{l\bar{l}}]_c^1+[D_9]_c^1 b\\
&= -\tfrac{1}{4s_W^2}-\tfrac{38}{27}+\tfrac{4}{9}L, & &= -\tfrac{1}{s_W^2}-\tfrac{524}{729}+\tfrac{128}{243}\pi^2+\tfrac{16}{3}L+\tfrac{128}{81}L^2,\\
C_{10}^{c(1)} &= \tfrac{1}{s_w^2}[B_9^{l\bar{l}}]_c^0, & C_{10}^{c(2)} &= \tfrac{1}{s_w^2}[B_9^{l\bar{l}}]_c^1\\
&= \tfrac{1}{4s_W^2}, & &= \tfrac{1}{s_W^2},
\end{aligned}
$$

where

$$
\begin{aligned}
T(x) &= -(16x+8)\sqrt{4x-1}\,Cl_2\left(2\arcsin\frac{1}{2\sqrt{x}}\right)+\left(16x+\frac{20}{3}\right)\ln x+32x+\frac{112}{9},\\
[B_9^{l\bar{l}}]_c^0 &= \frac{1}{4},\\
[B_9^{l\bar{l}}]_c^1 &= 1,\\
[D_9]_c^0 &= -\frac{38}{27}+\frac{4}{9}L,\\
[D_9]_c^1 &= \frac{524}{729}+\frac{128}{243}\pi^2+\frac{16}{3}L+\frac{128}{81}L^2.
\end{aligned}
\tag{9.3}
$$

9.1.2 Charm Sector in the THDM

Due to the Yukawa-coupling of the charged Higgs to the charm quark, the charm contributions come with a relative suppression factor $\frac{m_c m_b}{m_t^2}$ or $\frac{m_c^2}{m_t^2}$. They induce only dimension 8 operators which are neglected in our treatment.

9.2 Top Sector

The one-loop and two-loop matching conditions in the top sector are

$$
\begin{aligned}
C_3^{t(1)} &= 0, & C_3^{t(2)} &= [G_3]^1, \\
C_4^{t(n)} &= [E_4]^{(n-1)}, & & \\
C_5^{t(1)} &= 0, & C_5^{t(2)} &= -\frac{1}{10}[G_3]^1 + \frac{2}{15}[E_4]^0, \\
C_6^{t(1)} &= 0, & C_6^{t(2)} &= -\frac{3}{16}[G_3]^1 + \frac{1}{4}[E_4]^0, \\
C_7^{t(n)} &= [A_7]^{(n-1)}, & & \\
C_8^{t(n)} &= -\frac{1}{2}[F_8]^{(n-1)}, & & \\
C_9^{t(n)} &= \frac{1-4s_W^2}{s_W^2}[C_9^{l\bar{l}}]^{(n-1)} - \frac{1}{s_W^2}[B_9^{l\bar{l}}]^{(n-1)} + [D_9]^{(n-1)}, & & \\
C_{10}^{t(n)} &= \frac{1}{s_W^2}([B_{10}^{l\bar{l}}]^{(n-1)} - [C_9^{l\bar{l}}]^{(n-1)}). & & (9.4)
\end{aligned}
$$

The various functions $[X]^n$ in (9.4) indicate their origin when matching the $b \to s+$(light particles) Greens functions of the full and effective theory:

$[A]$: on-shell part of 1PI $b \to s\,\gamma$ (see fig. 9.1),

$[B^{l\bar{l}}]$: $b \to s l^+ l^-$ mediated by box-diagrams(see fig. 9.2),

$[C^{l\bar{l}}]$: $b \to s l^+ l^-$ mediated by Z^0 penguin diagrams (see fig. 9.1) ,

$[D]$: off-shell part of 1PI $b \to s\,\gamma$, contributing to $b \to s l^+ l^-$ (see fig. 9.1),

$[E]$: off-shell part of 1PI $b \to sg$, contributing to $b \to sq\bar{q}$ (see fig. 6.3),

$[F]$: on-shell part of 1PI $b \to sg$ (see fig. 6.3),

$[G]$: 1PI two-loop diagrams $b \to sq\bar{q}$.

The index n corresponds to the number of loops in the diagrams which can be classified into tree-level ($n = 0$), NLO ($n = 1$) and NNLO ($n = 2$) contributions (see also chapter 6). Furthermore each function $[X]^n$ receives contributions from different virtual particle exchange

$$[X]^n = \sum_{i=\{W,H\}} [X]_i^n. \tag{9.5}$$

The index i corresponds to

$i = W$: "top quark – W boson"and "top quark – Would-be-Goldstone-boson" SM-loop-contributions,

$i = H$: "top quark – charged Higgs boson" THDM-loop-contributions in type-II THDM models

receiving virtual gluon corrections at NNLO. Discarding the contributions H in the sum of (9.5) one recovers the SM results. Besides different conventions for $[A_7]$ and $[D_9]$ we followed the conventions given in [64]:

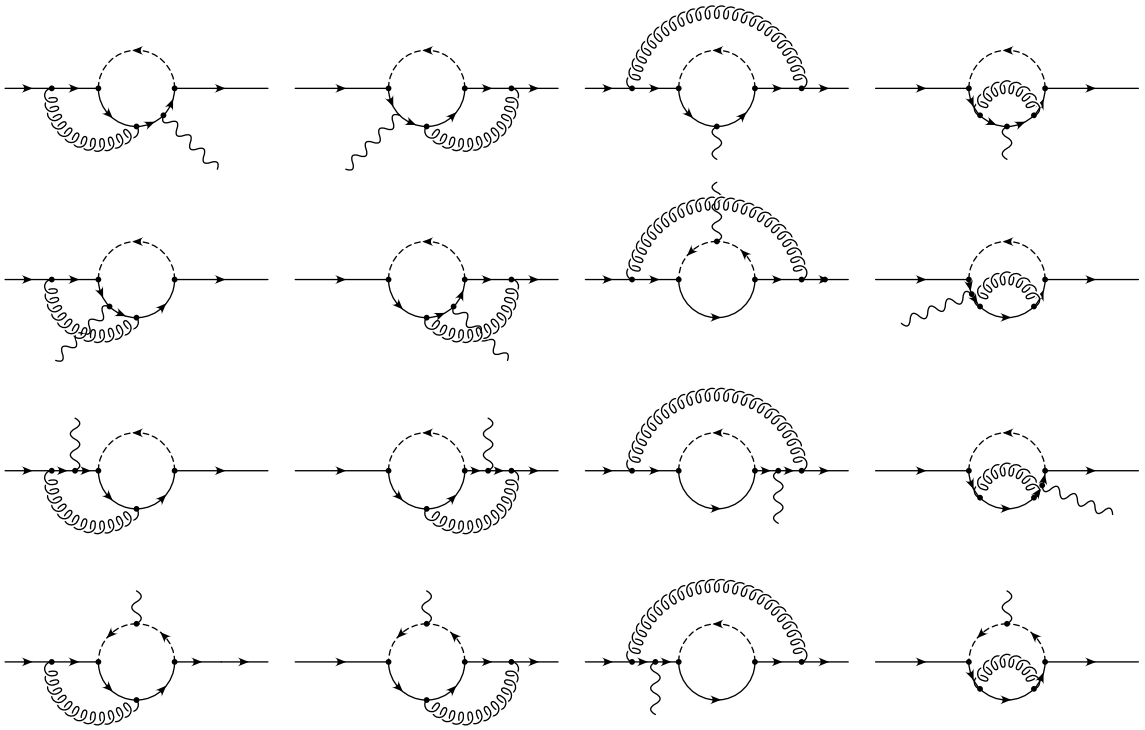

Figure 9.1: 1PI two-loop contributions to the functions $[A_7]_i^1, [C_9^{l\bar{l}}]_i^1, [D_9]_i^1$ $(i = W, H)$ The external solid quark lines solid denote the incoming b-quark and the outgoing s-quark, while the wavy line denotes a virtual photon or a Z^0-boson (gluon). The off-shell part of this contributions decays to a l^+l^--pair. The internal dashed lines denote the $W^\pm/\pi^\pm$ (SM) and $H^\pm$ (THDM)-contributions, the solid lines the u, c, t-quark and the curly line the gluon, respectively. The one-loop contributions can be obtained by removing the gluon line.

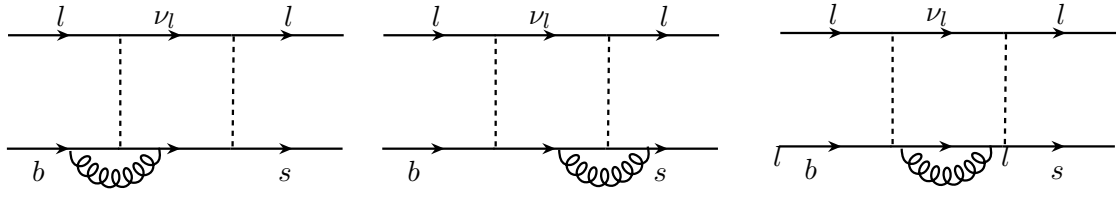

Figure 9.2: 1PI two-loop contributions to the functions $[B_9^{l\bar{l}}]_i^1$ $(i = W, H)$ The internal dashed lines denote the $W^\pm$ and/or $\pi^\pm$, the solid lines the u, c, t-quark and the curly line the gluon, respectively. The one-loop contributions can be obtained by removing the gluon line.

9.2.1 Top Sector in the SM

The evaluation of Feynman diagrams contributing to $b \to s+$(light particles) Greens functions within the SM mediated by "top quark - W boson" loops yields the functions

denoted by the index $i = W$ in (9.5). The explicit form is summarized in table 9.1 [50]. The one-loop contributions $[X]^0_W$ were calculated in [57, 65–67].

Contributions deriving from W-boson two-loop diagrams $[X]^1_W$ have been first calculated in the following papers: $[A_7]^1_W$ and $[F_8]^1_W$ in [14, 18, 68–71], $[B_9^{l\bar{l}}]^1_W$ and $[C_9^{l\bar{l}}]^1_W$ in [56, 58, 72, 73] and $[D_9]^1_W$, $[E_4]^1_W$ and $[G_3]^1_W$ in [42].

9.2.2 Top Sector in the THDM

Top Sector in the THDM of type II

The evaluation of Feynman diagrams contributing to $b \to s+$(light particles) Greens functions within the THDM of type II mediated by "top quark - charged Higgs boson" loops and denoted by the index $i = H$ in (9.5) yields the contributions summarised in table 9.2 [64]. The one-loop contributions to charged Higgs bosons $[X]^0_H$ were before calculated in [61, 74] The contributions from charged Higgs boson $[X]^1_H$ have been calculated by various groups:

- The on-shell part of 1PI $b \to s\ \gamma$ leading to $[A_7]^1_H$ and the on-shell part of 1PI $b \to s\ g$ leading to $[F_8]^1_H$ have been calculated in [14–18].

- $[C_9^{l\bar{l}}]^1_H$ originating from $b \to s l^+ l^-$ mediated by Z penguin diagrams has been first published in [59] and has been published by myself and the Bern group in [19].

- The function $[D_9]^1_H$ arising from the off-shell part of 1PI $b \to s\ \gamma$ contributing to $b \to l^+ l^-$ have been calculated independently by two groups: the Bern group (C. Greub, N. Salzmann and B. Toedtli) and myself. They have been first published in [19]. The same results have been obtained in the PhD thesis of Christoph Bobeth [60] and have been published in [64].

- The results for the functions $[E_4]^1_H$ and $[G_3]^1_H$ have been first published in [64]. Note that contributions deriving from the box diagrams ($[B_9^{l\bar{l}}]^1_H$ and $[B_{10}^{l\bar{l}}]^1_H$) vanish due to the approximation of vanishing lepton masses.

It should be mentioned that the THDM-contributions to C_9 and C_{10} do not depend on X, but are proportional to Y^2. As $Y^2 = \cot\beta$ both in type-I and type-II these contributions do not change by going from type-II to type-I models, thus $[D_9]^{0,1}_H$ and $[C_9]^{0,1}_H$ given in table 9.2 have exactly the same form in type-I models.

9.3 List of all Derived Wilson Coefficients

The below table gives a complete list of all with the help of the programs *Fermions* and *Integrals* (re)derived top-contributions to Wilson coefficients .

Wilson Coefficient	corresponding functions
$C_4^{t(1)}$	$[E_4]_W^0(x),\ [E_4]_H^0(x)$
$C_7^{t(1)}$	$[A_7]_W^0(x),\ [A_7]_H^0(x)$
$C_8^{t(1)}$	$[F_8]_W^0(x),\ [F_8]_H^0(x)$
$C_9^{t(1)}$	$[B_9]_W^0(x),\ [C_9]_W^0(x),\ [C_9]_H^0(x),\ [D_9]_W^0(x),\ [D_9]_H^0(x)$
$C_{10}^{t(1)}$	$[B_{10}]_W^0(x),\ [C_9]_W^1(x),\ [C_9]_H^1(x)$
$C_7^{t(2)}$	$[A_7]_W^1(x),\ [A_7]_H^1(x)$
$C_9^{t(2)}$	$[B_9]_W^1(x),\ [C_9]_W^1(x),\ [C_9]_H^1(x),\ [D_9]_W^1(x),\ [D_9]_W^1(x)$
$C_{10}^{t(2)}$	$[B_{10}]_W^1(x),\ [C_9]_W^1(x),\ [C_9]_H^1(x)$

In the charm sector the following SM-contributions have been rederived:

$$C_1^{c(1)},\ C_2^{c(1)},\ \ C_4^{c(1)},\ C_7^{c(1)},\ C_7^{c(2)},\ \ C_9^{c(1)},\ C_9^{c(2)},\ \ C_{10}^{c(1)},\ C_{10}^{c(2)}.$$

$$[A_7]^0_W(x) = \frac{3x^3-2x^2}{4(1-x)^4}\ln x + \frac{46-205\,x+312\,x^2-145\,x^3}{72\,(-1+x)^4}, \tag{9.6}$$

$$\begin{aligned}[B_9^{l\bar{l}}]^0_W(x) &= [B_{10}^{l\bar{l}}]^0_W(x)\\ &= \frac{x}{4(1-x)^2}\ln x + \frac{1}{4(1-x)},\end{aligned} \tag{9.7}$$

$$[[C_9^{l\bar{l}}]^0_W(x) = \frac{3x^2+2x}{8(1-x)^2}\ln x + \frac{-x^2+6x}{8(1-x)}, \tag{9.8}$$

$$[D_9]^0_W(x) = \frac{3x^4-30x^3+54x^2-32x+8}{18(1-x)^4}\ln x + \frac{47x^3-237x^2+312x-104}{108(1-x)^3}, \tag{9.9}$$

$$[E_4]^0_W(x) = \frac{-9x^2+16x-4}{6(1-x)^4}\ln x + \frac{-7x^3-21x^2+42x+4}{36(1-x)^3}, \tag{9.10}$$

$$[F_8]^0_W(x) = \frac{3x^2}{2(1-x)^4}\ln x + \frac{5x^3-9x^2+30x-8}{12(1-x)^3}, \tag{9.11}$$

$$\begin{aligned}[A_7]^1_W(x) &= \frac{-16x^4+122x^3+80x^2-8x}{9(1-x)^4}\mathrm{Li}_2\big(1-\tfrac{1}{x}\big) + \frac{372x^4+1413x^3-997x^2+65x-4}{81(1-x)^5}\ln x\\ &\quad - \frac{-94x^4-18665x^3+20682x^2-9113x+2006}{486(1-x)^4}\\ &\quad + \left[\frac{6x^4+46x^3-28x^2}{3(1-x)^5}\ln x + \frac{34x^4+101x^3+402x^2-397x+76}{27(1-x)^4}\right]L_t,\end{aligned} \tag{9.12}$$

$$\begin{aligned}[B_9^{l\bar{l}}]^1_W(x) &= [B_{10}^{l\bar{l}}]^1_W(x)\\ &= \frac{-2x}{(1-x)^2}\mathrm{Li}_2\big(1-\tfrac{1}{x}\big) + \frac{-x^2+17x}{3(1-x)^3}\ln x + \frac{13x+3}{3(1-x)^2} + \left[\frac{2x^2+2x}{(1-x)^3}\ln x + \frac{4x}{(1-x)^2}\right]L_t,\end{aligned} \tag{9.13}$$

$$\begin{aligned}[C_9^{l\bar{l}}]^1_W(x) &= \frac{-x^3-4x}{(1-x)^2}\mathrm{Li}_2\big(1-\tfrac{1}{x}\big) + \frac{3x^3+14x^2+23x}{3(1-x)^3}\ln x + \frac{4x^3+7x^2+29x}{3(1-x)^2}\\ &\quad + \left[\frac{8x^2+2x}{(1-x)^3}\ln x + \frac{x^3+x^2+8x}{(1-x)^2}\right]L_t,\end{aligned} \tag{9.14}$$

$$\begin{aligned}[D_9]^1_W(x) &= -\frac{380x^4-1352x^3+1656x^2-784x+256}{81(1-x)^4}\mathrm{Li}_2\big(1-\tfrac{1}{x}\big) - \frac{304x^4+1716x^3-4644x^2+2768x-720}{81(1-x)^5}\ln x\\ &\quad - \frac{-6175x^4+41608x^3-66723x^2+33106x-7000}{729(1-x)^4}\\ &\quad - \left[\frac{648x^4-720x^3-232x^2-160x+32}{81(1-x)^5}\ln x + \frac{-352x^4+4912x^3-8280x^2+3304x-880}{243(1-x)^4}\right]L_t,\end{aligned} \tag{9.15}$$

$$\begin{aligned}[E_4]^1_W(x) &= \frac{515x^4-614x^3-81x^2-190x+40}{54(1-x)^4}\mathrm{Li}_2\big(1-\tfrac{1}{x}\big) + \frac{-1030x^4+435x^3+1373x^2+1950x-424}{108(1-x)^5}\ln x\\ &\quad + \frac{-29467x^4+45604x^3-30237x^2+66532x-10960}{1944(1-x)^4}\\ &\quad + \left[\frac{-1125x^3+1685x^2+380x-76}{54(1-x)^5}\ln x + \frac{133x^4-2758x^3-2061x^2+11522x-1652}{324(1-x)^4}\right]L_t,\end{aligned} \tag{9.16}$$

$$\begin{aligned}[F_8]^1_W(x) &= \frac{4x^4-40x^3-41x^2-x}{3(1-x)^4}\mathrm{Li}_2\big(1-\tfrac{1}{x}\big) + \frac{-144x^4+3177x^3+3661x^2+250x-32}{108(1-x)^5}\ln x\\ &\quad + \frac{-247x^4+11890x^3+31779x^2-2966x+1016}{648(1-x)^4}\\ &\quad + \left[\frac{17x^3+31x^2}{(1-x)^5}\ln x + \frac{-35x^4+170x^3+447x^2+338x-56}{18(1-x)^4}\right]L_t,\end{aligned} \tag{9.17}$$

$$\begin{aligned}[G_3]^1_W(x) &= \frac{10x^4-100x^3+30x^2+160x-40}{27(1-x)^4}\mathrm{Li}_2\big(1-\tfrac{1}{x}\big) + \frac{30x^3-42x^2-332x+68}{81(1-x)^4}\ln x\\ &\quad + \frac{-6x^3-293x^2+161x+42}{81(1-x)^3} + \left[\frac{90x^2-160x+40}{27(1-x)^4}\ln x + \frac{35x^3+105x^2-210x-20}{81(1-x)^3}\right]L_t,\end{aligned} \tag{9.18}$$

Table 9.1: Top-contributions to SM-Wilson coefficients

$$[A_7]_H^0 = \tfrac{3y^2-2y}{6(y-1)^3}\ln y + \tfrac{-5y^2+3y}{12(y-1)^2} + \cot^2\beta\left\{\tfrac{3y^3-2y^2}{12(y-1)^4}\ln y + \tfrac{-8y^3-5y^2+7y}{72(y-1)^3}\right\}, \tag{9.19}$$

$$[B_9^{l\bar{l}}]_H^0 = [B_9^{l\bar{l}}]_H^1 = [B_{10}^{l\bar{l}}]_H^0 = [B_{10}^{l\bar{l}}]_H^1 = 0, \tag{9.20}$$

$$[C_9^{l\bar{l}}]_H^0 = \tfrac{x}{8y}\cot^2\beta\left\{\tfrac{-y^2}{(y-1)^2}\ln y + \tfrac{y^2}{y-1}\right\}, \tag{9.21}$$

$$[D_9]_H^0 = -\cot^2\beta\left\{\tfrac{-3y^4+6y^2-4y}{18(y-1)^4}\ln y + \tfrac{47y^3-79y^2+38y}{108(y-1)^3}\right\}, \tag{9.22}$$

$$[E_4]_H^0 = \cot^2\beta\left\{\tfrac{3y^2-2y}{6(y-1)^4}\ln y + \tfrac{7y^3-29y^2+16y}{36(y-1)^3}\right\}, \tag{9.23}$$

$$[F_8]_H^0 = \tfrac{y}{(y-1)^3}\ln y + \tfrac{y^2-3y}{2(y-1)^2} + \cot^2\beta\left\{\tfrac{y^2}{2(y-1)^4}\ln y + \tfrac{y^3-5y^2-2y}{12(y-1)^3}\right\}, \tag{9.24}$$

$$\begin{aligned}[A_7]_H^1 = {}& \tfrac{32y^3-112y^2+48y}{9(y-1)^3}\mathrm{Li}_2\Big(1-\tfrac{1}{y}\Big) + \tfrac{14y^3-128y^2+66y}{9(y-1)^4}\ln y + \tfrac{-8y^3+52y^2-28y}{3(y-1)^3} \\ & + \left[\tfrac{-12y^3-56y^2+32y}{9(y-1)^4}\ln y + \tfrac{-16y^3+94y^2-42y}{9(y-1)^3}\right]L_t \\ & + \cot^2\beta\left\{\tfrac{16y^4-74y^3+36y^2}{9(y-1)^4}\mathrm{Li}_2\Big(1-\tfrac{1}{y}\Big) + \tfrac{63y^4-807y^3+463y^2-7y}{81(y-1)^5}\ln y\right. \\ & \left. - \tfrac{1202y^4-7569y^3+5436y^2-797y}{486(y-1)^4} + \left[\tfrac{-6y^4-46y^3+28y^2}{9(y-1)^5}\ln y + \tfrac{-14y^4+135y^3-18y^2-31y}{27(y-1)^4}\right]L_t\right\},\end{aligned} \tag{9.25}$$

$$\begin{aligned}[C_9^{l\bar{l}}]_H^1 = {}& \tfrac{x}{y}\cot^2\beta\left\{\tfrac{-y^3+2y^2}{(y-1)^2}\mathrm{Li}_2\Big(1-\tfrac{1}{y}\Big) + \tfrac{-3y^3+11y^2}{3(y-1)^3}\ln y + \tfrac{4y^3-12y^2}{3(y-1)^2}\right. \\ & \left. + \left[\tfrac{2y^2}{(y-1)^3}\ln y + \tfrac{1y^3-3y^2}{(y-1)^2}\right]L_t\right\},\end{aligned} \tag{9.26}$$

$$\begin{aligned}[D_9]_H^1 = {}& -\cot^2\beta\left\{\tfrac{380y^4-528y^3+72y^2+128y}{81(y-1)^4}\mathrm{Li}_2\Big(1-\tfrac{1}{y}\Big) + \tfrac{596y^4-672y^3+64y^2+204y}{81(y-1)^5}\ln y\right. \\ & + \tfrac{-6175y^4+9138y^3-3927y^2-764y}{729(y-1)^4} \\ & \left. + \left[\tfrac{432y^4-456y^3+40y^2+128y}{81(y-1)^5}\ln y + \tfrac{-352y^4-972y^3+1944y^2-1052y}{243(y-1)^4}\right]L_t\right\},\end{aligned} \tag{9.27}$$

$$\begin{aligned}[E_4]_H^1 = {}& \cot^2\beta\left\{\tfrac{515y^4-906y^3+99y^2+182y}{54(y-1)^4}\mathrm{Li}_2\Big(1-\tfrac{1}{y}\Big) + \tfrac{1030y^4-2763y^3-15y^2+980y}{108(y-1)^5}\ln y\right. \\ & + \tfrac{-29467y^4+68142y^3-6717y^2-18134y}{1944(y-1)^4} \\ & \left. + \left[\tfrac{-375y^3-95y^2+182y}{54(y-1)^5}\ln y + \tfrac{133y^4-108y^3+4023y^2-2320y}{324(y-1)^4}\right]L_t\right\},\end{aligned} \tag{9.28}$$

$$\begin{aligned}[F_8]_H^1 = {}& \tfrac{-17y^3+25y^2-36y}{3(y-1)^3}\mathrm{Li}_2\Big(1-\tfrac{1}{y}\Big) + \tfrac{-34y^3+7y^2-165y}{6(y-1)^4}\ln y + \tfrac{29y^3-44y^2+143y}{4(y-1)^3} \\ & + \left[\tfrac{-34y^2-38y}{3(y-1)^4}\ln y + \tfrac{7y^3-16y^2+81y}{3(y-1)^3}\right]L_t \\ & + \cot^2\beta\left\{\tfrac{-13y^4+17y^3-30y^2}{3(y-1)^4}\mathrm{Li}_2\Big(1-\tfrac{1}{y}\Big) + \tfrac{-468y^4+321y^3-2155y^2-2y}{108(y-1)^5}\ln y\right. \\ & \left. + \tfrac{4451y^4-7650y^3+18153y^2-1130y}{648(y-1)^4} + \left[\tfrac{-17y^3-31y^2}{3(y-1)^5}\ln y + \tfrac{7y^4-18y^3+261y^2+38y}{18(y-1)^4}\right]L_t\right\},\end{aligned} \tag{9.29}$$

$$\begin{aligned}[G_3]_H^1 = {}& \cot^2\beta\left\{\tfrac{10y^4+30y^2-20y}{27(y-1)^4}\mathrm{Li}_2\Big(1-\tfrac{1}{y}\Big) + \tfrac{30y^3-66y^2-56y}{81(y-1)^4}\ln y + \tfrac{6y^3-187y^2+213y}{81(y-1)^3}\right. \\ & \left. + \left[\tfrac{-30y^2+20y}{27(y-1)^4}\ln y + \tfrac{-35y^3+145y^2-80y}{81(y-1)^3}\right]L_t\right\}.\end{aligned} \tag{9.30}$$

Table 9.2: THDM-contributions to Wilson-coefficients

Chapter 10

Cold Dark Matter and the decays $\tilde{\tau} \longrightarrow \tau\ \tilde{a}\ \gamma$ and $\tilde{\tau} \longrightarrow \tau\ \tilde{a}$

WMAP [75] measured the cold dark matter (CDM) density to be

$$0.095 < \Omega_{CDM} h^2 < 0.130. \tag{10.1}$$

The SM offers no suitable particle to describe this density: as the neutrinos are at most hot dark matter, we are obliged to search for CDM candidates beyond the SM. If low energy supersymmetry is realised and R-parity[1] is conserved, than the lightest supersymmetric particle (LSP) is a natural candidate for CDM [76, 77]. The LSP is massive and stable and has to be neutral in order to be a good DM candidate.

In the (C)MSSM the LSP is pretty naturally a neutralino with weak couplings. The most popular LSP candidate is the lightest neutralino χ arising already in the MSSM. It is a mixture $\chi = Z_{11}\widetilde{B} + Z_{12}\widetilde{W}_3 + Z_{13}\widetilde{H}_b^0 + Z_{14}\widetilde{H}_t^0$ of the respective fermionic partners (denoted by a tilde) of the electrically neutral gauge bosons B and W_3, and Higgs bosons H_b and H_u. Its thermal abundance falls relatively often in the right ball park. This scenario is known under the Weakly Interacting Massive Particle (WIMP)-scenario. For low $\tan\beta$ the "bulk" region is already excluded by LEP searches [22,24,25] and not much parameter space is left. An outcome of this situation is a fine tuning of the left parameter space. An alternative is to go even behind the CMSSM and consider another candidate, the axino. It is a very weakly interacting particle which does not belong to the WIMP candidates. In the following two sections we will give a short introduction to the physics of axions and their supersymmetric partner, the axinos.

[1] The general superpotential of MSSM contains terms where the baryon and the lepton numbers are violated. In order to cure this, a new symmetry, called R-parity, where the quantum number is given by

$$R = (-1)^{3(B-L)+2S} \tag{10.2}$$

for a particle with spins S and baryon- and lepton number B and L. This symmetry has a great influence on the phenomenology of the MSSM, since it requires that supersymmetric particles always are produced in pairs. Otherwise this would lead to results in conflict with observation, for instance flavour changing neutral currents. In addition to that, the conservation of R-parity means that the LSP is absolutely stable making it thus a good candidate for cold dark matter [76, 77].

10.1 Axions

Very light neutral (pseudo) scalar bosons which couple to stable matter arise if there is a global symmetry in the theory that is spontaneously broken in the vacuum. If the symmetry is exact, it results in a massless Nambu-Goldstone (NG) boson. If there is a small explicit breaking of the symmetry, either already in the Lagrangian or due to quantum mechanical effects such as anomalies, the would-be Nambu-Goldstone boson acquires a finite mass; then it is called a pseudo-NG boson. Axions (A^0) associated with spontaneously broken Peccei-Quinn symmetry [20,78] are typical examples of such pseudo-NG bosons.

An axion gives a natural solution to the strong CP problem [31]: why the effective θ-parameter in the QCD-Lagrangian

$$\mathcal{L}_{\text{eff}} = \Theta_{eff} \frac{\alpha_s}{8\pi} F^{\mu\nu a} \tilde{F}^a_{\mu\nu} \tag{10.3}$$

is so small:

$$\Theta_{eff} \lesssim 10^{-9}, \tag{10.4}$$

as required by the current limits on the neutron electric dipole moment, even though $\Theta_{eff} \sim \mathcal{O}(1)$ is perfectly allowed by QCD gauge invariance. Θ_{eff} is the effective Θ-parameter after the diagonalisation of the quark masses. $F^{\mu\nu a}$ is the gluon field strength and $\tilde{F}^a_{\mu\nu} = \frac{1}{2}\epsilon_{\mu\nu\rho\sigma}F^{\rho\sigma a}$. An axion is a pseudo-NG boson of a spontaneously broken Peccei-Quinn symmetry, which is an exact symmetry at the classical level, but is broken quantum mechanically due to the triangle anomaly with the gluons. As a result of the triangle anomaly, the axion acquires an effective coupling to gluons

$$\mathcal{L} \;=\; \left(\Theta_{eff} - \frac{\phi_A}{f_A}\right) \frac{\alpha_s}{8\pi} F^{\mu\nu a} \tilde{F}^a_{\mu\nu}, \tag{10.5}$$

where ϕ_A is the axion field. The axion decay constant f_A is often defined with this Lagrangian [79]. The QCD nonperturbative effect induces a potential for $\phi_a = \Theta_{eff} f_A$ cancelling Θ_{eff}, thus solving the strong CP problem. The mass of the the axion is inversely proportional to f_A. It is generated at the QCD transition by instanton's effects [80] and is given by

$$m_a = 6.2 \times 10^{-5} eV \left(\frac{10^{11}\ \text{GeV}}{f_A}\right). \tag{10.6}$$

The original axion model [20, 78] assumes $f_A \sim v$, where $v = (\sqrt{2}G_F)^{-\frac{1}{2}}$ is the scale of electroweak symmetry breaking. It has two Higgs doublets as minimal ingredient. By requiring tree-level flavour conservation the axion mass and this couplings are completely fixed in terms of the parameter $\tan\beta$, the ratio of the vacuum expectation values of two Higgs fields (see section 3). This model is experimentally ruled out [31].

A popular way to save the Peccei-Quinn idea are the so called invisible axion models [21], [81]: The idea is to introduce a new scale $f_A \gg v$ weakening the A^0 coupling and thus avoiding all the existing experimental limits. Two classes of models are discussed in the literature: The KSVZ axion model [21,26] introduces a new heavy quark carrying

Peccei-Quinn charge, while the usual quarks and leptons do not. In the DFSZ or "GUT"- axion model [81, 82] no additional quarks are needed, but two Higgs doublets are required and all quarks and leptons carry Peccei-Quinn charges.
Both type of models contain at least one electroweak singlet scalar boson which acquires an expectation values and breaks Peccei-Quinn symmetry. The invisible axion with a large decay constant $f_A \sim 10^{12}$ GeV was found to be good candidate for the cold dark matter component of the universe. The constraints on the invisible axion from astrophysics are derived from interactions of the axion with either photons, electrons or nucleons. A model independent generic limit for the axion mass is given by $m_A \leq 0.01$ eV [31].

10.2 Axinos

The axino arises as the spin-1/2 superpartner of the axion by extending the MSSM with the Peccei-Quinn mechanism in order to solve the strong CP problem. Depending on the model and the SUSY breaking scheme, the mass of the axino can range between the eV and the GeV scale [83]. The axino is a singlet with respect to the gauge groups of the SM. The axino's interactions are suppressed by the Peccei-Quinn scale $f_a \gtrsim 5 \times 10^9$ GeV and the (reduced) Planck scale [31]. Therefore in the axino LSP case the next-to-lightest supersymmetric particle (NLSP) - which could be a neutralino or a slepton typically has a long lifetime. For axino cold dark matter, an NLSP with a mass of 100 GeV has a lifetime of $\mathcal{O}$ (1 sec) [83]. Because of their extremely weak interaction, the direct detection of axinos seems hopeless.

Likewise, their direct production at colliders is very strongly suppressed. Instead, one expects a large sample of NLSPs from pair production or cascade decays of heavier superparticles provided the NLSP belongs to the MSSM spectrum. These NLSPs will appear as quasi-stable particles which will eventually decay into the axino LSP. A significant fraction of these NLSP decays will take place outside of the detector and thus will escape detection. For the charged slepton NLSP scenario, however, there have been recently proposals which discuss how such NLSPs could be stopped and collected for an analysis of their decays into the LSP. It was found that up to $\mathcal{O}(10^3\text{-}10^4)$ and $\mathcal{O}(10^3\text{-}10^5)$ of charged NLSPs can be trapped per year at the Large Hadron Collider (LHC) and the International Linear Collider (ILC), respectively, by placing 1-10 ktons of massive additional material around planned collider detectors [27, 28, 83]. In the following we assume that the NLSP is a charged slepton. We focus on the case where the $\tilde{\tau}$ is the NLSP. In general the $\tilde{\tau}$ is a linear combination of $\tilde{\tau}_R$ and $\tilde{\tau}_L$, $\tilde{\tau} = \cos\theta_\tau \tilde{\tau}_R + \sin\theta_\tau \tilde{\tau}_L$. For simplicity, we concentrate on a pure right-handed $\tilde{\tau}_R$, which is a good approximation at least for small $\tan\beta$ [83]. Then the neutralino - stau coupling is dominated by the bino coupling. In addition, we assume for simplicity that the lightest neutralino is a pure bino. We will give the relevant interaction Lagrangians (section 10.3) and give the total decay rate of the three body decay $\tilde{\tau}_R \to \tau\ \tilde{a}\ \gamma$ (section 10.5) and of the two-body $\tilde{\tau}_R \to \tau\ \tilde{a}$ (sec. 10.6) in supersymmetric KSVZ models. These decays have previously been considered in [83, 84]. In these papers the decay rate was estimated with the help of an effective Lagrangian integrating out the heavy (s)quarks introduced in supersymmetric KSVZ models. Here a more rigorous approach is performed. We

will calculate the decay rate with the help of the Heavy-Mass-Expansion (HME) [45] (for an introduction to this method see sec. 6.1).

10.3 Superpotential and Lagrangians

In order to calculate the decay rate of $\tilde{\tau_R} \to \tau_R \tilde{a}$ and $\tilde{\tau_R} \to \tau_R \tilde{a} \gamma$ we consider the following superpotential:

$$W = y\ \Phi\ Q_1\ Q_2, \tag{10.7}$$

where Φ, Q_1 and Q_2 are axion and heavy quark multiplets

$$\begin{aligned} Q_1 &= \tilde{Q_1} + \sqrt{2}\ q_1\theta + F_1\theta\theta, & (10.8)\\ Q_2 &= \tilde{Q_2} + \sqrt{2}\ q_2\theta + F_2\theta\theta, & (10.9)\\ \Phi &= \phi\ \ + \sqrt{2}\ \chi\theta\ + F_\phi\theta\theta, & (10.10) \end{aligned}$$

where θ is an anticommuting commutator and F_1, F_2 are auxiliary fields of mass dimension 2, to shorten the notation the indices of the component fields χ, q_1 and q_2 are suppressed. These two-component, complex, anticommuting objects are part of the 4-component fermions defined by [85]

$$\begin{aligned} \tilde{a} &= \begin{pmatrix} \chi_\alpha \\ \chi^{\dagger\,\dot{\alpha}} \end{pmatrix}, \quad \tilde{a} = (\chi^\alpha, \chi^\dagger_{\dot{\alpha}}): \quad \text{axino : Majorana fermion}, & (10.11)\\ Q &= \begin{pmatrix} q_{1\,\alpha} \\ q_2^{\dagger\,\dot{\alpha}} \end{pmatrix}, \quad \overline{Q} = (q_2^\alpha, q_{1\,\dot{\alpha}}^\dagger): \quad \text{heavy quark : Dirac Fermion} & (10.12) \end{aligned}$$

with $\alpha = 1, 2$ and $\dot{\alpha} = 1, 2$ [2].
The expectation value of ϕ is given by

$$\langle\phi\rangle = f_a. \tag{10.13}$$

contributions. As the neutralino-stau coupling is dominated by the bino coupling in the low $\tan\beta$ region the relevant fields are given by

	$\widetilde{a}$	$\tilde{Q}_1$	$\tilde{Q}_2$	Q	B	$\overline{\tilde{B}}$	γ	Z	τ
$U(1)_{em} : Q$	0	e_Q	$-e_Q$	e_Q	0	0	0	0	-1
$U(1)_Y : Y$	0	e_y	$-e_y$	e_y	0	0	0	0	-1

We make the assumption, that the heavy quarks are $SU(2)$-singlets, thus $e_y = e_Q$ in the following. In the supersymmetric limit, heavy (s)quark masses are given by

$$m_{\tilde{Q}_1} = m_{\tilde{Q}_2} = m_{\tilde{Q}} = y\langle\phi\rangle = y f_a. \tag{10.14}$$

[2] A short introduction to the two-component notation is given in appendix F

Here and hereafter, we take y and $\langle\phi\rangle = f_a$ to be real by field redefinitions.
The interaction Lagrangians are given by [86]

$$
\begin{aligned}
i\mathcal{L}_{\tilde{a}Q\tilde{Q}_1} &= -i\, y\, \overline{Q}\, P_L\, \widetilde{a}\, \cdot\, \tilde{Q}_1 - i\, y\, \overline{\widetilde{a}}\, P_R\, Q \cdot\, \tilde{Q}_1^\star, && (10.15)\\
i\mathcal{L}_{\tilde{a}Q\tilde{Q}_2} &= -i\, y\, \overline{Q}\, P_R\, \widetilde{a} \cdot\, \tilde{Q}_2^\star - i\, y\, \overline{\widetilde{a}}\, P_L\, Q\, \cdot\, \tilde{Q}_2, && (10.16)\\
i\mathcal{L}_{\text{gauge, Z}} &= i\, \frac{e(e_Q s_W)}{c_W}\, Z_\mu \overline{Q}\, \gamma^\mu Q \\
&\quad -\frac{e(e_Q s_W)}{c_W} Z_\mu(\tilde{Q}_1^\star\, \partial^\mu\, \tilde{Q}_1 - \tilde{Q}_1\, \partial^\mu\, \tilde{Q}_1^\star) \\
&\quad -\frac{e(e_Q s_W)}{c_W} Z_\mu(\tilde{Q}_2\, \partial^\mu\, \tilde{Q}_2^\star - \tilde{Q}_2^\star\, \partial^\mu\, \tilde{Q}_2), && (10.17)\\
i\mathcal{L}_{\text{gauge}} &= -i\, e(e_q)\, A_\mu \overline{Q}\, \gamma^\mu Q \\
&\quad +e(e_q) A_\mu(\tilde{Q}_1^\star\, \partial^\mu\, \tilde{Q}_1 - \tilde{Q}_1\, \partial^\mu\, \tilde{Q}_1^\star) \\
&\quad +e(e_q) A_\mu(\tilde{Q}_2\, \partial^\mu\, \tilde{Q}_2^\star - \tilde{Q}_2^\star\, \partial^\mu\, \tilde{Q}_2), && (10.18)\\
& && (10.19)\\
i\mathcal{L}_{Q\tilde{B}\tilde{Q}_1} &= -i\sqrt{2}\frac{e}{c_W} e_Q\, \overline{\tilde{B}}\, P_L\, Q\, \cdot\, \tilde{Q}_1^\star - i\sqrt{2}\frac{e}{c_W} e_Q\, \overline{Q}\, P_R\, \tilde{B}\, \cdot\, \tilde{Q}_1, && (10.20)\\
i\mathcal{L}_{Q\tilde{B}\tilde{Q}_2} &= i\sqrt{2}\frac{e}{c_W} e_Q\, \overline{\tilde{B}}\, P_R\, Q\, \cdot\, \tilde{Q}_2 + i\sqrt{2}\frac{e}{c_W} e_Q\, \overline{Q}\, P_L\, \tilde{B}\, \cdot\, \tilde{Q}_2^\star. && (10.21)
\end{aligned}
$$

From the above Lagrangians we can derive the Feynman rules given in section G.4.3.

10.4 The Bino-Photon-Axino-Loop

In both the two body $\tilde{\tau}_R \to \tau\, \tilde{a}$ and the tree-body decay $\tilde{\tau}_R \to \tau\, \tilde{a}\, \gamma$ the bino-photon-axino-loops given in fig. 10.1 appears. Therefore we will calculate in this section the unintegrated sum of all this four one-loop diagrams. Using the Feynman rules given in section G.4.3 we get for the matrix elements in the supersymmetric limit (eq. (10.14)):

$$
\begin{aligned}
i\mathcal{M}(QQ\tilde{Q}_1) &= i^6\sqrt{2}\, e\, e_Q\, \frac{e}{c_W} e_Q\, y\, \bar{u}_{\tilde{a}}(p)(-P_R) \\
&\quad \left(\int \frac{dq^4}{(2\pi)^4} prop\ (\not{q} + m_Q)(\gamma^\mu)(\not{q} + \not{k} + m_Q)\right)(-P_R) u_{\tilde{\tilde{B}}}(k+p) \cdot \epsilon_\mu^*(k) \\
&= -c_\gamma\, \bar{u}_{\tilde{a}}(p) P_R \left(\int \frac{dq^4}{(2\pi)^4} prop\ (\gamma^\mu \not{k} + 2q^\mu)\right)\, u_{\tilde{\tilde{B}}}(k+p) \cdot \epsilon_\mu^*(k), && (10.22)\\
i\mathcal{M}(QQ\tilde{Q}_2) &= i^6\sqrt{2}\, e\, e_Q\, \frac{e}{c_W} e_Q\, y\, \bar{u}_{\tilde{a}}(p)(-P_L) \\
&\quad \left(\int \frac{dq^4}{(2\pi)^4} prop\ (\not{q} + m_Q)(\gamma^\mu)(\not{q} + \not{k} + m_Q)\right) P_L u_{\tilde{\tilde{B}}}(k+p) \cdot \epsilon_\mu^*(k) \\
&= c_\gamma\, \bar{u}_{\tilde{a}}(p) P_L \left(\int \frac{dq^4}{(2\pi)^4} prop\ (\gamma^\mu \not{k} + 2q^\mu)\right)\, u_{\tilde{\tilde{B}}}(k+p) \cdot \epsilon_\mu^*(k), && (10.23)
\end{aligned}
$$

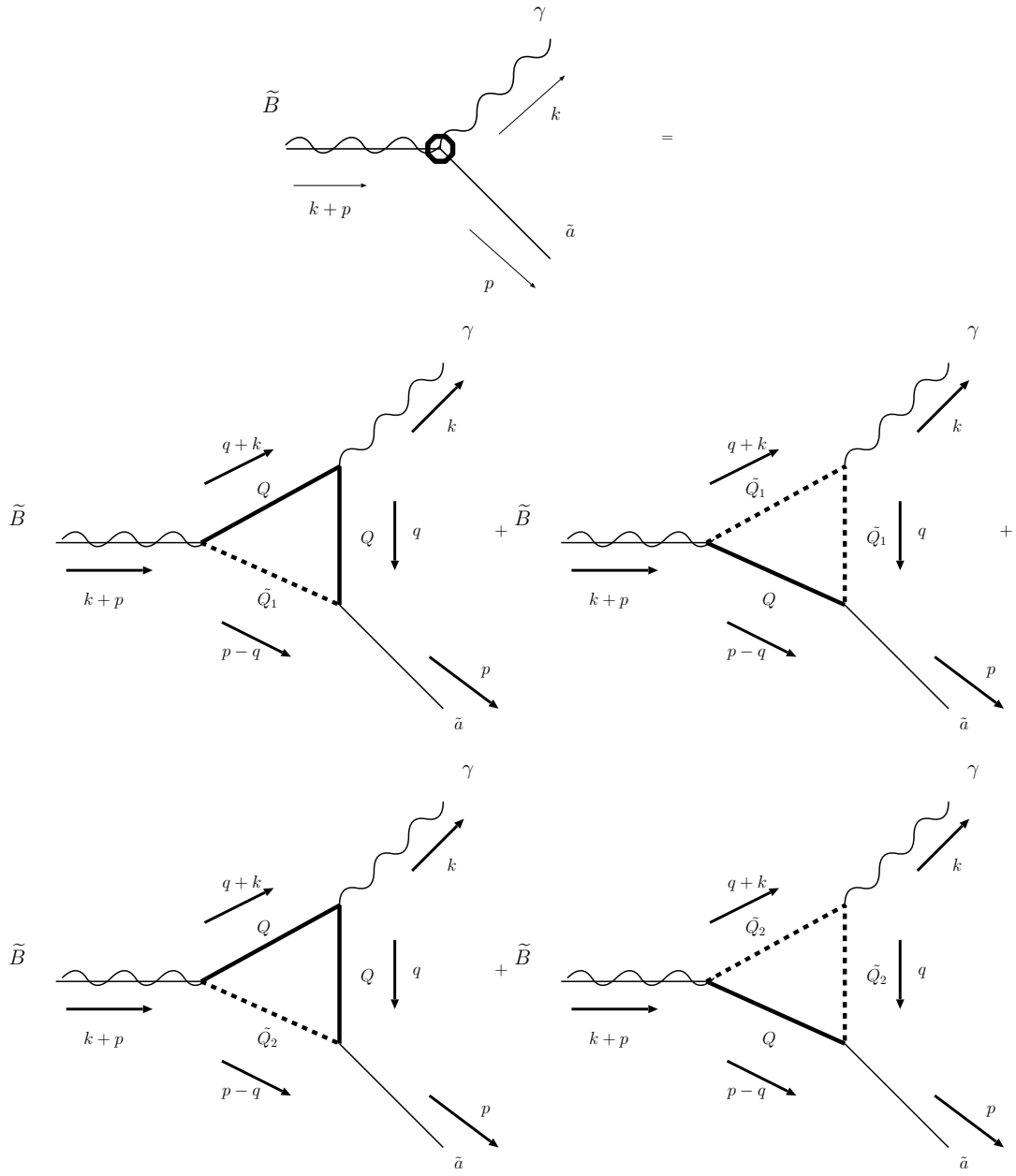

Figure 10.1: The bino-photon-axino loops.

$$
\begin{aligned}
i\mathcal{M}(Q\tilde{Q}_1\tilde{Q}_1) &= i^6\sqrt{2}\ e\ e_Q\ \frac{e}{c_W}e_Q\ y\ \bar{u}_{\tilde{a}}(p) \\
&\quad \left(\int \frac{dq^4}{(2\pi)^4} prop\ (-)(k^\mu + 2q^\mu)\ \ (-P_R)\ (\not{p} - \not{q} + m_Q)\right)(-P_R)\ u_{\tilde{\widetilde{B}}}(k+p)\cdot\epsilon^*_\mu(k) \\
&= c_\gamma \bar{u}_{\tilde{a}}(p) P_R\ u_{\tilde{\widetilde{B}}}(k+p)\cdot\epsilon^*_\mu(k)\ \int \frac{dq^4}{(2\pi)^4} prop\ (k^\mu + 2q^\mu), \qquad (10.24) \\
i\mathcal{M}(Q\tilde{Q}_2\tilde{Q}_2) &= i^6\sqrt{2}\ e\ e_Q\ \frac{e}{c_W}e_Q\ y\ \ \bar{u}_{\tilde{a}}(p) \\
&\quad \int \frac{dq^4}{(2\pi)^4} prop\ (-)(k^\mu + 2q^\mu)\ \ (-P_L)\ (\not{p} - \not{q} + m_Q) P_L\ u_{\tilde{\widetilde{B}}}(k+p)\cdot\epsilon^*_\mu(k) \\
&= -c_\gamma \bar{u}_{\tilde{a}}(p) P_L\ u_{\tilde{\widetilde{B}}}(k+p)\cdot\epsilon^*_\mu(k)\ \int \frac{dq^4}{(2\pi)^4} prop\ (k^\mu + 2q^\mu), \qquad (10.25)
\end{aligned}
$$

where

$$\begin{aligned} c_\gamma &= \sqrt{2}\, m_Q\, e^2\, e_Q^2\, \frac{y}{c_W} \\ prop &= \frac{1}{((q-p)^2-m_Q^2)(q^2-m_Q^2)((q+k)^2-m_Q^2)}. \end{aligned} \tag{10.26}$$

Thus we get for the sum of the diagrams containing two fermion legs

$$i\mathcal{M}(QQ\tilde{Q}_1)+i\mathcal{M}(QQ\tilde{Q}_2) = -c_\gamma\, \bar{u}_{\tilde{a}}(p)\gamma^5 \left(\int \frac{dq^4}{(2\pi)^4} prop\ (\gamma^\mu \not{k} + 2q^\mu)\right)\ u_{\tilde{\tilde{B}}}(k+p)\cdot\epsilon_\mu^*(k). \tag{10.27}$$

The diagrams containing two scalars give

$$i\mathcal{M}(Q\tilde{Q}_1\tilde{Q}_1)+i\mathcal{M}(Q\tilde{Q}_2\tilde{Q}_2) = c_\gamma \bar{u}_{\tilde{a}}(p)\gamma^5\ u_{\tilde{\tilde{B}}}(k+p)\cdot\epsilon_\mu^*(k)\ \int \frac{dq^4}{(2\pi)^4} prop\ (k^\mu + 2q^\mu). \tag{10.28}$$

Then we get for the sum of the four one-loop-diagrams

$$\begin{aligned} i\mathcal{M}_{\text{oneloop}} &= -c_\gamma \bar{u}_{\tilde{a}}(p)\gamma^5\ (\gamma^\mu \not{k} - k^\mu) u_{\tilde{\tilde{B}}}(k+p)\cdot\epsilon_\mu^*(k)\ \int \frac{dq^4}{(2\pi)^4} prop \\ &= -c_\gamma \bar{u}_{\tilde{a}}(p)\gamma^5\ \left(\frac{1}{2}[\gamma^\mu, \not{k}]\right) u_{\tilde{\tilde{B}}}(k+p)\cdot\epsilon_\mu^*(k)\ \int \frac{dq^4}{(2\pi)^4} prop. \end{aligned} \tag{10.29}$$

For the sum of all four one-loop diagrams we obtain

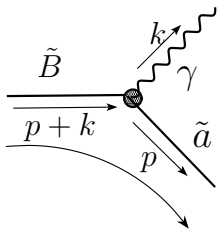

$$-c_\gamma\, \gamma^5\ \left(\frac{1}{2}[\gamma^\mu, \not{k}]\right)\ \int \frac{dq^4}{(2\pi)^4} prop. \tag{10.30}$$

Reverting the fermion flow we obtain with the help of the flip rule (G.6)

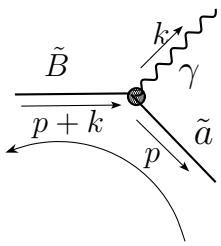

$$c_\gamma\, \gamma^5\ \left(\frac{1}{2}[\gamma^\mu, \not{k}]\right)\ \int \frac{dq^4}{(2\pi)^4} prop. \tag{10.31}$$

In the following sections we will discuss the three body decay $\tilde{\tau}_R \to \tau\ \tilde{a}\ \gamma$, which arises first at one-loop precision and the two body decay $\tilde{\tau}_R \to \tau\ \tilde{a}$ arising first at two-loop precision. Whereas the squared matrix element of the three body decay is of $\mathcal{O}(\alpha_{em}^3)$, the corresponding two body decay is of $\mathcal{O}(\alpha_{em}^4)$. This suppression of the two body decay by $\mathcal{O}(\alpha_{em})$ could be partly compensated by a the bigger phase space of this decay. In the following sections we will give an exact calculation of the three body decay rate, as well as an estimation of the two body decay rate under the assumption that the bino mass is much bigger than the stau mass.

10.5 The Three-Body Decay $\tilde{\tau}_R \to \tau\ \tilde{a}\ \gamma$

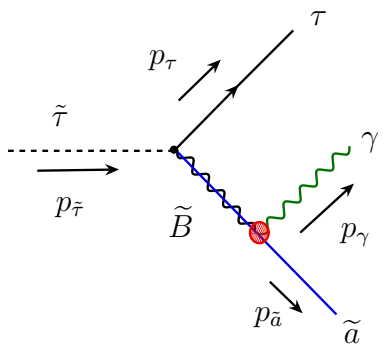

Figure 10.2: Three-body decay $\tilde{\tau}_R \to \tau\ \tilde{a}\ \gamma$. The blob symbolises the sum of the four one-loop diagrams given in fig. 10.1.

The three-body decay $\tilde{\tau}_R \to \tau\gamma\widetilde{a}$ shown in fig. 10.5 occurs first at one loop level. The photon energy E_γ and the cosine $\cos\theta$ of the opening angle between the photon and the tau direction seem to be the most accessible observables of these decays. Therefore we express the differential decay rate in these variables. The connection between differential decay rate and squared matrix element is given by [30]

$$d\Gamma = \frac{1}{2m_{\tilde{\tau}}} d\Pi_3 \sum_{\text{spins}} |\mathcal{M}(\tilde{\tau}_R \to \tau\,\gamma\,\widetilde{a})|^2. \tag{10.32}$$

The integral over final-state momenta in eq. (10.32) has the structure

$$\begin{aligned}\int d\,\Pi_3 &= \int \frac{d^3p_\tau}{(2\pi)^3}\frac{1}{2E_\tau}\int \frac{d^3p_{\widetilde{a}}}{(2\pi)^3}\frac{1}{2E_{\widetilde{a}}}\int \frac{d^3p_\gamma}{(2\pi)^3}\frac{1}{2E_\gamma}(2\pi)^4\delta^{(4)}(p_{\tilde{\tau}}-p_\tau-p_{\tilde{a}}-p_\gamma)\\ &= \frac{m_{\tilde{\tau}}^2}{128\pi^3}\int_{1-x_\gamma-A_{\widetilde{a}}}^{1-\frac{A_{\widetilde{a}}}{1-x_\gamma}} dx_\tau \int_0^{1-A_{\widetilde{a}}} dx_\gamma\\ &= \frac{m_{\tilde{\tau}}^2}{128\pi^3}\int_0^{1-A_{\widetilde{a}}} dx_\gamma \int_{-1}^{-1} d\cos\theta \frac{x_\gamma/2\,(1-A_{\widetilde{a}}-x_\gamma)}{[1-(x_\gamma/2)(1-\cos\theta)]^2}. \end{aligned} \tag{10.33}$$

From eq. (10.31) we get for the matrix element

$$\begin{aligned}i\mathcal{M}(\tilde{\tau}_R \to \tau\,\gamma\,\widetilde{a}) &= ic_\gamma \bar{u}(p_\tau)P_L\left(\frac{(-\not{p}_{\tilde{a}}-\not{p}_\gamma+m_{\widetilde{B}})\frac{1}{2}\gamma_5[\gamma^\mu,\not{p}_\gamma]}{(p_{\tilde{a}}+p_\gamma)^2-m_{\widetilde{B}}^2}\right.\\ &\left.\int\frac{dq^4}{(2\pi)^4}\frac{1}{((q-p_{\tilde{a}})^2-m_Q^2)(q^2-m_Q^2)((q+p_\gamma)^2-m_Q^2)}\right)v(p_{\tilde{a}}).\end{aligned} \tag{10.34}$$

As the mass of the heavy squarks is supposed to be of the $\mathcal{O}(10^9\ \text{GeV})$ we can neglect the external momenta $p_{\tilde{a}}$ and p_γ in the propagators of the loop integral. Thus we get for the matrix element

$$i\mathcal{M}(\tilde{\tau}_R \to \tau\,\gamma\,\widetilde{a}) = -i\frac{e^3\,e_Q}{32\,\pi^2\,c_W^2 f_a}\bar{u}(p_\tau)P_L\left(\frac{(-\not{p}_{\tilde{a}}-\not{p}_\gamma+m_{\widetilde{B}})\gamma_5[\gamma^\mu,\not{p}_\gamma]}{(p_{\tilde{a}}+p_\gamma)^2-m_{\widetilde{B}}^2}\right)v(p_{\tilde{a}}). \tag{10.35}$$

Squaring this matrix element we obtain

$$\sum_{\text{spins}}|\mathcal{M}(\tilde{\tau}_R \to \tau\,\gamma\,\widetilde{a})|^2 = \frac{\alpha_{em}^3 e_Q^2}{16\pi f_a^2 c_W^4}\,32\,\frac{p_{\tilde{a}}\cdot p_\gamma\,\left(2\,p_{\tilde{a}}\cdot p_\gamma\,p_{\tilde{a}}\cdot p_\tau+\left(-{m_{\widetilde{a}}}^2+{m_{\widetilde{B}}}^2\right)\,p_\gamma\cdot p_\tau\right)}{((p_{\tilde{a}}+p_\gamma)^2-m_{\widetilde{B}}^2)^2}. \tag{10.36}$$

Introducing

$$x_\gamma \equiv \frac{2E_\gamma}{m_{\tilde{\tau}}}\,,\qquad x_\tau \equiv \frac{2E_\tau}{m_{\tilde{\tau}}}\qquad A_{\widetilde{a}} \equiv \frac{m_{\widetilde{a}}^2}{m_{\tilde{\tau}}^2}\,,\qquad A_{\widetilde{B}} \equiv \frac{m_{\widetilde{B}}^2}{m_{\tilde{\tau}}^2} \tag{10.37}$$

we can write the squared matrix elements in terms of these new variables:

$$\sum_{\text{spins}}|\mathcal{M}(\tilde{\tau}_R \to \tau\,\gamma\,\widetilde{a})|^2 = \frac{\alpha_{em}^3 e_Q^2}{16\pi c_W^4}\frac{8m_{\tilde{\tau}}^2}{f_a^2}F_{\text{diff}}^{(\widetilde{a})}(x_\gamma,x_\tau,A_{\widetilde{a}},A_{\widetilde{B}}), \tag{10.38}$$

where

$$F_{\text{diff}}^{(\widetilde{a})}(x_\gamma,x_\tau,A_{\widetilde{a}},A_{\widetilde{B}}) = 1-A_{\widetilde{B}}-x_\gamma-\frac{\left(A_{\widetilde{a}}-A_{\widetilde{B}}\right)^2\left(A_{\widetilde{B}}-1\right)}{\left(A_{\widetilde{B}}+x_\tau-1\right)^2}-\frac{\left(A_{\widetilde{a}}-A_{\widetilde{B}}\right)\left(-2+2\,A_{\widetilde{B}}+x_\gamma\right)}{A_{\widetilde{B}}+x_\tau-1}. \tag{10.39}$$

Thus we get for the total decay rate

$$\begin{aligned}\Gamma(\tilde{\tau}_R \to \tau\gamma\widetilde{a}) &= \frac{\alpha_{em}^3 e_Q^2}{2\pi c_W^4}\frac{m_{\tilde{\tau}}^2}{f_a^2}\ \frac{m_{\tilde{\tau}}^2}{128\pi^3}\frac{1}{2m_{\tilde{\tau}}}\int_{1-x_\gamma-A_{\widetilde{a}}}^{1-\frac{A_{\widetilde{a}}}{1-x_\gamma}} dx_\tau \int_0^{1-A_{\widetilde{a}}} dx_\gamma F_{\rm diff}^{(\widetilde{a})}(x_\gamma, x_\tau, A_{\widetilde{a}}, A_{\widetilde{B}}) \\ &= \frac{\alpha_{em}^3 e_Q^2}{512\pi^4 c_W^4}\frac{m_{\tilde{\tau}}^3}{f_a^2}\left[\frac{1}{6} + \frac{15\,A_{\widetilde{a}}}{4} - 2\,A_{\widetilde{a}}{}^2 - \frac{23\,A_{\widetilde{a}}{}^3}{12} - \frac{3\,A_{\widetilde{a}}{}^2}{2\,A_{\widetilde{B}}} + \frac{3\,A_{\widetilde{a}}{}^3}{2\,A_{\widetilde{B}}} - \frac{13\,A_{\widetilde{B}}}{4} - \frac{5\,A_{\widetilde{a}}\,A_{\widetilde{B}}}{2}\right. \\ &+ \frac{23\,A_{\widetilde{a}}{}^2\,A_{\widetilde{B}}}{4} + \frac{7\,A_{\widetilde{B}}^2}{2} - \frac{7\,A_{\widetilde{a}}\,A_{\widetilde{B}}^2}{2} - \frac{A_{\widetilde{a}}{}^2\left(3\,A_{\widetilde{B}}+A_{\widetilde{a}}\left(-3+2\,A_{\widetilde{B}}\right)\right)\ln(A_{\widetilde{a}})}{2\,A_{\widetilde{B}}^2} \\ &- \left.\frac{\left(A_{\widetilde{a}}-A_{\widetilde{B}}\right)^2\left(-1+A_{\widetilde{B}}\right)\left(\left(3-7\,A_{\widetilde{B}}\right)A_{\widetilde{B}}+A_{\widetilde{a}}\left(3+A_{\widetilde{B}}\right)\right)\ln(\frac{-1+A_{\widetilde{B}}}{-A_{\widetilde{a}}+A_{\widetilde{B}}})}{2\,A_{\widetilde{B}}^2}\right]. \end{aligned} \tag{10.40}$$

From eq. (10.40) we obtain with [3]

$$\begin{aligned} m_{\tilde{\tau}} &= 100\,\text{GeV}, \qquad m_{\widetilde{B}} = 110\,\text{GeV}, \qquad m_{\widetilde{a}} = 10\ \text{GeV}, \\ e_Q &= 1, \qquad \alpha_{em}\,(M_Z) = 1/129, \qquad f_a = 10^{11}\text{GeV} \end{aligned} \tag{10.41}$$

for the total decay rate

$$\Gamma(\tilde{\tau}_R \to \tau\gamma\widetilde{a}) = 2.1 \cdot 10^{-28}\ \text{GeV} = 3.2 \cdot 10^{-4}\ s^{-1}, \tag{10.42}$$

where we have used the conversion factor between GeV and inverse seconds:

$$1\text{GeV} = 1.51925 \cdot 10^{24} s^{-1}. \tag{10.43}$$

Taking the limit $A_{\widetilde{a}} \to 0$ and not changing all over variables we obtain

$$\Gamma(\tilde{\tau}_R \to \tau\gamma\widetilde{a}) = 2.2 \cdot 10^{-28}\ \text{GeV} = 3.3 \cdot 10^{-4}\ s^{-1}. \tag{10.44}$$

This weak dependence on the chosen value of $A_{\widetilde{a}}$ is illustrated in fig. 10.5, where we varied the value of $A_{\widetilde{a}}$ between 0 and 1/100. For all other parameters we have chosen the values given in eq. (10.41).

In fig. (10.4) we varied the bino mass between 100 GeV and 200 GeV and fixed all other values to the values given in eq. (10.41). Increasing $A_{\widetilde{B}}$ from 1 to 2.5 the total decay rate varies about ±87%, whereas varying $A_{\widetilde{B}}$ between 2.5 and 4 the total decay rate varies only about ±33%. Varying $A_{\widetilde{B}}$ over the whole range from 1 to 4 changes the total decay rate about ±93%. The above changes demonstrate the strong dependence of the total decay rate on the relation of bino and stau mass, especially for low values of $A_{\widetilde{B}}$. Doubling the stau, bino and axino mass to

$$\begin{aligned} m_{\tilde{\tau}} &= 200\,\text{GeV}, \qquad m_{\widetilde{B}} = 220\,\text{GeV}, \qquad m_{\widetilde{a}} = 20\ \text{GeV}, \end{aligned} \tag{10.45}$$

the total decay rate increases by a factor 8, as it is proportional to $m_{\tilde{\tau}}^3$ and the dimensionless variables $A_{\widetilde{B}}$ and $A_{\widetilde{a}}$ remain unchanged by doubling the masses of stau, bino and axino. Thus we get

$$\Gamma(\tilde{\tau}_R \to \tau\gamma\widetilde{a}) = 16.7 \cdot 10^{-28}\ \text{GeV} = 25.3 \cdot 10^{-4}\ s^{-1}. \tag{10.46}$$

[3] Note that the actual limits for the stau mass in [31] ($m_{\tilde{\tau}} > 81.9$GeV, CL=95%, $m_{\tilde{\tau}_R} - m^0_{\chi_1} > 15$GeV) are obtained under the assumption that the neutralino is the LSP. In our model we make the assumption that the axino is the LSP.

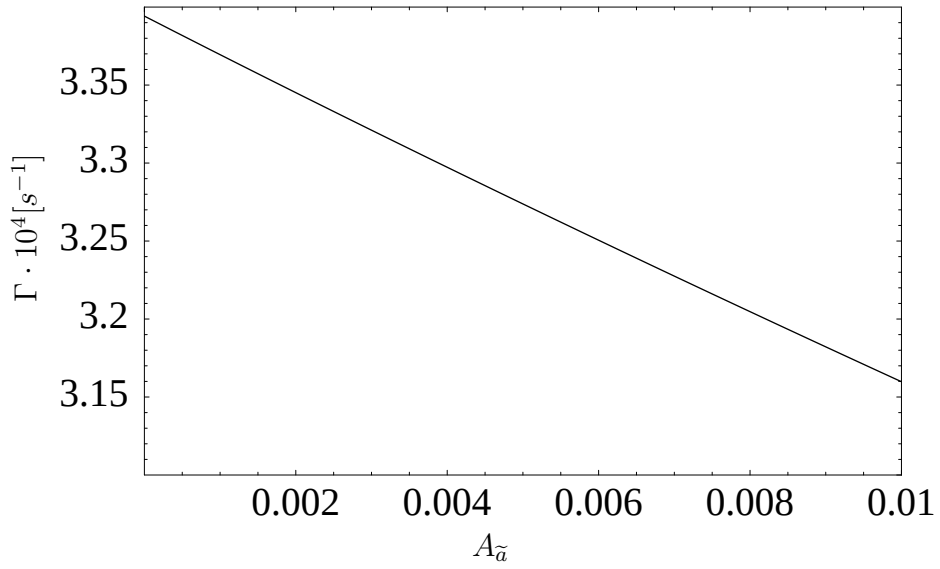

Figure 10.3: Dependence of the total decay rate Γ on $A_{\tilde{a}}$ for $m_{\tilde{\tau}} = 100\,\mathrm{GeV}$ and $m_{\widetilde{B}} = 110$ GeV.

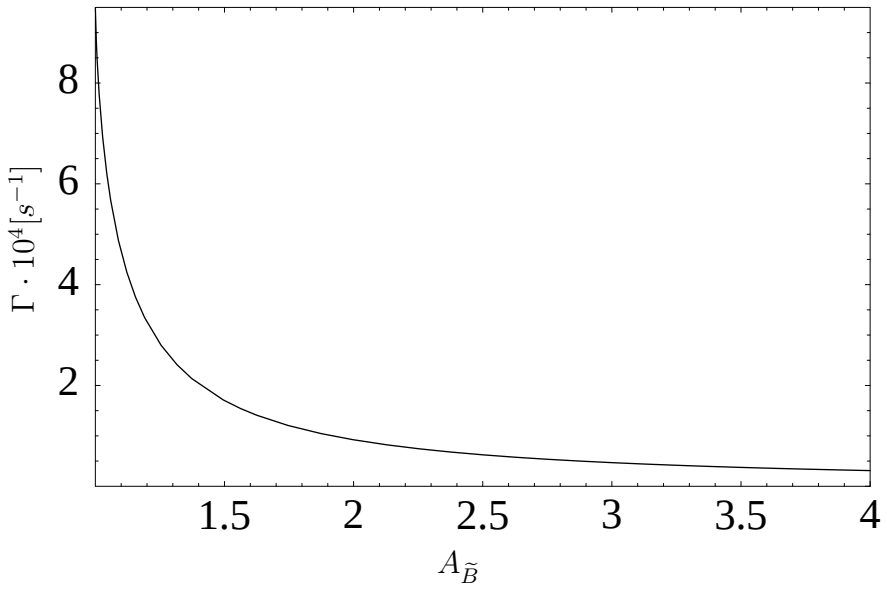

Figure 10.4: Dependence of the total decay rate Γ on $A_{\widetilde{B}}$ for $m_{\tilde{\tau}} = 100\,\mathrm{GeV}$ and $m_{\tilde{a}}^2/m_{\tilde{\tau}}^2 = 10^{-2}$.

The observables which seem to be most accessible are the photon energy E_γ and $\cos\theta$, the opening angle between the photon and the tau direction. Therefore we will additionally give the double differential decay rate expressed in the observable variables x_γ

and $\cos\theta$

$$\frac{d^2\Gamma(\tilde{\tau}_R \to \tau\,\gamma\,\widetilde{a})}{dx_\gamma\, d\cos\theta} = \frac{m_{\tilde{\tau}}}{512\pi^3}\,\frac{x_\gamma(1-A_{\widetilde{a}}-x_\gamma)}{[1-(x_\gamma/2)(1-\cos\theta)]^2}\sum_{\text{spins}}|\mathcal{M}(\tilde{\tau}_R \to \tau\,\gamma\,\widetilde{a})|^2, \qquad (10.47)$$

where

$$\sum_{\text{spins}}|\mathcal{M}(\tilde{\tau}_R \to \tau\,\gamma\,\widetilde{a})|^2 \;=\; \frac{\alpha_{em}^3 e_Q^2}{2\pi c_W^4}\frac{m_{\tilde{\tau}}^2}{f_a^2}F_{\text{diff}}^{(\widetilde{a})}(x_\gamma,\cos\theta,A_{\widetilde{a}},A_{\widetilde{B}}) \qquad (10.48)$$

and

$$F_{\text{diff}}^{(\widetilde{a})}(x_\gamma,\cos\theta,A_{\widetilde{a}},A_{\widetilde{B}}) = \frac{x_\gamma^2(1-A_{\widetilde{a}}-x_\gamma)[1+\cos\theta+A_{\widetilde{a}}(1-\cos\theta)][1+\cos\theta+A_{\widetilde{B}}(1-\cos\theta)]}{\{x_\gamma(1+\cos\theta)+2A_{\widetilde{a}}-A_{\widetilde{B}}[2-x_\gamma(1-\cos\theta)]\}^2}. \qquad (10.49)$$

Eq. (10.49) corresponds to the first line of eq. (7) of [83]. Numerical Integration of eq. (10.47) reproduces the life times given in eq. (10.42) and (10.44) [4].

10.5.1 Differential Distribution in the Three-Body Decay

Finally, we consider the differential distributions of the visible decay products in the three–body decay $\tilde{\tau}_R \to \tau + \gamma + \widetilde{a}$ in terms of the quantity

$$\frac{1}{\Gamma(\tilde{\tau}_R \to \tau\,\gamma\,\widetilde{a}\,)}\;\frac{d^2\Gamma(\tilde{\tau}_R \to \tau\,\gamma\,\widetilde{a})}{dx_\gamma d\cos\theta} \qquad (10.50)$$

which is independent of the total NLSP decay rate and the Peccei–Quinn scale. In fig. 10.5 we plot the normalised differential distributions of the visible decay products in the decays $\tilde{\tau}_R \to \tau\gamma\widetilde{a}$ for the axino LSP scenario for $m_{\tilde{\tau}} = 100\,\text{GeV}$, $m_{\widetilde{B}} = 110\,\text{GeV}$, $m_{\widetilde{a}}^2/m_{\tilde{\tau}}^2 = 10^{-2}$. The events are peaked in the regions where the photons carry a large energy fraction.

10.6 The Two-Body Decay $\tilde{\tau}_R \to \tau\ \tilde{a}$

The two-body decay $\tilde{\tau}_R \to \tau\ \tilde{a}$ arises first at two-loop level by the diagrams given in fig. 10.6. Its total decay rate is proportional to α_{em}^4 and is thus suppressed by a factor α_{em} compared to the three-body decay. This suppression by α_{em} could be (partially) compensated by the bigger phase space factor

$$\Pi_2 = \frac{m_{\tilde{\tau}}^2 - m_{\tilde{a}}^2}{8\pi m_{\tilde{\tau}}^2}, \qquad (10.51)$$

of the two-body decay. In this section we will calculate the two-body decay rate in order to find out if the two- or three-body decay give rise to the dominant contribution to the total decay rate of staus into axinos.

[4] Eq. (10.47) is in agreement with eq. (4) of [83], if we set in eq. (10.47) $e_Q^2 = 2C_{aYY}^2$ and consider only the first line of eq. (7).

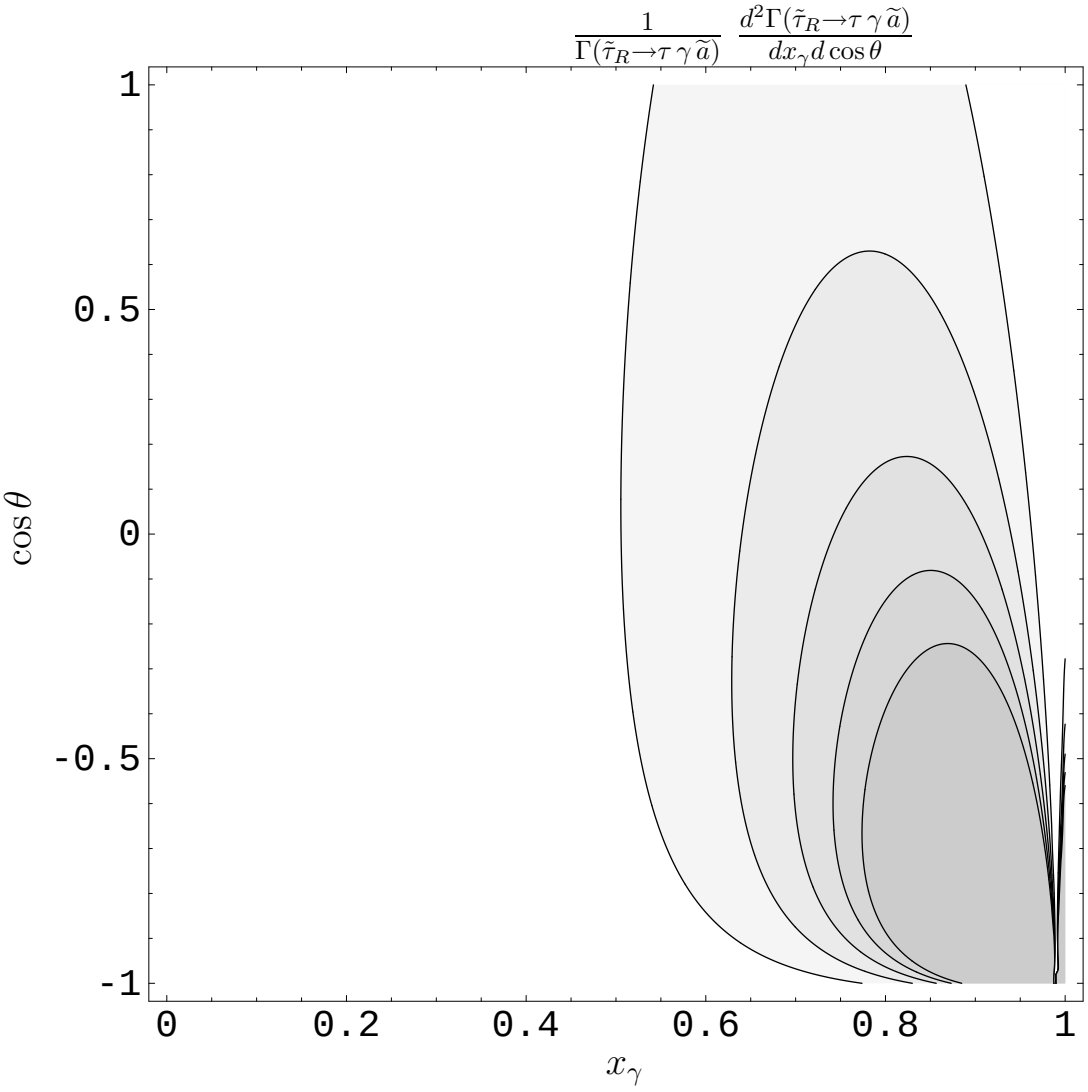

Figure 10.5: The normalized differential distributions of the visible decay products in the decays $\tilde{\tau}_R \to \tau\gamma\widetilde{a}$ for the axino LSP scenario for $m_{\tilde{\tau}} = 100\,\mathrm{GeV}$, $m_{\widetilde{B}} = 110\,\mathrm{GeV}$, $m^2_{\widetilde{a}}/m^2_{\tilde{\tau}} = 10^{-2}$. The contour lines represent the values 0.2, 0.4, 0.6, 0.8, and 1.0, where darker shading implies a higher number of events.

As in the case of the three-body decay we concentrate on a pure right-handed $\tilde{\tau}_R$. In contrast to the three-body decay we also have to consider a Z-boson when calculating the "effective" vertex. With a Z-boson in the loop the sum of the four one-loop diagrams eq. (10.31) gets changed to

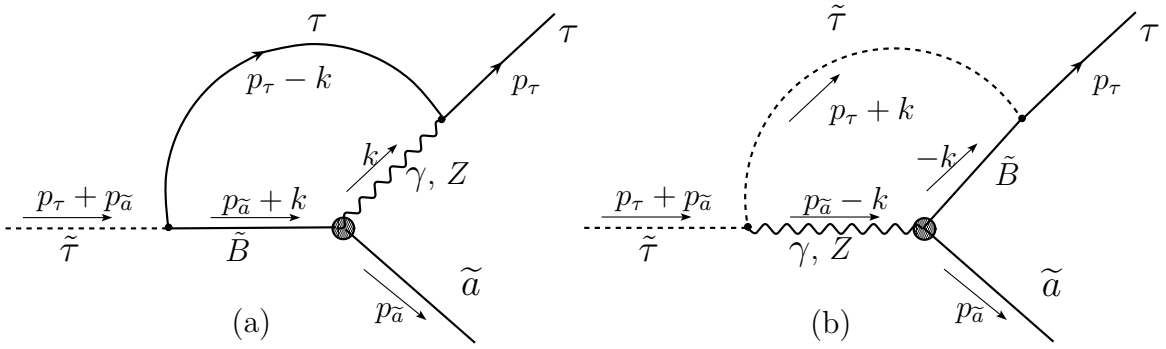

Figure 10.6: Two-body decay $\tilde{\tau} \to \tau\tilde{a}$

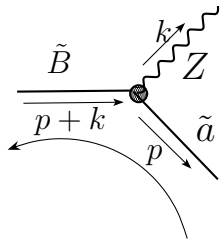

$$c_Z\,\gamma^5\,\left(\frac{1}{2}[\gamma^\mu, \not{k}]\right)\,\int \frac{dq^4}{(2\pi)^4} prop_1, \tag{10.52}$$

where

$$\begin{aligned} c_Z &= (-\sqrt{2} m_Q \frac{e^2}{c_W^2} e_Q^2 y s_W), \\ prop_1 &= \frac{1}{((q - p_{\tilde{a}})^2 - m_Q^2)(q^2 - m_Q^2)((q+k)^2 - m_Q^2)}. \end{aligned} \tag{10.53}$$

We start our calculation with diagram (a) of fig. 10.6. With the help of the Feynman rules given in section G and the the sum of the one-loop diagrams given in eq. (10.31) and eq. (10.31) we get for an incoming right handed $\tilde{\tau}_R$ and a photon (Z) in the loop

$$\begin{aligned} i\mathcal{M}_{R_{(a)}\,k} &= -i \int \frac{dq^4}{(2\pi)^4} \int \frac{dk^4}{(2\pi)^4} prop_1\ prop_{2\,k} \\ &\quad \bar{u}(p_\tau) \left(ie\gamma^\mu \;\; i(-\not{k} + \not{p}_\tau) \;\; (-i\sqrt{2} e P_L) \;\; i(-)(\not{k} + \not{p}_{\tilde{a}} - m_{\widetilde{B}}) \;\; c_k \gamma^5 \frac{1}{2}[\gamma^\mu, \not{k}] \right) v(p_{\tilde{a}}) \\ &= ie^4 m_Q y \frac{e_Q}{c_W}\ f_k \;\; \int \frac{dq^4}{(2\pi)^4} \int \frac{dk^4}{(2\pi)^4}\ prop_1\ prop_{2\,k} \\ &\quad \bar{u}(p_\tau) \left(\gamma^\mu \;\; (-\not{k} + \not{p}_\tau) \;\; P_L \;\; (\not{k} + \not{p}_{\tilde{a}} - m_{\widetilde{B}}) \;\; \gamma^5 [\gamma^\mu, \not{k}] \right) v(p_{\tilde{a}}), \end{aligned} \tag{10.54}$$

where $k = \gamma,\ Z$ and

$$\begin{aligned} prop_{2\,\gamma} &= \frac{1}{(k^2)(k-p_\tau)^2((k+p_{\tilde{a}})^2 - m^2_{\widetilde{B}})}, \\ prop_{2\,Z} &= \frac{1}{(k^2 - M_Z^2)(k-p_\tau)^2((k+p_{\tilde{a}})^2 - m^2_{\widetilde{B}})}, \\ f_\gamma &= -e_Q, \qquad f_Z = -e_Q \frac{s_W^2}{c_W^2}. \end{aligned} \tag{10.55}$$

Next we calculate the the matrix elements of diagram (b) in fig. 10.6. Replacing k with $-p_{\tilde{a}} + k$ and p with $p_{\tilde{a}}$ we get from eq. (10.31) for the effective vertex

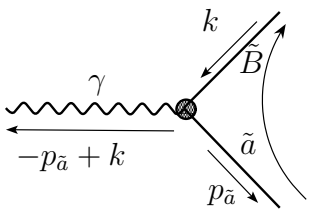

$$\begin{aligned} & c_k\,\gamma^5\ \left(\frac{1}{2}[\gamma^\mu, -\not{p}_{\tilde{a}} + \not{k}]\right) \int \frac{dq^4}{(2\pi)^4}\ prop_3 \\ &= -c_k\,\gamma^5\ \left(\frac{1}{2}[\gamma^\mu, \not{p}_{\tilde{a}} - \not{k}]\right) \int \frac{dq^4}{(2\pi)^4}\ prop_3, \end{aligned} \tag{10.56}$$

where

$$prop_3 = \frac{1}{((q-p_{\tilde{a}})^2 - m_Q^2)(q^2 - m_Q^2)((q-p_{\tilde{a}}+k)^2 - m_Q^2)}. \tag{10.57}$$

Thus we get for an incoming right handed $\tilde{\tau}$ [5]

$$\begin{aligned} i\mathcal{M}_{R_{(b)}\,k} &= \int \frac{dq^4}{(2\pi)^4} \int \frac{dk^4}{(2\pi)^4} prop_3\ prop_{4\,k} \\ & \quad \bar{u}(p_\tau) \left(-ie\sqrt{2}eP_L\ \ i(-\not{k} + m_{\widetilde{B}})\ \ \left(-c_\gamma \gamma^5 \frac{1}{2}[\gamma^\mu, \not{p}_{\tilde{a}} - \not{k}]\right)\right) v(p_{\tilde{a}}) \\ & \quad (-i)\, i\, e(2p_\tau + p_{\tilde{a}} + k)^\mu\, i \\ &= ie^4 m_Q y \frac{e_Q}{c_W}\ f_k \ \ \int \frac{dq^4}{(2\pi)^4} \int \frac{dk^4}{(2\pi)^4}\ prop_3\ prop_{4\,k} \\ & \quad \bar{u}(p_\tau)\left(P_L(-\not{k} + m_{\widetilde{B}})\ \ \gamma^5[\gamma^\mu, \not{p}_{\tilde{a}} - \not{k}]\right) v(p_{\tilde{a}})\,(2p_\tau + p_{\tilde{a}} + k)^\mu, \end{aligned} \tag{10.58}$$

where

$$\begin{aligned} prop_{4\,\gamma} &= \frac{1}{(k^2 - m^2_{\widetilde{B}})((k+p_\tau)^2 - m^2_{\tilde{\tau}})(k-p_{\tilde{a}})^2)}, \\ prop_{4\,Z} &= \frac{1}{(k^2 - m^2_{\widetilde{B}})((k+p_\tau)^2 - m^2_{\tilde{\tau}})(k-p_{\tilde{a}})^2 - M_Z^2)}\ . \end{aligned} \tag{10.59}$$

[5] The corresponding expression $i\mathcal{M}_{L_{(a)}}$ and $i\mathcal{M}_{L_{(b)}}$ for incoming lefthanded $\tilde{\tau}_s$ can be simply obtained from eq. (10.54) and (10.58) by replacing P_L with $-P_R$.

The integrals in eq. (10.54) and 10.58) are without approximations extremely difficult (not?) to solve analytically. In section A we explain on the example of rare B-decays the necessary steps to solve two-loop-integrals depending on two different mass scales and external momenta. The basic idea is to reduce the integrals to scalar integrals only depending on loop momenta and heavy masses with the help of the Heavy Mass Expansion (HME). Recurrence relations (see appendix B) bring then the scalar integrals to integrals where the highest power of each occurring propagator is 1. These "master integrals" can be solved analytically. The explicit formulae are given in section A.12. Details of these steps (and necessary intermediate steps) can be found in sections A.5 -A.9. In the two-body decay have to distinguish the following mass scales:

- particles with zero or small masses: photon, tau ($m_\tau = 1.8$ GeV), axino ($m_{\tilde{a}} \lesssim 1/10\ m_{\tilde{\tau}}$),
- particles with masses of $\mathcal{O}(100$ GeV): stau, Z, bino,
- heavy quarks.

We can divide the above mass scales in two classes: the "heavy" masses (heavy quarks and squarks) and light masses (all other particles).
Applying the HME we have to Taylor expand all subdiagrams which

- contain all heavy masses M_{Q_i} and $M_{\tilde{Q}_i}$ $(i = 1, 2)$ and
- consist of connected components that are 1PI with respect to lines with the small masses

in small masses and small momenta (for details see section 6.1.1.). On the example of diagram (a) of fig. 10.6 we show in fig. 10.7 the two subdiagrams which fulfil these requirements. With the above sketched procedure we get for the decaying right handed $\tilde{\tau}$ for contributions deriving from the Taylor expansion of the full diagrams (a) and (b) in small masses $m_{\widetilde{B}}$, M_Z, $m_{\tilde{\tau}}$ and in the external momenta $p_{\tilde{a}}$ and p_τ:

$$\begin{aligned} i\mathcal{M}_{R_{(a)}k} &= ie^4 m_Q y \tfrac{e_Q}{c_W} f_k \tfrac{1}{256\pi^8} \tfrac{1}{m_Q} \left[-4\tfrac{m_{\tilde{a}}}{m_Q} + 5\sqrt{x} + \tfrac{3}{\epsilon}\left(\tfrac{m_{\tilde{a}}}{2m_Q} - x\right)\right] \bar{u}(p_\tau) P_L v(p_{\tilde{a}}) + \mathcal{O}\left(\tfrac{p^4}{m_Q^4}\right), \\ i\mathcal{M}_{R_{(b)}k} &= ie^4 m_Q y \tfrac{e_Q}{c_W} f_k \tfrac{1}{256\pi^8} \tfrac{m_{\tilde{a}}}{m_Q^2} \left[\tfrac{7}{4} - \tfrac{1}{\epsilon}\tfrac{3}{2}\right] \bar{u}(p_\tau) P_L v(p_{\tilde{a}}) + \mathcal{O}\left(\tfrac{p^4}{m_Q^4}\right), \end{aligned} \tag{10.60}$$

where

$$x = \frac{m_{\widetilde{B}}^2}{m_Q^2} \tag{10.61}$$

and p is of the order of the external momenta. The above divergencies are only cancelled by calculating diagrams of type II in fig. 10.7. Thus we have to Taylor expand the loop containing the heavy masses in the external momenta of the loop ($p_{\tilde{a}}$ and k) and multiply this integral with the remaining legs and vertices of the outer loop (see eq. (6.2)). The calculation of these integrals is work in progress and will be included in a forthcoming publication.

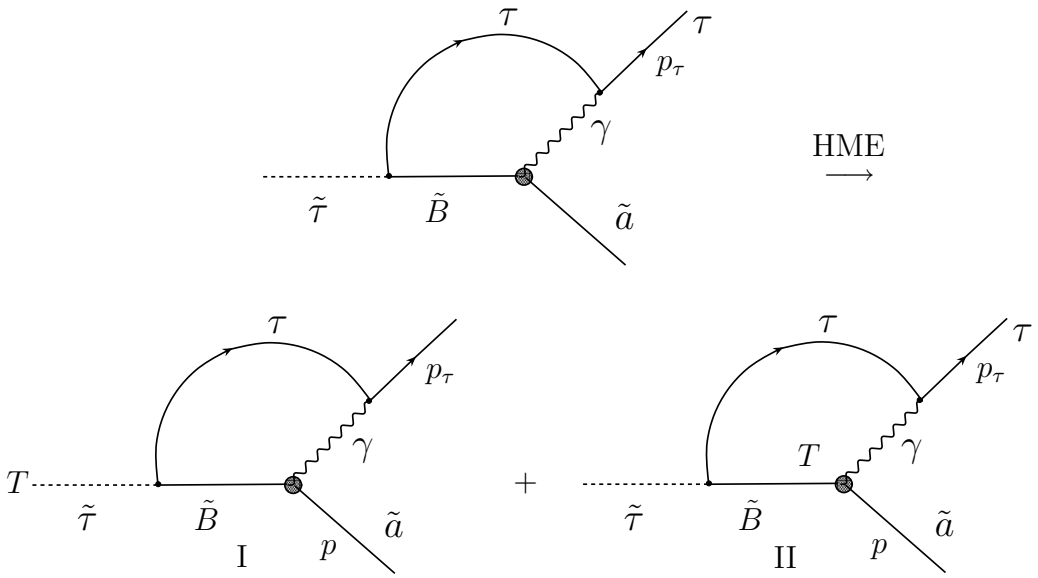

Figure 10.7: HME expansion of diagram (a) of fig. 10.6: The arising subdiagrams are the full diagram (diagram I) and the loop containing the heavy quarks and squarks (diagram II). The T symbolises the Taylor expansion in the small masses and the external momenta of the corresponding subdiagram.

Summing the contributions from all arising subdiagrams the total decay rate is given by

$$\Gamma(\tilde{\tau}_R \to \tau\ \widetilde{a}) = \frac{1}{2m_{\tilde{\tau}}}\Pi_2 \sum_{\text{spins}} |\mathcal{M}(\tilde{\tau}_R \to \tau\ \widetilde{a})|^2, \tag{10.62}$$

where

$$\Pi_2 = \frac{1}{4\pi}\frac{m_{\tilde{\tau}}^2 - m_{\tilde{a}}^2}{2m_{\tilde{\tau}}^2}. \tag{10.63}$$

Appendix A

Calculation of the Integrals of the Full SM and THDM Side

In the following we will display the major steps in performing the calculation of the arising integrals in $b \to s l^+ l^-$ and $b \to s\ \gamma$ and $b \to s\ g$ decays in the SM and THDM with the help of the *Mathematica* notebook "`mastertwo.nb`". This notebook calls all routines described in the following sections. In the initialisation step a routine "init.m" calls the following subprograms:

- *constants.m*: The *FeynArts*-output is loaded and all necessary declarations of momenta, masses and indices are made. By setting flags (further details can be found in the header of the program) it is defined which kind of process should be calculated (self-energies, penguins or boxes) and which model should be used (SM or THDM).

- *Fermions*: This package written by Patrick Liniger summarises all necessary routines needed to perform the Dirac Algebra. For a detailed documentation of this program we refer to his PhD-thesis [87].

- *Integrals*: This package summarises all routines concerning the tensor reduction, partial fraction and integrations of scalar integrals.

The usage of all occurring routines is explained in the head of the packages "*Integrals*" and "*Fermions*". The same information is obtained by using the online *Mathematica*-help function by typing ?`routine-name`. The new written routines are furthermore documented in section C[1].

A.1 Generation of the Feynman Integrands

The one- and two-loop Feynman integrands are generated with the help of the program *FeynArts* [88]. As we used the Background field (BGF)-formalisms even for diagrams

[1]The packages *Fermions* and *Integrals* are combined to the package *MasterTwo* which can be downloaded from `http://krone.physik.unizh.ch/~sschilli/MasterTwoWebPage.html`. A manual describing all functions of *MasterTwo* is in preparation.

including QCD-corrections we had to modify the existing model files for the QCD-extension of the SM-model and the THDM (further details of the generation of model files can be found in the *FeynArts* manual [88]).

A.2 Translation of the FeynArts Output

The Feynman-amplitudes generated by *FeynArts* are not appropriate for the routines used in `mastertwo.nb`. In a first section of the program the integrands generated by *FeynArts* are therefore transformed in such a way that the integration of the integrands can be performed fully automatically by the routines described in the following sections with the help of the routine. This part of `mastertwo.nb` depends very much on the concrete process to be calculated and has to be adapted when using new model files, calculating different processes, using new versions of *FeynArts* etc.. For the calculated B- and $\tilde{\tau}$-decays this translation is automatically performed by the function `FeynArtstoMasterTwo`.

A.3 Dirac Algebra

The routine `DiracAlgebra` performs standard transformations of the Dirac Algebra in the called naive dimensional regularisation scheme (NDR) described in section 4.1.1. The hermitian conjugate of γ^μ is taken to be

$$\gamma^{\mu\dagger} = \gamma^0\gamma^\mu\gamma^0, \tag{A.1}$$

so that according to the definition (4.8) we have

$$\gamma^{5\,\dagger} = \gamma^5 \tag{A.2}$$

From the definitions (4.7) and (4.8) it follows that

$$(\gamma^0)^2 = \mathbf{1} \quad (\gamma^i)^2 = -\mathbf{1}, \quad (\gamma^5)^2 = \mathbf{1}. \tag{A.3}$$

Scalars and mass factors are automatically factored out from the fermion chain such that it contains only gamma matrices and slashed momenta. From eq. (4.8) we get for the projectors $P_R = (1+\gamma^5)/2$ and $P_L = (1-\gamma^5)/2$

$$\gamma^0 P_R = P_L\gamma^0, \; \gamma^0 P_L = P_R\gamma^0. \tag{A.4}$$

Subsequent application of eq. (A.4) brings all the projectors to the left of the Fermion chains. The routine `ContractAllIndices` then performs all Lorentz contractions possible at this stage. This step significantly increases the number of fermion chains, but decreases the number of Lorentz indices simplifying the subsequent tensor reduction.

A.4 Colour Algebra

Integrals with outgoing gluons or quarks can lead to a quite complicated colour structures. Therefore it is necessary to provide a program performing the colour algebra

automatically. This is done by the routine `color.m` .
The following relations can be derived in the fundamental representation of $SU(N)$ with the help of eq. (E.2) and (E.14 – E.15) [2]:

$$f^{bac}\mathbf{T}^c\mathbf{T}^b = \frac{1}{2}\, i\, N\mathbf{T}^a, \tag{A.5}$$

$$\mathbf{T}^c\mathbf{T}^d f^{dba} f^{acb} = \mathbf{T}^c\mathbf{T}^d N\delta^{dc} = \frac{N^2-1}{2N}N = \frac{N^2-1}{2}. \tag{A.6}$$

From (A.5) and (E.16) we get

$$\mathbf{T}^a\mathbf{T}^e f^{adc} f^{dek} f^{ckb} = \frac{N}{2}\mathbf{T}^a\mathbf{T}^e f^{abe} = -i\frac{N^2}{4}\mathbf{T}^b. \tag{A.7}$$

Eq. (A.5)-(A.7) with $N = 3$ are implemented in the rule `colorrules`.

A.5 Taylor Expansion

The expansion of each propagator in external momenta up to $\mathcal{O}[(\text{external momenta})^2/M^2]$, where M is a heavy mass (M_W or M_H in the case of rare B-decays) is explicitly given by

$$\frac{1}{(q_i+k)^2-M^2} = \frac{1}{q_i^2-M^2}\left[1-\frac{k^2+2kq_i}{q_i^2-M^2}+\frac{4(kq_i)^2}{(q_i^2-M^2)^2}\right]+\mathcal{O}[k^4/M^4], \tag{A.8}$$

$$\frac{1}{(q_1+q_2+k)^2-M^2} = \frac{1}{(q_1+q_2)^2-M^2} \left[1-\frac{k^2+2kq_1+2kq_2}{(q_1+q_2)^2-M^2}+\frac{4(kq_1)^2+4(kq_2)^2+8q_1kq_2}{((q_1+q_2)^2-M^2)^2}\right]+\mathcal{O}[k^4/M^4], \tag{A.9}$$

where q_i $(i = 1, 2)$ are the loop momenta, M is a heavy mass and k an arbitrary external momentum. The expansions in external momenta are implemented in the routine `TaylorExpansion`. Analogously we get for the expansion in small masses

$$\frac{1}{q_i^2-m^2} = \frac{1}{q_i^2}\left[1+\frac{m^2}{q^2}\right]+\mathcal{O}[m^4/q^4], \tag{A.10}$$

where m is a small mass. This expansion is implemented in the routine `TaylorMass`, but was not applied in the matching calculations, as we directly set all the light masses (except the bottom mass) to zero, thus remaining in zeroth order of the expansion (A.10).

A.6 Scaling

After factoring the Taylor expanded integrands all light masses (in our case only the bottom mass) and external momenta are scaled with a factor x. As we are only

[2] For a short introduction to Lie Algebras we refer to section E and [89].

interested in Wilson coefficients corresponding to operators of mass dimension six, we set all terms x^n with $n > 2$ to zero. Keeping terms with $n > 2$ would correspond to the calculation of contributions to Wilson coefficients of higher mass dimensions.

A.7 Partial Fraction Decomposition

The remaining integrals depend only on loop momenta and two heavy masses: m_t and M_W (SM) or M_H (THDM). Subsequent application of the partial fraction decomposition

$$\frac{1}{(q^2-m_1^2)(q^2-m_2^2)} = \frac{1}{m_1^2-m_2^2}\left[\frac{1}{q^2-m_1^2}-\frac{1}{q^2-m_2^2}\right], \tag{A.11}$$

$$\frac{q^2}{(q^2-m_1^2)(q^2-m_2^2)} = \frac{1}{m_1^2-m_2^2}\left[\frac{m_1^2}{q^2-m_1^2}-\frac{m_2^2}{q^2-m_2^2}\right] \tag{A.12}$$

allows a reduction of all the integrals to those in which a single mass parameter occurs in the propagator denominators together with a given loop momentum.

A.8 Simplification of the Numerator

With the following relations the numerators successively get rid of loop momenta:

$$\frac{(q^2)^n}{(q^2-m^2)} = (q^2)^{n-1}+\frac{(q^2)^{n-1}m^2}{(q^2-m^2)}, \tag{A.13}$$

$$\begin{aligned}\frac{(q_1q_2)^n}{(q_1^2-m_1^2)(q_2^2-m_2^2)((q_1+q2)^2-m_3^2)} &= \frac{1}{2}(q_1q_2)^{n-1}\left[\frac{1}{(q_1^2-m_1^2)(q_2^2-m_2^2)}\right.\\ &- \frac{1}{(q_2^2-m_2^2)((q_1+q_2)^2-m_3^2)}\\ &- \frac{1}{(q_1^2-m_2^2)((q_1+q_2)^2-m_3^2)}\\ &+ \left.\frac{m_3^2-m_1^2-m_2^2}{(q_1^2-m_1^2)(q_2^2-m_2^2)((q_1+q2)^2-m_3^2)}\right];n\geq 1.\end{aligned} \tag{A.14}$$

The sections "Partial Fraction Decomposition" and "Simplification of the Numerator" are summarised in the routines `PartialFractionOne` (one-loop case) and `PartialFraction` (two-loop case).

A.9 Tensor Reduction

After Taylor expansion, partial fractioning and simplification of the numerators, the integrands of rare B-decays have at most four free Lorentz indices. Furthermore - provided all the light particle masses are set to zero - the corresponding integrals

always have at least one massless term in their denominators. In this case all two-loop integrals are relatively simple. A typical integrand has the following form:

$$I = \frac{q_1^\alpha q_1^\beta q_1^\gamma q_2^\delta}{(q_1^2 - m_1^2)^a (q_2^2 - m_2^2)^b ((q_1+q_2)^2)^c} \,. \tag{A.15}$$

The only entries depending on Lorentz indices are the loop momenta (being the integration variables) and the metric tensors. As integrals over an antisymmetric integrand with symmetric integration boundaries are zero, all integrands with an odd number of loop momenta $q_i^\alpha, (i = 1, 2)$ in the nominator can be set to zero. The idea of the tensor reduction is to express tensor integrals in terms of scalar integrals:
For the one loop case we get

$$\int d^D q q^\alpha q^\beta A(q^2) = \frac{1}{D} \int d^D q^2 g^{\alpha\beta} A(q^2), \tag{A.16}$$

$$\int d^D q q^\alpha q^\beta q^\gamma q^\delta A(q^2) = \frac{1}{D^2 + 2D} \int d^D q^4 (g^{\alpha\beta} g^{\gamma\delta} + g^{\alpha\gamma} g^{\beta\delta} + g^{\alpha\delta} g^{\beta\gamma}) A(q^2), \tag{A.17}$$

$$\int d^D q q^{\alpha_1} q^{\alpha_2} \dots q^{\alpha_{2k}} A(q^2) = \frac{\Gamma - 2\epsilon}{\Gamma(2 - \ +k)} \int d^D q^{2k} \mathbf{X} A(q^2), \tag{A.18}$$

where $A(q^2)$ is an arbitrary scalar function depending on Lorentz invariants of the loop momentum q. Usually it is a product of powers of propagators

$$\frac{1}{(q^2 - m_1^2)^{n_1}} \tag{A.19}$$

times a polynomial of q^2. $\mathbf{X}$ stands for permutations of metric tensor components $g^{\alpha_j \alpha_k}$. The tensor reduction for the one-loop case is implemented in the routine `UnderIntegration` for up to nine Lorentz indices. The above relations can be generalised to the case of two-loop integrals [90]

$$\int d^D q_1 d^D q_2 \ \ q_1^\alpha q_2^\beta A(q_1^2, q_2^2, q_1 q_2) = \frac{1}{D} \int d^D q_1 d^D q_2 q_1 \cdot q_2 g^{\alpha\beta} A(q_1^2, q_2^2, q_1 q_2), \tag{A.20}$$

$$\int d^D q_1 d^D q_2 \ \ q_1^\alpha q_1^\beta q_1^\gamma q_2^\delta A(q_1^2, q_2^2, q_1 q_2) = \frac{1}{D^2 + 2D} \int d^D q_1 d^D q_2 \ q_1^2 \ q_1 \cdot q_2 \ (g^{\alpha\beta} g^{\gamma\delta} + g^{\alpha\gamma} g^{\beta\delta} + g^{\alpha\delta} g^{\beta\gamma}) A(q_1^2, q_2^2, q_1 q_2), \tag{A.21}$$

$$\begin{aligned} \int d^D q_1 d^D q_2 \ \ q_1^\alpha q_1^\beta q_2^\gamma q_2^\delta A(q_1^2, q_2^2, q_1 q_2) &= \frac{1}{D^3 + D^2 - 2D} \int d^D q_1 d^D q_1 A(q_1^2, q_2^2, q_1 q_2) \\ &\quad \left[\left((1+D) q_1^2 q_2^2 - 2 (q_1^2 q_2^2)^2 \right) g^{\alpha\beta} g^{\gamma\delta} \right. \\ &+ \left. \left(-q_1^2 q_2^2 + D (q_1^2 q_2^2)^2 (g^{\alpha\beta} g^{\gamma\delta} + g^{\alpha\gamma} g^{\beta\delta} + g^{\alpha\delta} g^{\beta\gamma}) \right) \right], \end{aligned} \tag{A.22}$$

where $A(q_1^2, q_2^2, q_1 q_2)$ is an arbitrary scalar function of q_1 and q_2. It is usually a product of powers of propagators

$$\frac{1}{(q_1^2 - m_1^2)^a (q_2^2 - m_2^2)^b) ((q_1+q_2)^2 - m_3^2)^c} \tag{A.23}$$

times a polynomial in q_1^2, q_1^2, $q_1 q_2$, but the concrete form of this function has no importance for the tensor reduction.

The routine `TensorReduction` performs the tensor reduction for two-loop integrals. In the case of factorising integrals (corresponding to $c = 0$ in the integrand of eq. (A.15)), the one-dimensional tensor reduction calling the routine `UnderIntegration` is performed. From the tensor reduction we obtain additional terms of $q_1^2,\ q_2^2$ or $q_1 q_2$ in the numerator. Second usage of the identities described in section A.8 finally leads to a numerator not depending on loop momenta.

A.10 Substitutions

In rare B-decays we always have to deal with the special case that one of the occurring masses in the propagators is zero. This simplifies the loop integration significantly. Factoring out all scalar constants the two-loop integrals of rare B-decays are proportional to

$$\begin{aligned}
&\int d^D q_1 d^D q_2 \frac{1}{(q_1^2)^{n_3}(q_2^2 - m_2^2)^{n_2}((q_1+q_2)^2 - m_1^2)^{n_1}} \\
&= \int d^D q_1 d^D q_2 \frac{1}{(q_1^2 - m_2^2)^{n_2}(q_2^2)^{n_3}((q_1+q_2)^2 - m_1^2)^{n_1}} \\
&= \int d^D q_1 d^D q_2 \frac{1}{(q_1^2 - m_1^2)^{n_1}(q_2^2 - m_2^2)^{n_2}((q_1+q_2)^2)^{n_3}}. \qquad \text{(A.24)}
\end{aligned}$$

The last line of eq. (A.24) is the ordering of propagator denominators needed for the following loop integration routines. This form is characterised by the fact that the propagator denominator with overlapping loop momenta has always no additional mass term ($m_3 = 0$).

With the help of the routine `subrule` which is part of the function `SimplifyPropagator` all denominators are brought into this form. The ordering of the propagator denominators is very important, as the two-loop integrals are represented in the program generally as a non-commuting list.

A.11 Scalar One-Loop Integrals

The non-vanishing integrals obtained at one-loops are given by:

$$\begin{aligned}
\mu^{2\epsilon} \int \frac{d^D q}{(2\pi)^D} \frac{1}{(q^2 - m^2)^n} &= \frac{\mu^{2\epsilon}}{(2\pi)^D} \frac{\pi^{D/2}\,\Gamma(1+\epsilon)}{(m^2)^{n-D/2}}\, C_n^{(1)} \\
&= \frac{1}{16\pi^2} \frac{1}{(m^2)^{n-2}} \left(\left(\frac{\mu^2}{m^2} \right) 2^{2\epsilon} \pi^{\epsilon}\, \Gamma(1+\epsilon) \right)\, C_n^{(1)} \\
&= \frac{1}{16\pi^2} \frac{1}{(m^2)^{n-2}} N_\epsilon^{(1)}(m)\, C_n^{(1)}, \qquad \text{(A.25)}
\end{aligned}$$

where

$$\begin{aligned} N_\epsilon^{(1)}(m) &= \left(\frac{\mu^2}{m^2}\right)^\epsilon 2^{2\epsilon}\pi^\epsilon\,\Gamma(1+\epsilon) \\ &= 1-\epsilon\kappa+\epsilon^2\left(\frac{1}{12}\pi^2+\frac{1}{2}\kappa(m)^2\right)+\mathcal{O}(\epsilon)^3, \qquad \text{(A.26)} \\ \kappa(m) &= \gamma_E-\ln(4\pi)+\ln\frac{m^2}{\mu^2} \qquad \text{(A.27)} \end{aligned}$$

and arbitrary n and m. The prefactors of $C_n^{(1)}$ are chosen such that $C_n^{(1)}$ is free of common factors of the one-loop integration. The factor $N_\epsilon^{(1)}(m_1)$ summarises the ϵ-dependent part of the common prefactors. Defining the Pochhammer symbol

$$(a)_k=\frac{\Gamma(a+k)}{\Gamma(a)}=\begin{cases} a(a+1)(a+2)...(a+k-1), & k\geq 1, \\ 1, & k=0, \\ 1/[(a-1)(a-2)...(a-|k|)], & k\leq -1, \end{cases} \qquad \text{(A.28)}$$

for integer k and complex a, we can write $C_n^{(1)}$ in a compact way [91]:

$$C_n^{(1)}=i\frac{(-1)^n}{(n-1)!}(1+\epsilon)_{n-3}, \qquad \text{(A.29)}$$

which vanishes for $n\leq 0$. The routine `facruleone` calculates integrals proportional to eq. (A.25), but the trivial prefactor $1/(16\pi^2)$ is *not* included in the definition of `facruleone`. Thus the output of `facruleone` hast to be multiplied by $1/(16\pi^2)$ in order to get integrals of the form eq. (A.25).

A.12 Scalar Two-Loop Integrals

Including all phase-space factors we get for the D-dimensional two-loop integral

$$\begin{aligned} &\frac{\mu^{4\epsilon}}{(2\pi)^{2D}}\int\frac{d^Dq_1\,d^Dq_2}{(q_1^2-m_1^2)^{n_1}(q_2^2-m_2^2)^{n_2}[(q_1-q_2)^2]^{n_3}} \\ =\;& \frac{\mu^{4\epsilon}\pi^D\,\Gamma(1+\epsilon)^2}{(2\pi)^{2D}(m_1^2)^{n_1+n_2+n_3-D}}C^{(2)}_{n_1n_2n_3} \\ =\;& \frac{1}{256\pi^8}\frac{1}{(m_1^2)^{n_1+n_2+n_3-4}}\left(\left(\frac{\mu^2}{m_1^2}\right)^{2\epsilon}2^{4\epsilon}\pi^{2\epsilon}\,\Gamma(1+\epsilon)^2\right)\,C^{(2)}_{n_1n_2n_3} \\ =\;& \frac{1}{256\pi^8}\frac{1}{(m_1^2)^{n_1+n_2+n_3-4}}N_\epsilon^{(2)}(m_1)\,C^{(2)}_{n_1n_2n_3}, \end{aligned} \qquad \text{(A.30)}$$

with arbitrary integer powers n_1, n_2 and n_3 and with m_1 and $m_2\neq 0$.
$N_\epsilon^{(2)}(m)$ is given by

$$\begin{aligned} N_\epsilon^{(2)}(m) &= (N_\epsilon^{(1)}(m))^2=\left(\frac{\mu^2}{m^2}\right)^{2\epsilon}2^{4\epsilon}\pi^{2\epsilon}\,\Gamma(1+\epsilon)^2 \\ &= 1-2\epsilon\kappa+\epsilon^2\left(\frac{1}{6}\pi^2+2\kappa(m)^2\right)+\mathcal{O}(\epsilon)^3. \qquad \text{(A.31)} \end{aligned}$$

$C^{(2)}_{n_1n_2n_3}$ is free of common factors of all two-loop-integrals, whereas the constant $N^{(2)}_\epsilon(m)$ collects all ϵ-dependent parts of the common prefactors. All two-loop- integrals represented are represented in the program as a **non-commuting list** of the form

$$\begin{aligned} G^{m_1,m_2,0}_{n1,n2,n3} &= \frac{\mu^{4\epsilon}}{(2\pi)^{-4\epsilon}} \int d^Dq_1 d^Dq_2 \frac{1}{(q_1^2-m_1^2)^{n_1}(q_2^2-m_2^2)^{n_2}((q_1+q_2)^2-m_3^2)^{n_3}} \\ &= \frac{1}{(m_1^2)^{n_1+n_2+n_3-4}} N^{(2)}_\epsilon(m_1)\; C^{(2)}_{n_1n_2n_3}. \end{aligned} \tag{A.32}$$

The trivial phase space factor $1/(256\pi^8)$) not included in eq. (A.32) and is thus not part of the output of the corresponding integration routines. The output of all the integration routines described in the following subsections has thus to multiplied by $1/(258\pi^8)$ to get the results for the standard integrals of the form of general two-loop integral (A.30). Performing the integration in eq. (A.32) we have to distinguish the following cases: two of the masses are equal, the second mass m_2 vanishes, both masses m_1 and m_2 are different and one of the powers n_i $(i = 1, 2, 3)$ is zero. As the first three cases have the prefactor$N^{(2)}_\epsilon(m_1)/((m_1^2)^{n_1+n_2+n_3-4})$ in common we will only display the corresponding values of $C^{(2)}_{n_1n_2n_3}$.

A.12.1 Vanishing Integrals

All the two-loop integrals defined in eq. (A.32) vanish when either n_1 or n_2 is non-positive. Finally we should mention that by calculating the integrals we used the fact that for all massless integrals we have [92]

$$\int d^Dq \frac{1}{q^{2\alpha}} = 0. \tag{A.33}$$

This properties are implemented in the rule `deletprop` being part of the function `SimplifyPropagator`.

A.12.2 Two Equal Masses

With the help of Feynman-parameterisation [50] we get for two equal masses

$$C^{(2)}_{n_1n_2n_3} = (-1)^{n_1+n_2+n_3+1} \frac{(2-\epsilon)_{-n_3}(1+\epsilon)_{n_1+n_3-3}(1+\epsilon)_{n_2+n_3-3}}{(n_1-1)!(n_2-1)!(n_1+n_2+n_3-4+2\epsilon)_{n_3}}, \tag{A.34}$$

which is implemented in the routine `TwoEqual`.

A.12.3 Two Masses Zero

If also the second mass $m_2 = 0$ we again derive with the help of Feynman-parameterisation

$$C^{(2)}_{n_1n_2n_3} = (-1)^{n_1+n_2+n_3+1} \frac{(1+2\epsilon)_{n_1+n_2+n_3-5}(1+\epsilon)_{n_2+n_3-3}(1-\epsilon)_{1-n_2}(1-\epsilon)_{1-n_3}}{(n_1-1)!(n_2-1)!(n_3-1)!(1-\epsilon)(1-\frac{1}{3}\pi^2\epsilon^2+\mathcal{O}(\epsilon^3))}. \tag{A.35}$$

This case is implemented in the routine `TwoZero`.

A.12.4 Two Different Masses

If $m_1 \neq m_2$ and none of the two masses vanishes the routine `ScalInt` reduces all integrals with three positive indices to the master integral $G_1^{m_1\,m_2\,0}{}_1{}_1$ with the help of recurrence relations. $C_{111}^{(2)}$ is given by

$$\begin{aligned} C_{111}^{(2)} &= \frac{1}{2(1-\epsilon)(1-2\epsilon)} \\ &\left[-\frac{1+x}{\epsilon^2} + \frac{2}{\epsilon}x\ln x + (1-2x)\ln^2 x + 2(1-x)\mathrm{Li}_2\left(1-\frac{1}{\mathrm{x}}\right) + \mathcal{O}(\epsilon)\right], \end{aligned} \tag{A.36}$$

where we have introduced the mass relation

$$x = \frac{m_2^2}{m_1^2}. \tag{A.37}$$

The derivation of the recurrence relation is discussed in detail in section B.

A.12.5 Three Different Masses

In the two-loop matching for $\mathcal{O}_1^c$ and $\mathcal{O}_2^c$ scalar integrals with three different masses of the form

$$\begin{aligned} &\int \frac{d^Dq_1 d^Dq_2}{(2\pi)^{2D}} \frac{1}{(q_1^2-m_1^2)^{n_1}(q_2^2-m_1^2)^{n_2}((q_1-q_2)^2-m_2^2)^{n_3}} \\ &= \int \frac{d^Dq_1 d^Dq_2}{(2\pi)^{2D}} \frac{1}{(q_1^2-m_1^2)^{n_1}(q_2^2-m_2^2)^{n_3}((q_1+q_2)^2-m_1^2)^{n_2}} \\ &= \int \frac{d^Dq_1 d^Dq_2}{(2\pi)^{2D}} \frac{1}{(q_1^2-m_2^2)^{n_3}(q_2^2-m_1^2)^{n_1}((q_1+q_2)^2-m_1^2)^{n_2}}. \end{aligned} \tag{A.38}$$

With the help of the recurrence relations eq. (B.9), (B.11) and (B.12) we can reduce all these integrals to the following master integral:

$$\begin{aligned} G_1^{m_1\,m_2\,m_1}{}_1{}_1 &= \frac{\mu^{4\epsilon}}{(2\pi)^{-4\epsilon}} \int d^Dq_1 d^Dq_2 \frac{1}{(q_1^2-m_1^2)^{n_1}(q_2^2-m_2^2)^{n_2}((q_1+q_2)^2-m_1^2)^{n_3}} \\ &= m_1^2\, N_\epsilon^{(2)}(m_1)\, C_{111}^{a\,(2)}, \end{aligned} \tag{A.39}$$

where $C_{111}^{a\,(2)}$ is given by [46]

$$\begin{aligned} C_{111}^{a\,(2)} &= \frac{1}{(1-\epsilon)(1-2\epsilon)} \left[-\frac{1}{\epsilon^2}\right. \\ &\left.\left(1+\frac{x}{2}\right) + \frac{1}{\epsilon}\left(x_1\,\log(x)\right) - \frac{1}{2}\left(x_1\log(x)^2\right) + \left(2-\frac{x}{2}\right)\,\phi(x)\right]. \end{aligned} \tag{A.40}$$

If

$$x = \frac{m_2^2}{m_1^2} \ll 1 \tag{A.41}$$

then $\phi(x)$ is given by

$$\phi(x) = 4\sqrt{\frac{x}{4-x}}\ \mathrm{Cl}_2\ (2\arcsin\left(\frac{\sqrt{\mathrm{x}}}{2}\right)), \tag{A.42}$$

where Cl_2 is Clausen's integral function defined in section A.13.2.

The substitutions of eq. (A.38), the recurrence relations eq. (B.9), (B.11) and (B.12) as well as the integration of the master-integral (A.39) are implemented in the integration routine `ScalInt`.

A.12.6 Factorising Two-Loop Integrals

When two indices are positive, but one of the n_i in eq. (A.32) equals zero, the two-loop integrals reduce to products of oneloop integrals. Without restriction we can choose $n_3 = 0$ [3]. Then we get from eq. (A.29)

$$\begin{aligned} G^{m_1,m_2,0}_{n1,n2,0} &= \frac{1}{(m_1^2)^{n_1-2}(m_2^2)^{n_2-2}} N^{(1)}_\epsilon(m_1) N^{(1)}_\epsilon(m_2)\ C^{(1)}_{n_1} C^{(1)}_{n_2} \\ &= \frac{N^{(1)}_\epsilon(m_1) N^{(1)}_\epsilon(m_2)}{(m_1^2)^{n_1+n_2-4}} C^{(2)}_{n_1 n_2 0} + \mathcal{O}(\epsilon^3), \end{aligned} \tag{A.43}$$

where

$$C^{(2)}_{n_1 n_2 0} = C^{(1)}_{n_1} C^{(1)}_{n_2} = \frac{(-1)^n_1 (-1)^n_2}{(n_1-1)!(n_2-1)!} (1+\epsilon)_{n_1-3} (1+\epsilon)_{n_2-3}. \tag{A.44}$$

If $m_1 \neq m_2$ we get

$$N^{(1)}_\epsilon(m_1) N^{(1)}_\epsilon(m_2) = \frac{N^2_\epsilon(m_1)}{(m_1^2)^{n_1+n_2-4}} \left(1 - \ln(x)\ \epsilon + \frac{1}{2}\ \ln^2(x)\ \epsilon^2\right) x^{n_2-2} \tag{A.45}$$

with x defined in eq. (A.37).

If both masses equal m_1, we simply have

$$(N^{(1)}_\epsilon(m_1))^2 = N^{(2)}_\epsilon(m_1) \tag{A.46}$$

(see eq. (A.31)), if both masses equal m_2 we derive

$$(N^{(1)}_\epsilon(m_2))^2 = (1 - 2\epsilon \log(x) + 2\epsilon^2 \log(x)^2)\ N^{(2)}_\epsilon(m_1). \tag{A.47}$$

The routine `FacInt` integrates all factorising two-loop integrals of the form of (A.43) expressing all ϵ-dependent prefactors of $C^{(2)}_{n_1 n_2 0}$ in terms proportional to $N^{(1)}_\epsilon(m_1)$ as described in eq. (A.45-A.47).

[3] All other cases can by simple substitutions be transformed to this case.

A.13 Polylogarithms and Clausens's Function

A.13.1 Polylogarithms

In NLO - calculations we often have to deal with dilogarithms. They are a special case of the polylogarithm

$$\mathrm{Li_n(x)} = \sum_{\mathrm{k=1}}^{\infty} \frac{\mathrm{x^k}}{\mathrm{k^n}} \quad \mathrm{for}|\mathrm{x}| \leq 1 \tag{A.48}$$

for $n = 2$.
The dilogarithm can thus be defined as the sum [89]

$$\mathrm{Li_2(x)} = \sum_{\mathrm{n=1}}^{\infty} \quad \frac{\mathrm{x^n}}{\mathrm{k^2}} \quad \mathrm{for}|\mathrm{x}| \leq 1 \tag{A.49}$$

or the integral

$$\begin{aligned} \mathrm{Li_2(x)} &= -\int_0^x \frac{\ln(1-t)}{t} dt = -\int_0^1 \frac{\ln(1-xt)}{t} dt \\ &= -\int_{1-x}^1 \frac{\ln(t)}{1-t} dt = \int_0^1 \frac{\ln(t)}{t-1/x} dt. \end{aligned} \tag{A.50}$$

The major functional equations for the dilogarithm are given by

$$\mathrm{Li_2(x)} + \mathrm{Li_2(-x)} = -\frac{1}{2}\mathrm{Li_2(x^2)}, \tag{A.51}$$

$$\mathrm{Li_2(1-x)} + \mathrm{Li_2(1-1/x)} = -\frac{1}{2}\ln^2(x), \tag{A.52}$$

$$\mathrm{Li_2(x)} + \mathrm{Li_2(1-x)} = \frac{\pi^2}{6} - \ln(x)\ln(1-x), \tag{A.53}$$

$$\mathrm{Li_2(-x)} + \mathrm{Li_2(1-x)} + \frac{1}{2}\mathrm{Li_2(1-x^2)} = -\frac{\pi^2}{12} - \ln(x)\ln(x+1). \tag{A.54}$$

The definitions of eq. (A.50) correspond to the definitions used in *Mathematica* [93]. Unfortunately this is not the case for the conventions used in *Maple* [94]. We have the following connections between both conventions

$$\mathrm{Li_2^{\mathit{Mathematica}}(1-x)} = \mathrm{Li_2^{\mathit{Maple}}(x)}. \tag{A.55}$$

A.13.2 Clausen's Function

Define

$$S_n(x) \equiv \sum_{k=1}^{\infty} \frac{\sin(kx)}{k^n}, \tag{A.56}$$

$$C_n(x) \equiv \sum_{k=1}^{\infty} \frac{\cos(kx)}{k^n}, \tag{A.57}$$

and write

$$\mathrm{Cl_n(x)} \equiv \begin{cases} S_n(x), & n \text{ even} \\ C_n(x), & n \text{ odd.} \end{cases} \tag{A.58}$$

Then the Clausen function $\mathrm{Cl_n}$ can be given symbolically in terms of polylogarithm as [95]

$$\mathrm{Cl_n(x)} = \begin{cases} \frac{1}{2}[\mathrm{Li_n}(\mathrm{e^{-ix}}) - \mathrm{Li_n}(\mathrm{e^{ix}})], & n \text{ even} \\ \frac{1}{2}[\mathrm{Li_n}(\mathrm{e^{-ix}}) + \mathrm{Li_n}(\mathrm{e^{ix}})], & n \text{ odd.} \end{cases} \tag{A.59}$$

In NLO - calculations we often have to deal with the special case $n = 2$. Then eq. (A.59) becomes the Clausen's integral function

$$\mathrm{Cl_2(x)} = \mathrm{S_2(x)} = \Im[\mathrm{Li_2}(\mathrm{e^{ix}})] = -\int_0^{\mathrm{x}} \mathrm{dt} \ln|2\sin\left(\frac{\mathrm{t}}{2}\right)|. \tag{A.60}$$

Appendix B

Recurrence Relations

B.1 General Recurrence Relations

We will first give a general derivation of the recurrence relations for arbitrary masses $m_1,\ m_2\ m_3$ for the integral

$$G^{m_1,m_2,m_3}_{n_1,n_2,n_3} = \frac{\mu^{4\epsilon}}{(2\pi)^{-4\epsilon}} \int d^D q_1 d^D q_2 \frac{1}{(q_1^2-m_1^2)^{n_1}(q_2^2-m_2^2)^{n_2}((q_1+q_2)^2-m_3^2)^{n_3}}. \tag{B.1}$$

From this general expression, which will be needed for the calculation of two-loop integrals in the case $\tilde{\tau} \to \tau\widetilde{a}$, we will then derive the recurrence relations for the special case $m_3 = 0$.
The derivation of the recurrence relations starts with the following identities [46]:

$$\int d^D q_1 d^D q_2 \frac{\partial}{\partial q_1^\mu} \left(\frac{q_1^\mu}{(q_1^2-m_1^2)^{n_1}(q_2^2-m_2^2)^{n_2}((q_1+q_2)^2-m_3^2)^{n_3}} \right) = 0, \tag{B.2}$$

$$\int d^D q_1 d^D q_2 \frac{\partial}{\partial q_2^\mu} \left(\frac{q_2^\mu}{(q_1^2-m_1^2)^{n_1}(q_2^2-m_2^2)^{n_2}((q_1+q_2)^2)-m_3^2)^{n_3}} \right) = 0, \tag{B.3}$$

$$\int d^D q_1 d^D q_2 \frac{\partial}{\partial q_1^\mu} \left(\frac{q_1^\mu}{(q_1^2-m_1^2)^{n_1}((q_1+q_2)^2-m_2^2)^{n_2}(q_2^2-m_3^2)^{n_3}} \right) = 0, \tag{B.4}$$

Substitutions of the integration variables in eq. (B.2) lead to (B.3-B.4). With the help of the Gaussian integral theorem we can transform the integral to a vanishing surface integral with symmetric boundaries and an asymmetric integrand. In oder to simplify the notation we will use

$$G^{m_1,m_2,m_3}_{n_1,n_2,n_3} \equiv G_{n_1,n_2,n_3} \tag{B.5}$$

in this section. From eq. (B.2) we get

$$\begin{aligned}(D-2n_1-n_3)G_{n_1,n_2,n_3} &= 2n_1 m_1^2 G_{n_1+1,n_2,n_3} + a_3(G_{n_1-1,n_2,n_3+1} - G_{n_1,n_2-1,n_3+1}) \\ &\quad + a_3(m_1^2 - m_2^2 + m_3^2)G_{n_1,n_2,n_3+1},\end{aligned} \tag{B.6}$$

where we have used $G^{m_1,m_2,m_3}_{n_1,n_2,n_3} = G_{n_1,n_2,n_3}$. From eq. (B.3) or directly by replacing $n_1 \leftrightarrow n_2$ and $m_1 \leftrightarrow m_2$ in eq. (B.6) we get

$$\begin{aligned}(D-2n_2-n_3)G_{n_1,n_2,n_3} &= 2n_2 m_2^2 G_{n_1,n_2+1,n_3} + a_3(G_{n_1,n_2-1,n_3+1} - G_{n_1-1,n_2,n_3+1}) \\ &\quad + a_3(m_2^2 - m_1^2 + m_3^2)G_{n_1,n_2,n_3+1}.\end{aligned} \tag{B.7}$$

From (eq. (B.4)) we obtain

$$\begin{aligned}(D-2n_1-n_2)G_{n_1,n_2,n_3} &= 2n_1m_1^2G_{n_1+1,n_2,n_3}+a_2(G_{n_1-1,n_2+1,n_3}-G_{n_1,n_2+1,n_3-1})\\ &\quad +a_2(m_1^2+m_2^2-m_3^2)G_{n_1,n_2+1,n_3}. \qquad \text{(B.8)}\end{aligned}$$

The last three equations connect integrals with the sum of powers $a_1+a_2+a_3$ with integrals where the sum of the powers is lowered by 1. They form an equation system, which can be used to extract the integrals G_{n_1+1,n_2,n_3}, G_{n_1,n_2+1,n_3} G_{n_1,n_2,n_3+1}. Solving this equation system we obtain the following recurrence relations:

$$\begin{aligned}G_{n_1+1,n_2,n_3} &= \frac{1}{n_1\, m_1^2\, \Delta(m_1,m_2,m_3)}\\ &\quad \Big\{\big[n_2\,(m_1^2-m_3^2)(m_1^2-m_2^2+m_3^2)+n_3\,(m_1^2-m_2^2)(m_1^2+m_2^2-m_3^2)\\ &\quad D\,m_1^2\,(-m_1^2+m_2^2+m_3^2)-a_1\,\Delta\,(m_1,m_2,m_3)\big]\,G_{n_1,n_2,n_3}\\ &\quad +n_2\,m_2^3(m_1^2-m_2^2+m_3^2)\,[G_{n_1,n_2+1,n_3-1}-G_{n_1-1,n_2+1,n_3}]\\ &\quad +n_3\,m_3^2(m_1^2+m_2^2-m_3^2)\,[G_{n_1,n_2-1,n_3+1}-G_{n_1-1,n_2,n_3+1}]\Big\} \qquad \text{(B.9)}\end{aligned}$$

with the determinant of the corresponding equation system

$$\Delta(m_1,m_2,m_3)=2(m_1^2m_2^2+m_1^2m_3^2+m_2^2m_3^2)-(m_1^4+m_2^4+m_3^4). \qquad \text{(B.10)}$$

Replacing $n_1 \leftrightarrow n_2$ and $m_1 \leftrightarrow m_2$ in eq. (B.9) we get

$$\begin{aligned}G_{n_1,n_2+1,n_3} &= \frac{1}{n_2\, m_2^2\, \Delta(m_1,m_2,m_3)}\\ &\quad \Big\{\big[n_1\,(m_2^2-m_3^2)(m_2^2-m_1^2+m_3^2)+n_3\,(m_2^2-m_1^2)(m_1^2+m_2^2-m_3^2)\\ &\quad D\,m_2^2\,(-m_2^2+m_1^2+m_3^2)-a_2\,\Delta(m_1,m_2,m_3)\big]\,G_{n_1,n_2,n_3}\\ &\quad +n_1\,m_1^2(m_2^2-m_1^2+m_3^2)\,[G_{n_1+1,n_2,n_3-1}-G_{n_1+1,n_2-1,n_3}]\\ &\quad +n_3\,m_3^2(m_1^2+m_2^2-m_3^2)\,[G_{n_1-1,n_2,n_3+1}-G_{n_1,n_2-1,n_3+1}]\Big\}\,. \qquad \text{(B.11)}\end{aligned}$$

Replacing $n_1 \leftrightarrow n_3$ and $m_1 \leftrightarrow m_3$ in eq. (B.9) we obtain

$$\begin{aligned}G_{n_1,n_2,n_3+1} &= \frac{1}{n_3\, m_3^2\, \Delta(m_1,m_2,m_3)}\\ &\quad \Big\{\big[n_1(m_3^2-m_2)^2)(m_2^2-m_1^2+m_3^2)+n_2(m_3^2-m_1^2)(m_1^2+m_3^2-m_2^2)\\ &\quad D\,m_3^2(-m_3^2+m_1^2+m_2^2)-a_3\,\Delta(m_1,m_2,m_3)\big]\,G_{n_1,n_2,n_3}\\ &\quad +a_1\,m_1^2(m_2^2-m_1^2+m_3^2)\,[G_{n_1+1,n_2-1,n_3}-G_{n_1+1,n_2,n_3-1}]\\ &\quad +a_2\,m_2^2(m_1^2+m_3^2-m_2^2)\,[G_{n_1-1,n_2+1,n_3}-G_{n_1,n_2+1,n_3-1}]\Big\}\,. \qquad \text{(B.12)}\end{aligned}$$

The general recurrence relations (B.9), (B.11) and (B.12) are implemented in the rule `recurrence` which is part of the integration routine `ScalIntAxino`.

B.2 Recurrence Relations for Rare FCNC Decays Mediated by Penguins and W-Boxes

At least one mass is zero in the integrals appearing in the considered rare B-decays mediated by by penguins and W–boxes [1] . Without restrictions we can choose this

[1] This is not the case for the decay $b \to sc\bar{c}$, where three mass scales are present and the more general recurrence relations described in the previous section have to be used.

mass to be m_3. To shorten the notation we will now set

$$G^{m_1,m_2,0}_{n_1,n_2,n_3} \equiv G_{n_1,n_2,n_3} \tag{B.13}$$

in this section. Taking the limit $m_3 \to 0$ we get from eq. (B.9) and B.11)

$$\begin{aligned} G_{(n_1+1)\,n_2\,n_3} &= \tfrac{1}{m_1^2\,n_1(1-x)} \quad \{[D-n_1-n_2-n_3+x(n_1-n_3)]G_{n_1n_2n_3} \\ &\qquad + \quad xn_2 \quad \left[G_{(n_1-1)(n_2+1)n_3} - G_{n_1(n_2+1)(n_3-1)}\right]\}\,, \end{aligned} \tag{B.14}$$

$$\begin{aligned} G_{n_1\,(n_2+1)\,n_3} &= -\tfrac{1}{m_2^2 n_2 x(1-x)} \quad \{[x(D-n_1-n_2-n_3)+n_2-n_3]G_{n_1n_2n_3} \\ &\qquad + \quad n_1 \quad \left[G_{(n_1+1)(n_2-1)n_3}\right]\}\,, \end{aligned} \tag{B.15}$$

where $x = m_2^2/m_1^2$ [46]. From eq. (B.12) we see that the limit $m_3 \to 0$ does not exist for G_{n_1,n_2,n_3+1}. The recurrence relation for G_{n_1,n_2,n_3+1} in this limit can be derived from eq. (B.9) by eliminating G_{n_1+1,n_2,n_3} with the help of eq. (B.11) and G_{n_1,n_2+1,n_3} with the help of eq. (B.12). Thus we obtain

$$\begin{aligned} G_{n_1\,n_2\,(n_3+1)} &= \tfrac{1}{m_1^2 n_3(1-x)^2} \quad \{[(1+x)(-D)+2n_2+(1+3x)n_3]G_{n_1n_2n_3} \\ &\qquad + \quad 2xn_2 \quad \left[G_{n_1(n_2+1)(n_3-1)} - G_{(n_1-1)(n_2+1)n_3}\right] \\ &\qquad + \quad (1-x)n_3 \quad \left[G_{n_1(n_2-1)(n_3+1)} - G_{(n_1-1)n_2(n_3+1)}\right]\}\,. \end{aligned} \tag{B.16}$$

Eq. (B.3-B.16) are implemented in the rule `recurrenceb`. Furthermore this rule is part of the integration routine `ScalInt`.

Appendix C

Documentation of Basic Functions of Integrals

In this appendix we give a detailed documentation of the routines mentioned in section A. For the documentation of the routines in *Fermions* needed to perform the Dirac Algebra and the contraction of free indices we refer to [87].

C.1 Declarations

The following declarations are inherited from *Fermions*:

`DeclareIndex[`μ`]` declares any index μ you wish to use.

`DeclareMomentum[p]` declares any momentum p you wish to use.

`DeclareMass[m]` declares any mass `m` you wish to use with `DeclareMass[m]`. It can be used afterwards as `Dirac[m]` or `Dirac[p + m]`.

In order to make the functions `TaylorExpansion, TaylorMass, Scaling` and `Substitution` (see below) to run properly, we have to distinguish between small masses and heavy masses as well as between loop momenta and external momenta. Thus the general declarations of masses and momenta have to be replaced by the following declarations:

`DeclareLoopMomentum[q]` declares any loop momentum `q` appearing in one and two dimensional loop integrals. The declaration of loop momenta is needed for the correct usage of `TaylorExpansion` and `Substitution`.

`DeclareExternalMomentum[k]` declares any external momenta `k` appearing in one and two dimensional loop integrals. Needed for the correct usage of `TaylorExpansion` and `Scaling`.

`DeclareHeavyMass[M]` declares any heavy mass `M`. Needed for the correct usage of `TaylorMass`.

`DeclareSmassMass[m]` declares any small masses `m`. Needed for the correct usage of `Scaling`.

Momenta defined by `DeclareLoopMomentum[q]` and `DeclareExternalMomentum[k]` inherit the properties of `DeclareMomentum`, masses defined by `DeclareHeavyMass[M]` and `DeclareSmallMass[m]` inherit the properties of `DeclareMass`.

Propagators like

$$\frac{1}{(q1^2 - m1^2)^{n1}(q2 + k_1)^2 - m2^2)^{n2}((q1 + q2 + k_2)^2 - m3^2)^{n3}}, \tag{C.1}$$

are represented as a list of the following form:

$$\texttt{AD}\Big[\underbrace{den[q1, m1], ..., den[q1, m1]}_{\text{n1 terms}}, \underbrace{den[q2 + k1, m2], ..., den[q2 + k1, m2]}_{\text{n2 terms}}, \underbrace{den[q1 + q2 + k2, m3], ..., den[q1 + q2 + k2, m3]}_{\text{n3 terms}}\Big]. \tag{C.2}$$

C.2 Taylor Expansion

`TaylorExpansion[expr]` expands each propagator `den[a, M]` of `expr` in external momenta up to $\mathcal{O}[(\text{external momenta})^2/M^2]$, where `M` has to be declared as heavy mass with `DeclareHeavyMass[M]` (see eq. (A.8)).

`TaylorMass[expr]` expands each propagator `den[a, m]` of `expr` up to second order in the small mass `m`. This routine functions only if `m` is declared as small mass with `DeclareSmallMass[m]` (see eq. (A.10).

`Scaling[expr]` scales all external momenta and light masses with a factor x. All terms with x^n with $n > 2$ are set to zero (see section A.6). External momenta have to be declared with `DeclareExternalMomentum`, light masses have to be declared with `DeclareSmallMass`.

C.3 Tensor Reduction

`UnderIntegration[expr,var]` performs the one-dimensional tensor reduction of `expr` in `var`. It assumes that the denominator of `expr` is an arbitrary scalar function depending on Lorentz invariants of `var`. It can handle expressions `expr` with up to 9 Lorentz Indices.

`UnderTwo[expr,var]` works just like `UnderIntegration`, with one difference: it doesn't give out the various intermediate messages that indicate what the program is doing at a given time.

`TensorReduction[expr,var1,var2]` performs a two dimensional tensor reduction of expressions `expr` with up to 5 Lorentz Indices assuming that the denominator of `expr` is an arbitrary scalar function of the variables `var1` and `var2`. If the numerator of `expr` depends only on `var` (`var2`) it performs a one-dimensional tensor reduction in `var` (`var2`) using `UnderTwo[expr,var]`(`UnderTwo[expr,var2]`).

`TensorReductionTwo[expr,var,var2]` works like `TensorReduction` without intermediate Print-messages and a Taylor expansion of the output up to second order in `eps`.

The routines for the one-dimensional tensor reduction `UnderIntegration` and `UnderTwo` are modified versions of routines I got via private communication by the courtesy of Kai Bieri.

C.4 Partial Fraction

`PartialFraction[expr]` makes a partial fraction decomposition (see section A.7 of the denominators of the form (C.2) in the two-loop case. Not appropriate for one-loop calculation, as it sets denominators with only one loop-momentum to zero. Furthermore it gets the numerators successively rid of loop momenta as described in section A.8.

`PartialFractionOne[expr]` same as `PartialFraction` without setting denominators depending only on one loop momentum to zero.

C.5 Preparation of Loop Integrations

`Substitution[expr]` makes substitution in the integrands of factorising two-loop-integrals such that the propagator structure contains no overlapping loop momenta.

`SimplifyPropagator[expr]` transforms propagator structures in such a way that the routines for Loop Integration work properly. In a first step it the rule `delete` sets all vanishing integrals to zero (see A.12.1). Then propagators like

$$\texttt{AD}\Big[\underbrace{den[q1,m1],...,den[q1,m1]}_{\text{n1 terms}},\underbrace{den[q2,m2],...,den[q2,m2]}_{\text{n2 terms}},\underbrace{den[q1+q2,m3],...,den[q1+q2,m3]}_{\text{n3 terms}}\Big] \tag{C.3}$$

are brought to the form

$$\texttt{AD[i[m1, n1], i[m2, n2], i[m3, n3]]}. \tag{C.4}$$

Propagator structures with all $ni > 0$ and thus three list entries in eq. (C.4) are transformed to

$$\texttt{G[i[m1, n1], i[m2, n2], i[m3, n3]]}. \tag{C.5}$$

If one of the ni, $(i = 1, 2, 3)$ in C.3 is zero, we deal with a factorising integral. If e.g. $n3$ in (C.3) is zero, the propagator structure is then according to (C.4) represented as

$$\texttt{AD[i[m1, n1], i[m2, n2]]}. \tag{C.6}$$

In a last step `subrule` applies the substitution rules (A.24) and (A.38) to all non-factorising integrands of the form (C.5). Thus at the end all non-factorising propagator structures are either of the form `G[i[m1,n1],i[m2,n2],i[0,n3]]` or `G[i[m1,n1],i[m2,n2],i[m1,n3]]`.

C.6 Two-Loop Integration

C.6.1 General Remarks

Taylor Expansion: The output of all routines for two-loop integration is Taylor expanded in `eps` until 0. order.

Constants: The constant `N2[m1]` corresponds to $N\epsilon^{(2)}(m1)$ as defined in (A.31).

Phase Space Factor: The trivial phase space factor $1/(256\pi^8)$ has been omitted in the definition of loop integration routines below. In order to obtain the result for standard integrals of the form

$$\frac{G^{m_1,m_2,m_3}_{n_1,n_2,n_3}}{(2\pi)^8} = \frac{\mu^{4\epsilon}}{(2\pi)^{2D}} \int d^Dq1 d^Dq2 \frac{1}{(q_1^2-m_1^2)^{n1}(q_2^2-m_2^2)^{n_2}((q_1+q_2)^2-m_3^2)^{n_3}}$$

the output of all routines has to be multiplied by 256 π^8 (see also comments under eq. (A.32)).

C.6.2 Two-Loop-Integration Functions

`TwoEqual[expr]` replaces in `expr` expressions of the form `G[i[m1,n1],i[m1,n2],i[0,n3]]`, with the analytical result of the corresponding scalar twoloop integral $G^{m1,m1,0}_{n1,n2,n3}$ as defined in eq. (A.32).

`TwoZero[expr]` replaces in `expr` expressions of the form `G[i[m1,n1],i[0,n2],i[0,n3]]`, with the analytical result of the corresponding scalar twoloop integral $G^{m1,0,0}_{n1,n2,n3}$ as defined in eq. (A.32).

`ScalInt[expr]` replaces in `expr` expressions of the form `G[i[m1,n1],i[m2,n2],i[0,n3]]` with the analytical result of the corresponding scalar twoloop integral $G^{m1,m2,0}_{n1,n2,n3}$ as defined in eq. (A.32).

`ScalIntAxino[expr]` replaces in `expr` expressions of the form `G[i[m1,n1],i[m2,n2],i[m1,n3]]` with the analytical result for scalar twoloop integrals of the form $G^{m1,m2,m1}_{n1,n2,n3}$ as defined in eq. (A.39).

`FacInt[expr]` replaces in `expr` factorising two-loop integrals of the form `AD[i[m1,n1],i[m2,n2]]` with the analytical result for scalar twoloop integrals of the form $G^{m1,m2,0}_{n1,n2,0}$ as defined in eq. (A.43).

Appendix D

Non-Physical Operators

The class of non-physical operators can be subdivided into the Equation-Of-Motion (EOM)-vanishing operators and evanescent operators.

D.1 EOM-Vanishing Operators

The EOM-vanishing operators appear only in an *off-shell* calculation of $b \to s\ \gamma$ ($b \to s\ g$) Greens functions. Their Wilson coefficients contribute to the process $b \to s\ l^+l^-$ ($b \to s\ q\overline{q}$), when the off-shell photon (gluon) decays into a lepton (quark) pair. The used background field version maintains explicit gauge invariance allowing to perform the matching without making use of the CKM-matrix unitarity. Therefore our relevant EOM-vanishing operators contain background photon (gluon) fields and are invariant with respect to gauge transformations of the background field.

The gauge invariant EOM-vanishing operators $\mathcal{O}_{31,\ldots,36}$ can be chosen as [50]

$$\begin{aligned}
\mathcal{O}_{31} &= \frac{1}{g}(\bar{s}\gamma^\mu P_L \mathbf{T}^a b) D^\nu G^a_{\mu\nu} + \mathcal{O}_4, \qquad \text{(D.1)}\\
\mathcal{O}_{32} &= \frac{1}{g^2} m_b \bar{s} \not{D}\not{D} P b,\\
\mathcal{O}_{33} &= \frac{i}{g^2} \bar{s} \not{D}\not{D}\not{D} P_L b,\\
\mathcal{O}_{34} &= \frac{i}{g}\left[\bar{s}\ \overleftarrow{\not{D}}\ \sigma^{\mu\nu} P_L \mathbf{T}^a b\ G^a_{\mu\nu} - G^a_{\mu\nu}\bar{s}\mathbf{T}^a\sigma^{\mu\nu}\not{D} P_L b\right] + \mathcal{O}_8,\\
\mathcal{O}_{35} &= \frac{ie}{g^2}\left[\bar{s}\ \overleftarrow{\not{D}}\ \sigma^{\mu\nu} P_L b F_{\mu\nu} - F_{\mu\nu}\bar{s}\sigma^{\mu\nu}\not{D} P_L b\right] + \mathcal{O}_7,\\
\mathcal{O}_{36} &= \frac{e}{g^2}(\bar{s}\gamma^\mu P_L b)\partial^\nu F_{\mu\nu}\ -\ \mathcal{O}_9. \qquad \text{(D.2)}
\end{aligned}$$

Our sign convention in the covariant derivative acting on a quark field ψ is

$$D_\mu \psi = \left(\partial_\mu + igG^a_\mu \mathbf{T}^a + ieQ_\psi A_\mu\right)\psi. \qquad \text{(D.3)}$$

The corresponding sign convention in the covariant derivative acting on the gluon field-strength tensor $G_{\mu\nu}$ is

$$D^\nu_{ab} G^b_{\mu\nu} = \left(\partial_\nu \delta_{ab} + g_s f_{abc} G^{c,\nu}\right) G^b_{\mu\nu}. \qquad \text{(D.4)}$$

We can assume that the EOM-vanishing operators in eq. (D.1) contain only the background gluon field, because nothing but their tree-level matrix elements is needed for the off-shell matching.

D.2 Evanescent Operators

In intermediate steps of the calculation structures like

$$(\gamma_{\mu_1}\gamma_{\mu_2}\gamma_{\mu_3}\gamma_{\mu_4}P_A)(\gamma^{\mu_1}\gamma^{\mu_2}\gamma^{\mu_3}\gamma^{\mu_4}P_B) \tag{D.5}$$

with P_A, B being either P_L or P_R. Due to the appearance of the matrix γ_5 they cannot be reduced using D dimensional Dirac algebra. Only after the matching all divergencies cancel and the limit $D \to 4$ can be taken. Therefore so called *evanescent* operators must be introduced in the effective theory. The name "evanescent" originates from the fact that such operators vanish in 4 dimensions. The following evanescent operator appears when calculating box diagrams in the SM for the process $b \to sl^+l^-$ [1]. It is defined by ([58], [73])

$$\mathcal{O}_1^E = (\bar{s}\gamma_{\mu_1}\gamma_{\mu_2}\gamma_{\mu_3}P_L b)(\bar{b}\gamma^{\mu_1}\gamma^{\mu_2}\gamma^{\mu_3}P_L l) - 4\bar{s}\gamma_{\mu_1}P_L b)(\bar{l}\gamma^{\mu}P_L l) \tag{D.6}$$

For completeness we give also the evanescent operators appearing in the calculation of the anomalous dimension ([96], [97]) of the process $b \to s\gamma$, $b \to g$, $b \to sq\overline{q}$ are defined as follows

$$\begin{aligned}
\mathcal{O}_{11}^Q &= (\bar{s}\gamma_{\mu_1}\gamma_{\mu_2}\gamma_{\mu_3}P_L\mathbf{T}^a Q)(\bar{Q}\gamma^{\mu_1}\gamma^{\mu_2}\gamma^{\mu_3}P_L\mathbf{T}^a b) - 16\mathcal{O}_1^Q,\\
\mathcal{O}_{12}^Q &= (\bar{s}\gamma_{\mu_1}\gamma_{\mu_2}\gamma_{\mu_3}P_L Q)(\bar{Q}\gamma^{\mu_1}\gamma^{\mu_2}\gamma^{\mu_3}P_L b) - 16\mathcal{O}_2^Q,\\
\mathcal{O}_{15} &= (\bar{s}\gamma_{\mu_1}\gamma_{\mu_2}\gamma_{\mu_3}\gamma_{\mu_4}\gamma_{\mu_5}P_L b)\sum_q(\bar{q}\gamma^{\mu_1}\gamma^{\mu_2}\gamma^{\mu_3}\gamma^{\mu_4}\gamma^{\mu_5}q) - 20\mathcal{O}_5 + 64\mathcal{O}_3,\\
\mathcal{O}_{16} &= (\bar{s}\gamma_{\mu_1}\gamma_{\mu_2}\gamma_{\mu_3}\gamma_{\mu_4}\gamma_{\mu_5}P_L\mathbf{T}^a b)\sum_q(\bar{q}\gamma^{\mu_1}\gamma^{\mu_2}\gamma^{\mu_3}\gamma^{\mu_4}\gamma^{\mu_5}\mathbf{T}^a q) - 20\mathcal{O}_6 + 64\mathcal{O}_4,\\
\mathcal{O}_{21}^Q &= (\bar{s}\gamma_{\mu_1}\gamma_{\mu_2}\gamma_{\mu_3}\gamma_{\mu_4}\gamma_{\mu_5}P_L\mathbf{T}^a Q)(\bar{Q}\gamma^{\mu_1}\gamma^{\mu_2}\gamma^{\mu_3}\gamma^{\mu_4}\gamma^{\mu_5}P_L\mathbf{T}^a b) - 20\mathcal{O}_{11}^Q - 256\mathcal{O}_1^Q,\\
\mathcal{O}_{22}^Q &= (\bar{s}\gamma_{\mu_1}\gamma_{\mu_2}\gamma_{\mu_3}\gamma_{\mu_4}\gamma_{\mu_5}TP_L Q)(\bar{Q}\gamma^{\mu_1}\gamma^{\mu_2}\gamma^{\mu_3}\gamma^{\mu_4}\gamma^{\mu_5}P_L b) - 20\mathcal{O}_{12}^Q - 256\mathcal{O}_2^Q,\\
\mathcal{O}_{25} &= (\bar{s}\gamma_{\mu_1}\gamma_{\mu_2}\gamma_{\mu_3}\gamma_{\mu_4}\gamma_{\mu_5}\gamma_{\mu_6}\gamma_{\mu_7}b)\sum_q(\bar{q}\gamma^{\mu_1}\gamma^{\mu_2}\gamma^{\mu_3}\gamma^{\mu_4}\gamma^{\mu_5}\gamma^{\mu_6}\gamma^{\mu_7}q) - 336\mathcal{O}_5 + 1280\mathcal{O}_3,\\
\mathcal{O}_{26} &= (\bar{s}\gamma_{\mu_1}\gamma_{\mu_2}\gamma_{\mu_3}\gamma_{\mu_4}\gamma_{\mu_5}\gamma_{\mu_6}\gamma_{\mu_7}\mathbf{T}^a b)\sum_q(\bar{q}\gamma^{\mu_1}\gamma^{\mu_2}\gamma^{\mu_3}\gamma^{\mu_4}\gamma^{\mu_5}\gamma^{\mu_6}\gamma^{\mu_7}\mathbf{T}^a q) - 336\mathcal{O}_6 + 1280\mathcal{O}_4.
\end{aligned}$$

As before, the symbol Q stands either for u or for c.

The explicit form of the evanescent operators defines the meaning of the "MS" scheme in the effective theory. Changing the evanescent operators by terms proportional to $\epsilon = 2 - D/2$ will not affect the property of the operators to vanish in the limit $D \to 4$, but it will change the actual value of the Wilson coefficients, anomalous dimensions and matrix elements of physical operators.

[1] The corresponding diagrams in the THDM vanish, as the coupling of the charged Higgs is proportional to the mass of the lepton.

Appendix E

Basics about Lie Algebras

E.1 Lie Group

A continously generated group contains elements arbitrarily close to the identity, such that the general element can be reached by the repeated action of these infinitesimal elements. Then any infinitesimal group element g can be written as

$$g(\alpha) = 1 + i\alpha^a \hat{\mathbf{T}}^a + \mathcal{O}(\alpha^2), \tag{E.1}$$

where the coefficients of the infinitesimal group parameters α^a are Hermitian operators $\hat{\mathbf{T}}^a$, called the generators of the symmetry group. A continuous group with this structure is called a Lie group.

E.2 Lie Algebra

The set of generators $\hat{\mathbf{T}}^a$ of a Lie group must span the space of infinitesimal group transformations, so the commutator of generators $\hat{\mathbf{T}}^a$ must be a linear combination of generators. Thus the commutation relations of the generators $\hat{\mathbf{T}}^a$ can be written as [30]

$$[\hat{\mathbf{T}}^a, \hat{\mathbf{T}}^b] = i f^{abc} \mathbf{T}^c, \tag{E.2}$$

where the numbers f^{abc} are the so called structure constants. From the definition (E.2) follows directly that they are antisymmetric in the first two indices; $f_{abc} = -f_{bac}$. It can be shown that in every irreducible representation (see E.5) the structure constants are totally antisymmetric [89]. The vector space spanned by the generators with the additional operation of commutation, is called a Lie Algebra.
The elements of a Lie algebra satisfy the Jacobi identity [1]

$$[\hat{\mathbf{T}}^a, [\hat{\mathbf{T}}^b, \hat{\mathbf{T}}^c]] + [\hat{\mathbf{T}}^b, [\hat{\mathbf{T}}^c, \hat{\mathbf{T}}^a]] + [\hat{\mathbf{T}}^c, [\hat{\mathbf{T}}^a, \hat{\mathbf{T}}^b]] = 0 \tag{E.3}$$

leading with (E.2) to the relation

$$f^{abc} f^{ecd} + f^{cbe} f^{aed} + f^{dbe} f^{ace} \;=\; 0. \tag{E.4}$$

[1] The Jacobi identity is an axiom that must be satisfied in order for a given set of commutation rules to define a Lie algebra.

E.3 Classification of Lie Algebras

- *compact*: Lie-Algebra with finite number of generators.

- *semi-simple*: If one of the generators $\mathbf{T}^a$ commutes with all the others, it generats an independent continuous Abelian group. Such a group, which has the structure of the group of phase rotations

$$\Psi \to e^{i\alpha}\Psi \tag{E.5}$$

  is called $U(1)$. If the algebra contains no such commuting elements, so that the group contains no $U(1)$ factors, the algebra is called *semi-simple*.

- *simple*: Semi-simple Algebra which cannot be divided into two mutually commuting sets of generators.

E.4 Casimir Operator

For any simple Lie Algebra, the operator

$$\hat{\mathbf{T}}^2 = \hat{\mathbf{T}}^a\hat{\mathbf{T}}^a \tag{E.6}$$

commutes with all group generators

$$\begin{aligned} [\hat{\mathbf{T}}^b, \hat{\mathbf{T}}^a\hat{\mathbf{T}}^a] &= (if^{bac}\hat{\mathbf{T}}^c)\hat{\mathbf{T}}^a + \hat{\mathbf{T}}^a(if^{bac}\hat{\mathbf{T}}^c) && \text{(E.7)} \\ &= if^{bac}\{\hat{\mathbf{T}}^c, \hat{\mathbf{T}}^a\} = 0 && \text{(E.8)} \end{aligned}$$

due to the antisymmetry of f^{abc} in an irreducible representation. This means that $\hat{\mathbf{T}}^2$ is an invariant of the algebra. It takes a constant value on each irreducible representation. Thus the matrix representation of $\hat{\mathbf{T}}^2$ is proportional to

$$\mathbf{T}_r^a\mathbf{T}_r^a = C_F(r)\cdot\mathbf{1}, \tag{E.9}$$

where the index r indicates the chosen representation, $\mathbf{1}$ is the $d(r)\times d(r)$ dimensional unit matrix and $C_F(r)$ is a constant called the *quadratic Casimir operator*.

E.5 Representations

- *irreducible representation* of a group :
  representation that has no nontrivial invariant subspaces.

- *fundamental representation*:
  In $SU(N)$ the basic irreducible representation (often called the fundamental representation) is the N-dimensional complex vector.

– $SU(2)$:
For $SU(2)$ the fundamental two-dimensional representation is the spinor representation, which is given in terms of Pauli matrices by

$$\mathbf{T}^a = \frac{\sigma^a}{2} \tag{E.10}$$

They satisfy

$$Tr[\mathbf{T}^a, \mathbf{T}^b] = \frac{1}{2}\delta^{a,b} \tag{E.11}$$

– $SU(N)$:
We choose the generators of $SU(N)$ so that three of them are the generators (E.10) acting on the first two components of the N-vector ξ. Then we adopt as normalisation for any $N \times N$ matrices of the fundamental representation

$$Tr[\mathbf{T}^a, \mathbf{T}^b] = \frac{1}{2}\delta^{ab}. \tag{E.12}$$

From eq. (E.2 and E.12) and noting that the $\mathbf{T}^a$ together with the unitary matrix $\mathbf{1}$ form a set of of hermitian $N \times N$ matrices we can derive the useful formula [92]

$$\mathbf{T}^a_{ij}\mathbf{T}^a_{kl} = \frac{1}{2}\left[\delta_{il}\delta_{jk} - \frac{1}{N}\delta_{ij}\delta_{kl}\right]. \tag{E.13}$$

An immediate consequence of eq. (E.13) is that

$$(\mathbf{T}^a\mathbf{T}^a)_{ij} = C_F(f)\delta_{ij} = \frac{N^2-1}{2N}, \tag{E.14}$$

where $C_F(f) = \frac{N^2-1}{2N}$ is the quadratic Casimir operator in the fundamental representation. From eq. (E.2),(E.12) as well as (E.14) we get [92]

$$f^{acd}f^{bcd} = N\delta^{ab} \tag{E.15}$$

With the help of the Jacobi identity E.4 we obtain

$$f^{cba}f^{deb}f^{kae} = -\frac{N}{2}f^{cdk}. \tag{E.16}$$

∗ $SU(3)_C$:
The standard basis for the fundamental representation of $SU(3)_C$ are the Gell-Mann-Matrices:

$$\mathbf{T}_1 = \frac{1}{2}\begin{pmatrix} 0 & 1 & 0 \\ 1 & 0 & 0 \\ 0 & 0 & 0 \end{pmatrix}, \quad \mathbf{T}_2 = \frac{1}{2}\begin{pmatrix} 0 & -i & 0 \\ i & 0 & 0 \\ 0 & 0 & 0 \end{pmatrix}, \quad \mathbf{T}_3 = \frac{1}{2}\begin{pmatrix} 1 & 0 & 0 \\ 0 & -1 & 0 \\ 0 & 0 & 1 \end{pmatrix},$$

$$\mathbf{T}_4 = \frac{1}{2}\begin{pmatrix} 0 & 0 & 1 \\ 0 & 0 & 0 \\ 1 & 0 & 0 \end{pmatrix}, \quad \mathbf{T}_5 = \frac{1}{2}\begin{pmatrix} 0 & 0 & -i \\ 0 & 0 & 0 \\ i & 0 & 0 \end{pmatrix}, \quad \mathbf{T}_6 = \frac{1}{2}\begin{pmatrix} 0 & 0 & 0 \\ 0 & 0 & 1 \\ 0 & 1 & 0 \end{pmatrix},$$

$$\mathbf{T}_7 = \frac{1}{2}\begin{pmatrix} 0 & 0 & 0 \\ 0 & 0 & -i \\ 0 & i & 0 \end{pmatrix}, \quad \mathbf{T}_8 = \frac{1}{2\sqrt{3}}\begin{pmatrix} 1 & 0 & 0 \\ 0 & 1 & 0 \\ 0 & 0 & -2 \end{pmatrix}.$$

- *adjoint representation*:
  Representation to which the generators of the algebra belong. The representation matrices are given by the structure constants:

$$(\mathbf{T}^b)_{ac} = if^{abc} \tag{E.17}$$

  With this definition, the statement that $\mathbf{T}^a$ satisfies the Lie algebra

$$([\mathbf{T}^b, \mathbf{T}^c])_{ae} = if^{bcd}(\mathbf{T}^d)_{ae}, \tag{E.18}$$

  is just a rewriting of the Jacobi-identity for the structure constants eq. (E.4).

Appendix F

On Dirac Fermions and Weyl Spinors

In this chapter we will introduce the two-component fermion notation. We will specify our conventions[1]. by showing how they correspond to the four-component fermion language. A four-component Dirac fermion ψ_D [2] with mass M is described by the Lagrangian

$$\mathcal{L}_{\text{Dirac}} = i\overline{\psi}_D\gamma^\mu\partial_\mu\psi_D - M\overline{\psi}_D\psi_D\,. \tag{F.1}$$

We use a spacetime metric $g_{\mu\nu} = \text{diag}(1,-1,-1,-1)$. For our purposes it is convenient to use the *Weyl* or *chiral* representation of the 4×4 gamma matrices given in 2×2 blocks by

$$\gamma^\mu = \begin{pmatrix} 0 & \sigma^\mu \\ \overline{\sigma}^\mu & 0 \end{pmatrix}; \qquad \gamma^5 = \begin{pmatrix} 1 & 0 \\ 0 & -1 \end{pmatrix}, \tag{F.2}$$

where

$$\begin{aligned} \sigma^0 = \overline{\sigma}^0 &= \begin{pmatrix} 1 & 0 \\ 0 & 1 \end{pmatrix}; \qquad \sigma^1 = -\overline{\sigma}^1 = \begin{pmatrix} 0 & 1 \\ 1 & 0 \end{pmatrix}; \\ \sigma^2 = -\overline{\sigma}^2 &= \begin{pmatrix} 0 & -i \\ i & 0 \end{pmatrix}; \qquad \sigma^3 = -\overline{\sigma}^3 = \begin{pmatrix} 1 & 0 \\ 0 & -1 \end{pmatrix}. \end{aligned} \tag{F.3}$$

are the Pauli sigma matrices. In this basis, a four component Dirac spinor is written in terms of 2 two-component, complex, anticommuting objects $(\xi)_\alpha$ with $\alpha = 1,2$ and $(\chi^\dagger)^{\dot\alpha}$ with $\dot\alpha = 1,2$:

$$\psi_D = \begin{pmatrix} \xi_\alpha \\ \chi^{\dagger\dot\alpha} \end{pmatrix}; \qquad \overline{\psi}_D = \begin{pmatrix} \chi^\alpha & \xi^\dagger_{\dot\alpha} \end{pmatrix}. \tag{F.4}$$

The undotted (dotted) indices are used for the first (last) two components of a Dirac spinor. The heights of these indices are important; for example, comparing eq. (F.1)-(F.4), we observe that the matrices $(\sigma^\mu)_{\alpha\dot\alpha}$ and $(\overline{\sigma}^\mu)^{\dot\alpha\alpha}$ defined by eq. (F.3) carry indices

[1] Besides the different metric we will follow the conventions used by ref. [85]

[2] In this section Dirac spinors have an additional subscript $_D$ to distinguish them from Majorana spinors with the subscript $_M$. In all other chapters Dirac spinors are given without this additional index.

with the heights as indicated. The spinor indices are raised and lowered using the antisymmetric symbol $\epsilon^{12} = -\epsilon^{21} = \epsilon_{21} = -\epsilon_{12} = 1$; $\epsilon_{11} = \epsilon_{22} = \epsilon^{11} = \epsilon^{22} = 0$, according to

$$\xi_\alpha = \epsilon_{\alpha\beta}\xi^\beta; \qquad \xi^\alpha = \epsilon^{\alpha\beta}\xi_\beta; \qquad \chi^\dagger_{\dot\alpha} = \epsilon_{\dot\alpha\dot\beta}\chi^{\dot\beta\dagger}; \qquad \chi^{\dot\alpha\,\dagger} = \epsilon^{\dot\alpha\dot\beta}\chi^\dagger_{\dot\beta}\,. \tag{F.5}$$

This is consistent since $\epsilon_{\alpha\beta}\epsilon^{\beta\gamma} = \epsilon^{\gamma\beta}\epsilon_{\beta\alpha} = \delta^\gamma_\alpha$ and $\epsilon_{\dot\alpha\dot\beta}\epsilon^{\dot\beta\dot\gamma} = \epsilon^{\dot\gamma\dot\beta}\epsilon_{\dot\beta\dot\alpha} = \delta^{\dot\gamma}_{\dot\alpha}$. The field ξ is called a "left-handed Weyl spinor" and $\chi^\dagger$ is a "right-handed Weyl spinor". The names fit, because

$$\psi_{D\,L} = P_L\psi_D = \begin{pmatrix}\xi_\alpha\\0\end{pmatrix}; \qquad \psi_{D\,R} = P_R\psi_D = \begin{pmatrix}0\\\chi^{\dagger\dot\alpha}\end{pmatrix}. \tag{F.6}$$

The hermitian conjugate of a left-handed Weyl spinor is a right-handed Weyl spinor $(\psi_\alpha)^\dagger = (\psi^\dagger)_{\dot\alpha}$ and vice versa $(\psi^{\dagger\dot\alpha})^\dagger = \psi^\alpha$. Therefore any particular fermionic degrees of freedom can be described equally well using a Weyl spinor which is left-handed (with an undotted index) or by one which is right-handed (with a dotted index). By convention, all names of fermion fields are chosen so that left-handed Weyl spinors do not carry daggers and right-handed Weyl spinors do carry daggers, as in eq. (F.4).

It is useful to abbreviate expressions with two spinor fields by suppressing undotted indices contracted like ${}^\alpha{}_\alpha$ and dotted indices contracted like ${}_{\dot\alpha}{}^{\dot\alpha}$. In particular,

$$\xi\chi \equiv \xi^\alpha\chi_\alpha = \xi^\alpha\epsilon_{\alpha\beta}\chi^\beta = -\chi^\beta\epsilon_{\alpha\beta}\xi^\alpha = \chi^\beta\epsilon_{\beta\alpha}\xi^\alpha = \chi^\beta\xi_\beta \equiv \chi\xi \tag{F.7}$$

A minus sign appeared in eq. (F.7) from exchanging the order of anticommuting spinors, but it disappeared due to the antisymmetry of the ϵ symbol. Likewise we find

$$(\xi\chi)^* \;\equiv\; \xi^\dagger\chi^\dagger = \xi^\dagger_{\dot\alpha}\chi^{\dot\alpha\,\dagger} = \xi^\dagger_{\dot\alpha}\epsilon^{\dot\alpha\dot\beta}\chi^\dagger_{\dot\beta} = \chi^\dagger_{\dot\beta}\epsilon^{\dot\beta\dot\alpha}\xi^\dagger_{\dot\alpha} = \chi^{\dot\alpha\,\dagger}\xi_{\dot\alpha\,\dagger} = \chi^\dagger\xi^\dagger.$$

In a similar way,

$$\xi^\dagger\overline\sigma^\mu\chi = -\chi\sigma^\mu\xi^\dagger = (\chi^\dagger\overline\sigma^\mu\xi)^* = -(\xi\sigma^\mu\chi^\dagger)^* \tag{F.8}$$

stands for $\xi^\dagger_{\dot\alpha}(\overline\sigma^\mu)^{\dot\alpha\alpha}\chi_\alpha$, etc. With these conventions, the Dirac Lagrangian eq. (F.1) can now be rewritten:

$$\begin{aligned}\mathcal{L}_{\rm Dirac} &= i\overline\psi_D\gamma^\mu\partial_\mu\psi_D - M\overline\psi_D\psi_D &\text{(F.9)}\\ &= i\xi^\dagger\overline\sigma^\mu\partial_\mu\xi + i\chi^\dagger\overline\sigma^\mu\partial_\mu\chi - M(\xi\chi + \xi^\dagger\chi^\dagger), &\text{(F.10)}\end{aligned}$$

where we have dropped a total derivative piece $i\partial_\mu(\chi^\dagger\overline\sigma^\mu\chi)$ which does not affect the action.

A four-component Majorana spinor can be obtained from the Dirac spinor of eq. (F.4) by imposing the constraint $\chi = \xi$, so that

$$\psi_{\rm M} = \begin{pmatrix}\xi_\alpha\\\xi^{\dagger\dot\alpha}\end{pmatrix}; \qquad \overline\psi_{\rm M} = \begin{pmatrix}\xi^\alpha & \xi^\dagger_{\dot\alpha}\end{pmatrix}. \tag{F.11}$$

The Lagrangian for a Majorana fermion with mass M

$$\mathcal{L}_{\rm Majorana} = \frac{i}{2}\overline\psi_{\rm M}\gamma^\mu\partial_\mu\psi_{\rm M} - \frac{1}{2}M\overline\psi_{\rm M}\psi_{\rm M} \tag{F.12}$$

in the four-component Majorana spinor form can therefore be rewritten

$$\mathcal{L}_{\text{Majorana}} = i\xi^\dagger \overline{\sigma}^\mu \partial_\mu \xi - \frac{1}{2} M(\xi\xi + \xi^\dagger \xi^\dagger) \tag{F.13}$$

in the two-component Weyl spinor representation.

If one has any expression involving bilinears in four-component spinors

$$\psi_1 = \begin{pmatrix} \xi_1 \\ \chi_1^\dagger \end{pmatrix} \qquad \text{and} \qquad \psi_2 = \begin{pmatrix} \xi_2 \\ \chi_2^\dagger \end{pmatrix}, \tag{F.14}$$

then one can translate into two-component Weyl spinor language (or vice versa) using the dictionary:

$$\overline{\psi}_1 P_L \psi_2 = \chi_1 \xi_2; \qquad \overline{\psi}_1 P_R \psi_2 = \xi_1^\dagger \chi_2^\dagger; \tag{F.15}$$

$$\overline{\psi}_1 \gamma^\mu P_L \psi_2 = \xi_1^\dagger \overline{\sigma}^\mu \xi_2; \qquad \overline{\psi}_1 \gamma^\mu P_R \psi_2 = \chi_1 \sigma^\mu \chi_2^\dagger. \tag{F.16}$$

Next we will show how the Standard Model quarks and leptons can be described in this notation. The complete list of *left-handed* Weyl spinors can be given the following names

$$Q_i = (u\ d),\ (c\ s),\ (t\ b) \tag{F.17}$$

$$\overline{u}_i = \overline{u},\ \overline{c},\ \overline{t} \qquad \overline{d}_i = \overline{d},\ \overline{s},\ \overline{b} \tag{F.18}$$

$$L_i = (\nu_e\ e),\ (\nu_\mu\ \mu),\ (\nu_\tau\ \tau) \tag{F.19}$$

$$\overline{e}_i = \overline{e},\ \overline{\mu},\ \overline{\tau}, \tag{F.20}$$

where $i = 1, 2, 3$ is the family index. The unbarred fields are the left-handed pieces of a Dirac spinor, while the barred fields are the names given to the conjugates of the right-handed piece of a Dirac spinor. For example, e is e_L and $\overline{e}$ is the same as $e_R^\dagger$. Together they form a Dirac spinor:

$$\begin{pmatrix} e \\ \overline{e}^\dagger \end{pmatrix} \equiv \begin{pmatrix} e_L \\ e_R \end{pmatrix} \tag{F.21}$$

with similar equations for all of the other quark and charged lepton Dirac spinors (the neutrinos of the Standard Model are not part of a Dirac spinor).

Appendix G

Feynman Rules

In this appendix we give all Feynman rules used in this work. We used the Feynman-t'Hooft-gauge for all massive gauge bosons. All external gluons are background fields. Quarks and leptons carry generation indices $\{I, J\}$ running from $1-3$. All vertices are properly symmetrised.

G.1 Conventions and Abbreviations

G.1.1 Conventions

- In the following it will always be assumed that the elementary charge $e > 0$.
- Sign convention of the SU(2) covariant derivative:

  $$D_\mu = \partial_\mu + \sigma g_2 W_\mu$$

  Unfortunately two different sign conventions are used in the Standard Model and THDM model-files of FeynArts [88]: σ is $-$ in the SM and $+$ in the THDM model files. There is a simple rule for translating the two conventions: replace s_W by $-s_W$ and add an additional minus sign for each Higgs field that appears in a coupling. In order to combine SM and THDM results in a stringent way, we have used

  $$\sigma = -$$

  in the SM and in the self-written files THDM. This self-written files are simply modifications of the SM model files where only the THDM interactions needed for the rare B decays are added.
- Arrows on scalars indicate the charge flow. Momenta follow the charge flow.
- We assume that three matter generations exist, so the capital letters $I,\ J, ...$ run from 1-3 indicating the three matter generations.
- When implementing the vertices into a FeynArts-model file, it has to be taken into consideration that in FeynArts all momenta always point to the vertex.

G.1.2 Abbreviations

The following abbreviations will be used:

- F=Fermion, V=Vector, S=Scalar.
- $s_W = \sin\Theta_W$, $c_W = \cos\Theta_W$, where Θ_W is the Weinberg angle.

G.2 Propagators

1. Scalar particles (Higgs bosons):

$$\frac{i}{p^2 - m^2}$$

2. Vector bosons:

$$\frac{-ig_{\mu\nu}}{p^2 - m^2}$$

3. Fermions:
Fermions are denoted by solid lines. For Dirac fermions, each line carries an arrow which indicates the fermion number flow. Momentum flows from left to right. Thin arrows beneath the propagator denote the orientation of the fermion flow.

Dirac Fermions:

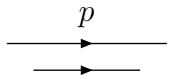

$$iS(p) = \frac{i}{p_\mu\gamma^\mu - m} = \frac{i\,(\not{p} + m)}{p^2 - m^2}$$

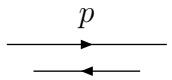

$$iS(-p) = \frac{i}{-p_\mu\gamma^\mu - m} = \frac{i\,(-\not{p} + m)}{p^2 - m^2}$$

Majorana fermions:

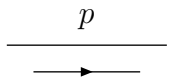

$$iS(p) = \frac{i}{p_\mu\gamma^\mu - m} = \frac{i\,(\not{p} + m)}{p^2 - m^2}$$

A more detailed discussion of Majorana fermions can be found in section G.4.3.
The propagators of gluons, quarks and squarks should be multiplied by a factor δ^{ab}, where a and b are as usual colour indices.

G.3 External Lines

Mass shell condition for external lines

$$p^2 = m^2. \tag{G.1}$$

Momentum flows always from left to right and is denoted by small arrows above the external lines. Thin arrows beneath the external line denote the orientation (fermion

flow).

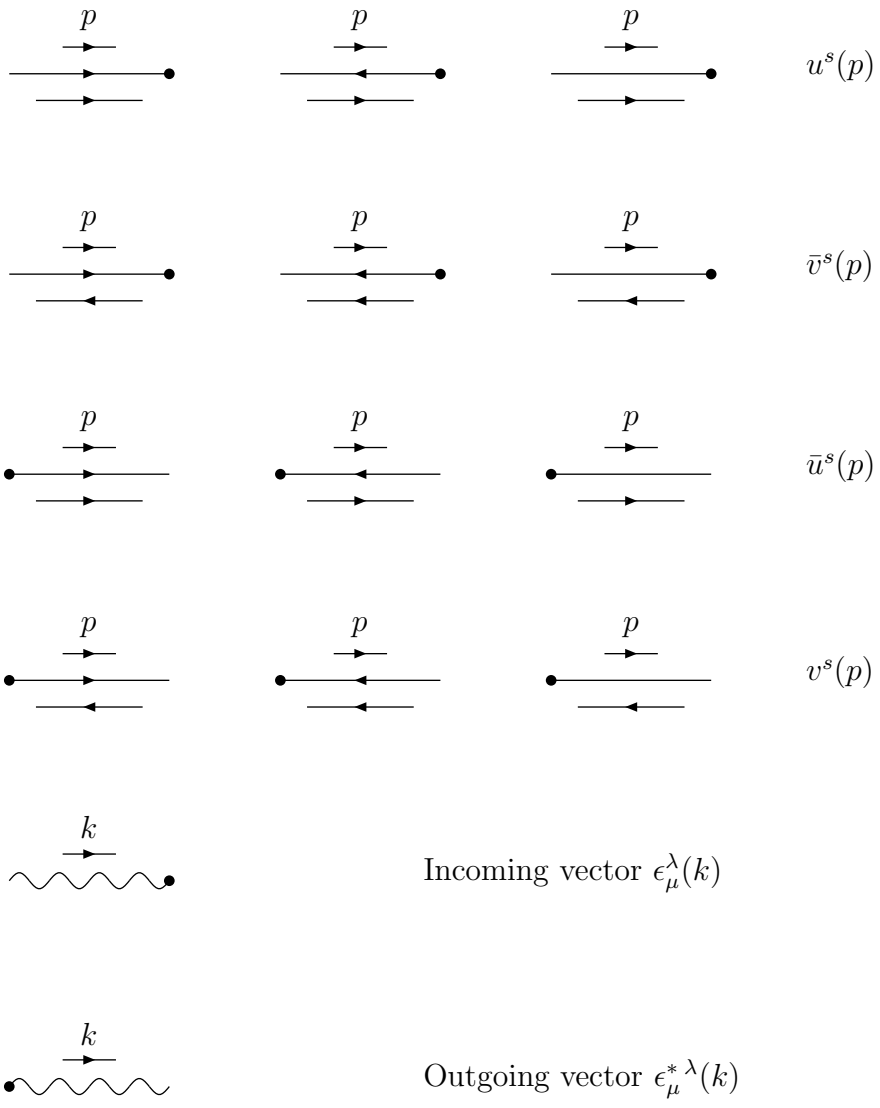

$s = 1, 2$ denotes the spin states, $\lambda = 1, 2$ the polarization states.

G.4 Vertices

In the following we will only display the vertices actually needed for our calculations.

G.4.1 Standard Model

FFV-couplings

1. Quark-quark-gauge boson

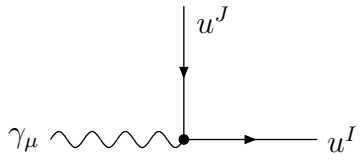

$$-ie\gamma^\mu Q_u \delta^{IJ} = -\frac{2}{3} ie\gamma^\mu \delta^{IJ}$$

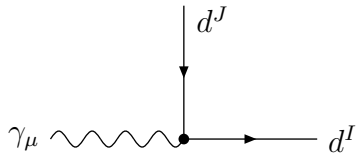

$$-ieQ_d \gamma^\mu \delta^{IJ} = \frac{1}{3} ie\gamma^\mu \delta^{IJ}$$

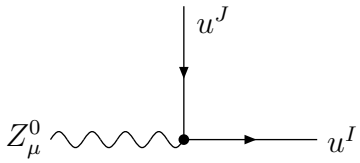

$$-\frac{ie}{2 s_W c_W} \gamma^\mu (P_L - \frac{4}{3} s_W^2) \delta^{IJ}$$

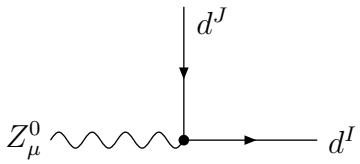

$$\frac{ie}{2 s_W c_W} \gamma^\mu (P_L - \frac{2}{3} s_W^2) \delta^{IJ}$$

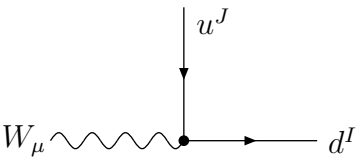

$$-\frac{ie}{\sqrt{2} s_W} V^{JI\star} \gamma^\mu P_L$$

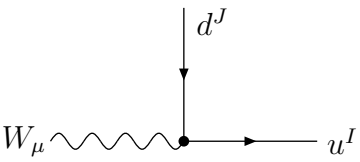

$$-\frac{ie}{\sqrt{2} s_W} V^{IJ} \gamma^\mu P_L$$

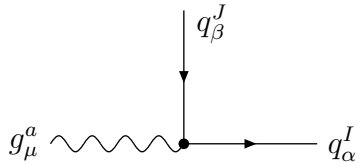

$$-ig_s (T^a)_{\alpha\beta} \gamma^\mu \delta^{IJ}$$

2. Lepton-lepton-gauge boson

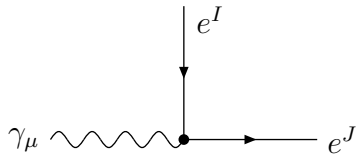

$$ie\gamma^\mu \delta^{IJ}$$

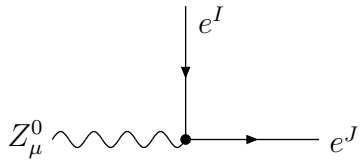

$$\frac{ie}{2s_W c_W}\gamma^\mu(P_L - 2s_W^2)\delta^{IJ}$$

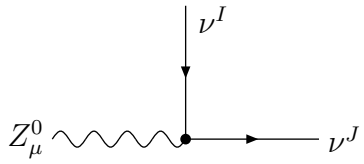

$$-\frac{ie}{2s_W c_W}\gamma^\mu P_L\delta^{IJ}$$

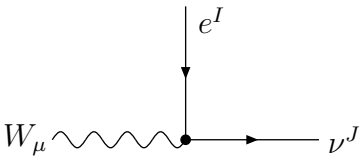

$$-\frac{ie}{\sqrt{2}s_W}\gamma^\mu P_L\delta^{IJ}$$

FFS-coupling

3. Quark-quark-Would-be Goldstone-boson

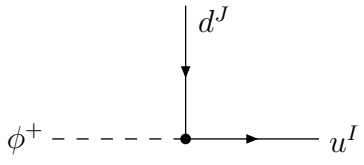

$$\frac{ie}{\sqrt{2}s_W}V^{IJ}\left[\frac{m_{u_I}}{M_W}P_L - \frac{m_{d_J}}{M_W}P_R\right]$$

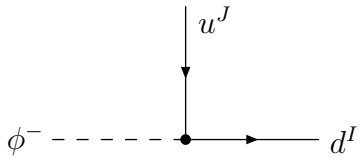

$$\frac{ie}{\sqrt{2}s_W}V^{JI\star}\left[-\frac{m_{d_I}}{M_W}P_L + \frac{m_{u_J}}{M_W}P_R\right]$$

G.4.2 THDM

SSV-coupling

1. Charged Higgs particle-gauge boson

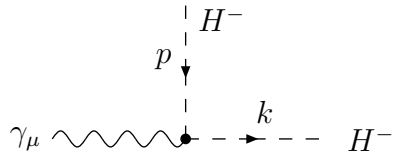

$$ie(p+k)^\mu$$

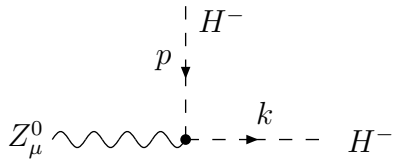

$$-ie\frac{c_W^2 - s_W^2}{2s_W c_W}(p+k)^\mu$$

FFS-coupling

2. Leptons and quarks -charged Higgs particles

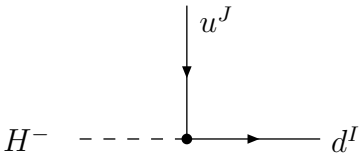

$$i\frac{e}{\sqrt{2}s_W M_W}(Xm_{d_I}P_L + Xm_{u_J}P_R)V^{JI\star}$$

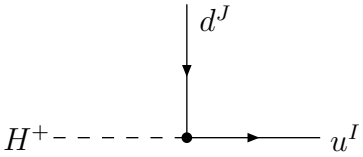

$$i\frac{e}{\sqrt{2}s_W M_W}(Ym_{u_I}P_L + Xm_{d_J}P_R)V^{IJ}$$

G.4.3 The Axino Diagram's Vertices

Fermion Flow and Majorana Fermions

Since photinos and axinos are Majorana fermions one has to cope with fermion number violating interactions when calculating the $\tilde{\tau}$ decays. As soon as fermion-number violating couplings are present, the fermion flow cannot be defined in the standard way. Feynman rules for Majorana fermions which yield nonetheless the correct relative minus signs between different interfering diagrams contributing to a process are proposed in [98]. The basic idea is to introduce an arbitrary continuous fermion flow for all fermion chains. Instead of ordering the fermion propagators according to the given fermion number flow, one *chooses* a direction for the fermion lines. This means that *the fermion number flow is replaced by a fermion flow* which corresponds to an orientation of each complete fermion chain. Is it possible to reverse the interaction Lagrangian $\overline{\psi}_1\,\Gamma\,\psi_2$ by introducing the charge-conjugate fields

$$\psi^c = C\overline{\psi}^T;\;\; \overline{\psi^c} = -\psi^T C^{-1}, \tag{G.2}$$

where the charge-conjugation matrix C fulfils

$$C^\dagger = C^{-1}, \quad C^T = -C, \quad C\Gamma^T C^{-1} = \eta_i\,\Gamma_i \tag{G.3}$$

(no summation over i) with

$$\eta = \begin{cases} \;\;1 & \text{for} \quad \Gamma \in \{1, \gamma^5, \gamma^5\gamma^\mu\} \\ -\;\;1 & \text{for} \quad \Gamma \in \{\gamma^\mu, \sigma^{\mu\nu}\}. \end{cases} \tag{G.4}$$

Thus

$$\begin{aligned} \overline{\psi}_1\,\Gamma\,\psi_2 &= g^i_{abc}\Phi_c\overline{\psi}_{1\,a}\Gamma_i\,\psi_{2\,b} = g^i_{abc}\Phi_c(\overline{\psi}_{1\,a}\Gamma_i\,\psi_{2\,b})^T = (-1)g^i_{abc}\Phi_c\psi^T_{2\,b}\Gamma_i^T\,\overline{\psi}^T_{1\,a} \\ &= g^i_{abc}\Phi_c(-\psi^T_{2\,b})\Gamma_i^T\,\overline{\psi}^T_{1\,a} = g^i_{abc}\Phi_c\overline{\psi^C}_{2\,b}C\,\Gamma_i^T\,C^-1\,\psi^C_{1\,a} \\ &= = g^i_{abc}\Phi_c\overline{\psi^C}_{2\,b}\eta_i\Gamma_i\,\psi^C_{1\,a} \\ &=: \overline{\psi}_2\,\Gamma\,\psi_1, \end{aligned} \tag{G.5}$$

where the so called "flip rule" is given by

$$\Gamma' = C\Gamma^T C^{-1} = \eta\,\Gamma = \begin{cases} \Gamma & \text{for} \quad \Gamma \in \{1, i\,\gamma^5, \gamma^5\gamma^\mu\} \\ -\Gamma & \text{for} \quad \Gamma \in \{\gamma^\mu, \sigma^{\mu\nu}\}. \end{cases} \tag{G.6}$$

For Majorana fermions we have

$$\psi^c = \psi. \tag{G.7}$$

Hence, when stating Feynman rules we can restrict ourselves to one fermion flow - even when dealing with vertices including Majorana fermions. Changing the fermion flow can be necessary, if the chosen directions is opposite to the actual fermion flow (arbitrarily chosen by a program like FeynArts).
The following Feynman rules are derived from the Lagrangians given in eq.(10.15)-(10.21). We will not display the Feynman rules for all three matter generations as in the case of the SM and THDM, but we will restrict ourself to the third generation, the matter generation we considered in our calculations.
In order to simplify our notation it is supposed that the fermion flow is always parallel to the momentum flow. Fermion flow and fermion number flow are supposed to have the same orientation. Opposite orientation of the fermion flow can be obtained by replacing Γ by $\Gamma' = \pm\Gamma$ according to eq. (G.6).

FFV-coupling

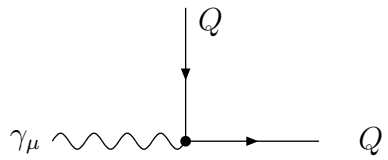

$$-ie\; e_Q \gamma^\mu$$

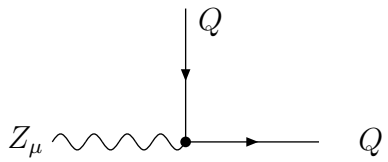

$$-i\frac{e}{2s_W\; c_W}\;\gamma^\mu(-2e_Q s_W^2) = i\frac{s_W}{c_W}\;\gamma^\mu e\; e_Q$$

FFS-coupling

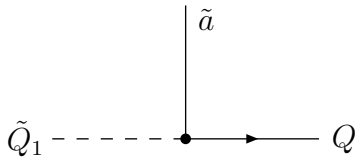

$$-iyP_L$$

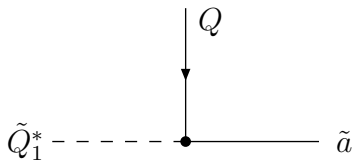

$$-iyP_R$$

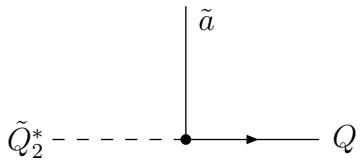

$$-iyP_R$$

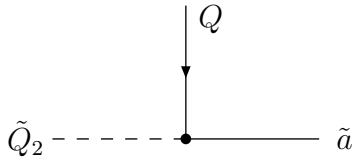

$$-iyP_L$$

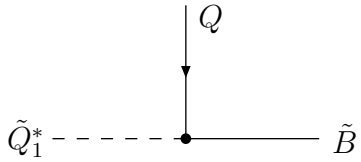

$$-i\sqrt{2}\frac{e}{c_W}\, e_Q\, P_L$$

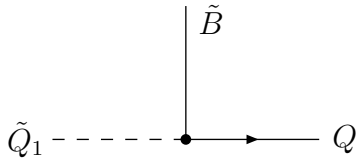

$$-i\sqrt{2}\frac{e}{c_W}\, e_Q\, P_R$$

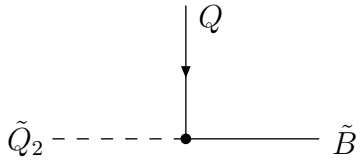

$$i\sqrt{2}\frac{e}{c_W}\, e_Q\, P_R$$

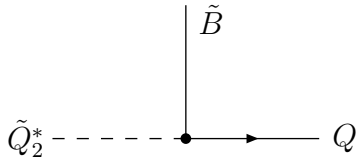

$$i\sqrt{2}\frac{e}{c_W}\, e_Q\, P_L$$

The $\tilde{\tau}\ \tau\ \tilde{B}$-vertices are given by

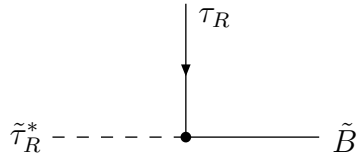

$$i\sqrt{2}\frac{e}{c_W}e_\tau P_R = -i\sqrt{2}\frac{e}{c_W}P_R$$

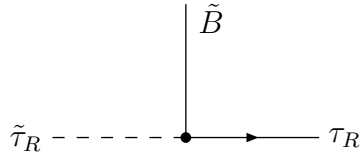

$$i\sqrt{2}\frac{e}{c_W}e_\tau P_L = -i\sqrt{2}\frac{e}{c_W}P_L$$

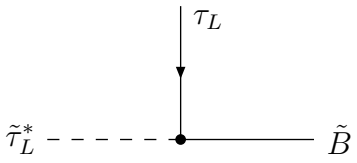

$$-i\sqrt{2}\frac{e}{c_W}e_\tau P_L = i\sqrt{2}\frac{e}{c_W}P_L$$

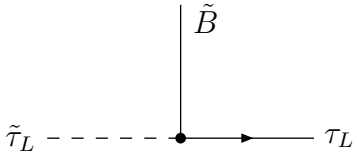

$$-i\sqrt{2}\frac{e}{c_W}e_\tau P_R = i\sqrt{2}\frac{e}{c_W}P_R$$

SSV-coupling

Arrows an scalars denote the momentum flow.

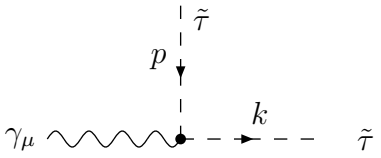

$$-ie\ e_\tau(p+k)^\mu = ie\ (p+k)^\mu$$

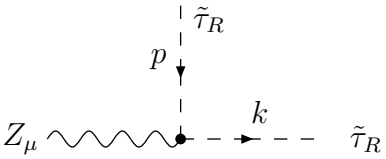

$$-i\frac{e}{c_W}\ (-e_\tau)s_W(p+k)^\mu = -ie\ \frac{s_W}{c_W}(p+k)^\mu$$

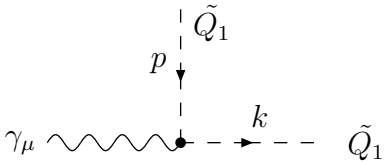

$$-ie\ e_Q(p+k)^\mu$$

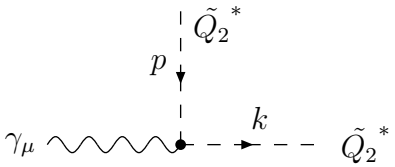

$$-ie\ e_Q(p+k)^\mu$$

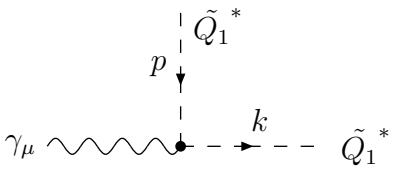

$$ie\ e_Q(p+k)^\mu$$

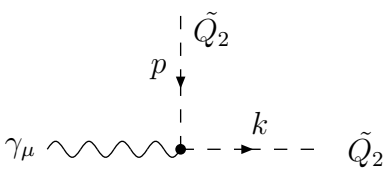

$$ie\ e_Q(p+k)^\mu$$

The above rules for the squark-squark-photon couplings can also be written as

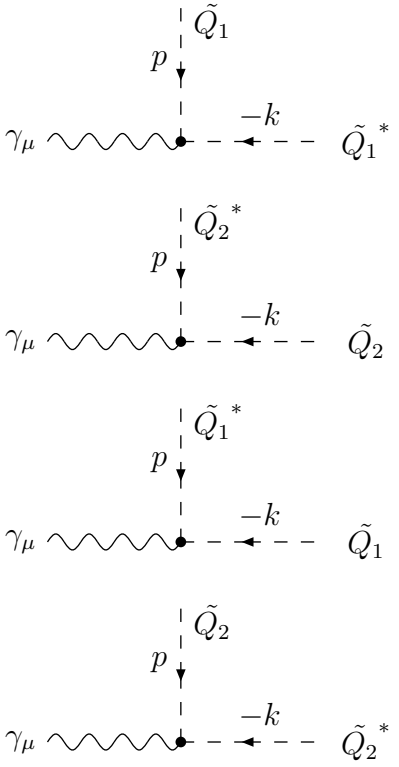

$-ie\ e_Q(p+k)^\mu$

$-ie\ e_Q(p+k)^\mu$

$ie\ e_Q(p+k)^\mu$

$ie\ e_Q(p+k)^\mu$

G.5 Formulation of the Feynman Rules

With the above ingredients the Feynman amplitudes are obtained as follows [98]:

- Draw all possible Feynman diagrams for a given process.
- Fix an *arbitrary* orientation (fermion flow) for each fermion chain.
- Start at an external leg (for closed loops at some arbitrary propagator) and write down the Dirac matrices proceeding opposite to the chosen orientation (fermion flow) through the chain.
- Insert the appropriate analytic expression for each internal propagator, external line and vertex. If the orientation (fermion flow) is opposite to the flow of fermion number the reversed vertices Γ', propagators S(-p) and spinors have to be taken.
- Multiply by a factor (-1) for every closed loop.
- Multiply by the permutation parity of the spinors in the obtained analytical expression with respect to some reference order.
- Majorana fermions behave exactly like real scalar or vector fields as far as the determination of the combinatorial factor is concerned.

Appendix H

Numerical Input Parameters

Below we give a compilation of input parameters that were used in the numerical parts of this thesis. All input parameters, if not quoted differently, are from [31, 62]

Running quark mass:

$$m_{\mathrm{t}}^{(\mathrm{pole})} = 178 \text{ GeV}$$

QCD and electroweak parameters:

$$\begin{array}{lcllcl} \alpha_s(M_Z) & = & 0.119 & \Lambda_{\overline{\mathrm{MS}}}{}^{(5)} & = & (225 \pm 85) \text{ MeV} \\ \alpha_{\mathrm{em}}(M_Z) & = & 1/129 & M_W & = & 80.4 \text{ GeV} \\ \sin\theta_{\mathrm{W}} & = & 0.231 & M_Z & = & \frac{M_W}{\cos\theta_{\mathrm{W}}} = 91.2 \end{array}$$

Bibliography

[1] P. W. Higgs, Phys. Lett. **12**, 132 (1964).

[2] P. W. Higgs, Phys. Rev. Lett. **13**, 508 (1964).

[3] P. W. Higgs, Phys. Rev. **145**, 1156 (1966).

[4] G. 't Hooft and M. J. G. Veltman, Nucl. Phys. **B44**, 189 (1972).

[5] B. W. Lee and J. Zinn-Justin, Phys. Rev. **D5**, 3121 (1972).

[6] ALEPH, R. Barate *et al.*, Phys. Lett. **B565**, 61 (2003), [hep-ex/0306033].

[7] N. Cabibbo, Phys. Rev. Lett. **10**, 531 (1963).

[8] M. Kobayashi and T. Maskawa, Prog. Theor. Phys. **49**, 652 (1973).

[9] J. H. Christenson, J. W. Cronin, V. L. Fitch and R. Turlay, Phys. Rev. Lett. **13**, 138 (1964).

[10] CDF, T. Affolder *et al.*, Phys. Rev. **D61**, 072005 (2000), [hep-ex/9909003].

[11] S. L. Glashow, J. Iliopoulos and L. Maiani, Phys. Rev. **D2**, 1285 (1970).

[12] P. Gambino and M. Misiak, Nucl. Phys. **B611**, 338 (2001), [hep-ph/0104034].

[13] H. F. A. Group(HFAG), hep-ex/0505100.

[14] M. Ciuchini, G. Degrassi, P. Gambino and G. F. Giudice, Nucl. Phys. **B527**, 21 (1998), [hep-ph/9710335].

[15] F. M. Borzumati and C. Greub, Phys. Rev. **D58**, 074004 (1998), [hep-ph/9802391].

[16] F. M. Borzumati and C. Greub, Phys. Rev. **D59**, 057501 (1999), [hep-ph/9809438].

[17] P. Ciafaloni, A. Romanino and A. Strumia, Nucl. Phys. **B524**, 361 (1998), [hep-ph/9710312].

[18] C. Bobeth, M. Misiak and J. Urban, Nucl. Phys. **B567**, 153 (2000), [hep-ph/9904413].

[19] S. Schilling, C. Greub, N. Salzmann and B. Toedtli, hep-ph/0407323.

[20] R. D. Peccei and H. R. Quinn, Phys. Rev. Lett. **38**, 1440 (1977).

[21] J. E. Kim, Phys. Rev. Lett. **43**, 103 (1979).

[22] L. Covi, J. E. Kim and L. Roszkowski, Phys. Rev. Lett. **82**, 4180 (1999), [hep-ph/9905212].

[23] G. L. Kane, C. F. Kolda, L. Roszkowski and J. D. Wells, Phys. Rev. **D49**, 6173 (1994), [hep-ph/9312272].

[24] J. R. Ellis, T. Falk, G. Ganis, K. A. Olive and M. Schmitt, Phys. Rev. **D58**, 095002 (1998), [hep-ph/9801445].

[25] K. Griest and L. Roszkowski, Phys. Rev. **D46**, 3309 (1992).

[26] M. A. Shifman, A. I. Vainshtein and V. I. Zakharov, Nucl. Phys. **B166**, 493 (1980).

[27] K. Hamaguchi, Y. Kuno, T. Nakaya and M. M. Nojiri, Phys. Rev. **D70**, 115007 (2004), [hep-ph/0409248].

[28] J. L. Feng and B. T. Smith, Phys. Rev. **D71**, 015004 (2005), [hep-ph/0409278].

[29] G. Buchalla, A. J. Buras and M. E. Lautenbacher, Rev. Mod. Phys. **68**, 1125 (1996), [hep-ph/9512380].

[30] M. E. Peskin and D. V. Schroeder, *An Introduction to Quantum Field Theory* (Reading, USA: Addison-Wesley, 1995).

[31] S. Eidelman *et al.*, Physics Letters B **592**, 1+ (2004).

[32] H. Georgi, Hadronic J. **1**, 155 (1978).

[33] J. F. Gunion, H. E. Haber, G. L. Kane and S. Dawson, hep-ph/9302272.

[34] J. F. Gunion, H. E. Haber, G. L. Kane and S. Dawson, SCIPP-89/13.

[35] J. F. Gunion and H. E. Haber, Nucl. Phys. **B272**, 1 (1986).

[36] S. L. Glashow and S. Weinberg, Phys. Rev. **D15**, 1958 (1977).

[37] A. J. Buras, hep-ph/9806471.

[38] P. Breitenlohner and D. Maison, Commun. Math. Phys. **52**, 11,39,55 (1977).

[39] G. Bonneau, Nucl. Phys. **B177**, 523 (1981).

[40] A. J. Buras and P. H. Weisz, Nucl. Phys. **B333**, 66 (1990).

[41] K. G. Wilson, Phys. Rev. **179**, 1499 (1969).

[42] C. Bobeth, M. Misiak and J. Urban, Nucl. Phys. **B574**, 291 (2000), [hep-ph/9910220].

[43] M. Misiak, Nucl. Phys. **B393**, 23 (1993).

[44] T. Hahn, Comput. Phys. Commun. **140**, 418 (2001), [hep-ph/0012260].

[45] V. A. Smirnov, Mod. Phys. Lett. **A10**, 1485 (1995), [hep-th/9412063].

[46] A. I. Davydychev and J. B. Tausk, Nucl. Phys. **B397**, 123 (1993).

[47] A. Ghinculov and J. J. van der Bij, Nucl. Phys. **B436**, 30 (1995), [hep-ph/9405418].

[48] M. J. Dugan and B. Grinstein, Phys. Lett. **B256**, 239 (1991).

[49] S. Herrlich and U. Nierste, Nucl. Phys. **B455**, 39 (1995), [hep-ph/9412375].

[50] C. Bobeth, M. Misiak and J. Urban, Nucl. Phys. **B574**, 291 (2000), [hep-ph/9910220].

[51] A. J. Buras and M. Munz, Phys. Rev. **D52**, 186 (1995), [hep-ph/9501281].

[52] K. G. Chetyrkin, M. Misiak and M. Munz, Nucl. Phys. **B520**, 279 (1998), [hep-ph/9711280].

[53] K. G. Chetyrkin, M. Misiak and M. Munz, Phys. Lett. **B400**, 206 (1997), [hep-ph/9612313].

[54] K. G. Chetyrkin, M. Misiak and M. Munz, Phys. Lett. **B400**, 206 (1997), [hep-ph/9612313].

[55] K. Baranowski and M. Misiak, Phys. Lett. **B483**, 410 (2000), [hep-ph/9907427].

[56] G. Buchalla and A. J. Buras, Nucl. Phys. **B398**, 285 (1993).

[57] T. Inami and C. S. Lim, Prog. Theor. Phys. **65**, 297 (1981).

[58] M. Misiak and J. Urban, Phys. Lett. **B451**, 161 (1999), [hep-ph/9901278].

[59] C. Bobeth, A. J. Buras, F. Kruger and J. Urban, Nucl. Phys. **B630**, 87 (2002), [hep-ph/0112305].

[60] C. Bobeth, *QCD Corrections to $\bar{B} \to X_s l^+ l^-$ in the Standard Model and Beyond*, PhD thesis, TU Munich, 2003, http://tumb1.biblio.tu-muenchen.de/publ/diss/ph/2003/bobeth.pdf.

[61] P. L. Cho, M. Misiak and D. Wyler, Phys. Rev. **D54**, 3329 (1996), [hep-ph/9601360].

[62] D0, V. M. Abazov *et al.*, Nature **429**, 638 (2004), [hep-ex/0406031].

[63] P. Gambino, M. Gorbahn and U. Haisch, Nucl. Phys. **B673**, 238 (2003), [hep-ph/0306079].

[64] C. Bobeth, A. J. Buras and T. Ewerth, hep-ph/0409293.

[65] A. Ali and C. Greub, Phys. Lett. **B259**, 182 (1991).

[66] A. J. Buras, M. Misiak, M. Munz and S. Pokorski, Nucl. Phys. **B424**, 374 (1994), [hep-ph/9311345].

[67] A. Ali, G. F. Giudice and T. Mannel, Z. Phys. **C67**, 417 (1995), [hep-ph/9408213].

[68] K. Adel and Y.-P. Yao, Phys. Rev. **D49**, 4945 (1994), [hep-ph/9308349].

[69] C. Greub and T. Hurth, Phys. Rev. **D56**, 2934 (1997), [hep-ph/9703349].

[70] C. Greub, T. Hurth and D. Wyler, Phys. Lett. **B380**, 385 (1996), [hep-ph/9602281].

[71] A. J. Buras, A. Kwiatkowski and N. Pott, Nucl. Phys. **B517**, 353 (1998), [hep-ph/9710336].

[72] G. Buchalla and A. J. Buras, Nucl. Phys. **B400**, 225 (1993).

[73] G. Buchalla and A. J. Buras, Nucl. Phys. **B548**, 309 (1999), [hep-ph/9901288].

[74] S. Bertolini, F. Borzumati, A. Masiero and G. Ridolfi, Nucl. Phys. **B353**, 591 (1991).

[75] WMAP, D. N. Spergel *et al.*, Astrophys. J. Suppl. **148**, 175 (2003), [astro-ph/0302209].

[76] B. W. Lee and S. Weinberg, Phys. Rev. Lett. **39**, 165 (1977).

[77] E. Diehl, G. L. Kane, C. F. Kolda and J. D. Wells, Phys. Rev. **D52**, 4223 (1995), [hep-ph/9502399].

[78] R. D. Peccei and H. R. Quinn, Phys. Rev. **D16**, 1791 (1977).

[79] G. G. Raffelt, Phys. Rept. **198**, 1 (1990).

[80] T. Schafer and E. V. Shuryak, Rev. Mod. Phys. **70**, 323 (1998), [hep-ph/9610451].

[81] A. R. Zhitnitsky, Sov. J. Nucl. Phys. **31**, 260 (1980).

[82] M. Dine and W. Fischler, Phys. Lett. **B120**, 137 (1983).

[83] A. Brandenburg, L. Covi, K. Hamaguchi, L. Roszkowski and F. D. Steffen, hep-ph/0501287.

[84] L. Covi, L. Roszkowski, R. Ruiz de Austri and M. Small, JHEP **06**, 003 (2004), [hep-ph/0402240].

[85] S. P. Martin, hep-ph/9709356.

[86] private communication with K. Hamaguchi and F. Steffen.

[87] P. Liniger, *Charmless B-Meson Decays in the Standard Model*, PhD thesis, University of Bern, 2001, http://www-itp.unibe.ch/thesis/liniger/thesis.ps.

[88] T. Hahn, Comput. Phys. Commun. **140**, 418 (2001), [hep-ph/0012260].

[89] R. Field, *Applications of perturbative QCD* (Addison-Wesley, 1989).

[90] K. G. Chetyrkin, M. Misiak and M. Munz, Nucl. Phys. **B518**, 473 (1998), [hep-ph/9711266].

[91] J. C. Collins, *Renormalization. An introduction to renormalization, the renormalization group, and the operator product expansion* (Cambridge, Uk: Univ. Pr., 1984).

[92] T. Muta, World Sci. Lect. Notes Phys. **57**, 1 (1998).

[93] Wolfram, *MATHEMATICA, Version 5.0* (Champaign, Illinois: Wolfram Research, Inc., 2003).

[94] A. Heck, *Introduction to Maple* (New York: Springer, 1993).

[95] M. Abramowitz and I. E. Stegun, *Handbook of Mathematical Functions* (New York: Dover, 1972).

[96] K. G. Chetyrkin, M. Misiak and M. Munz, Nucl. Phys. **B518**, 473 (1998), [hep-ph/9711266].

[97] P. Gambino, M. Gorbahn and U. Haisch, Nucl. Phys. **B673**, 238 (2003), [hep-ph/0306079].

[98] A. Denner, H. Eck, O. Hahn and J. Kublbeck, Nucl. Phys. **B387**, 467 (1992).

CURRICULUM VITAE

Personal data

Name	SCHILLING
First name	Sabine
Date of birth	31/01/1974
Nationality	german

Education

11/2001-08/2005	Postgraduate studies at the Department of Theoretical Physics of the University of Zurich, Switzerland PhD thesis: Two–Loop Techniques in Rare Decays Thesis supervisor: Prof. Daniel Wyler
10/2000	**Diplom** (M.S.) in physics at the University of Heidelberg
08/99-09/00	Diploma thesis: H1 collaboration at DESY (Hamburg): Implementation of BGF- processes in Monte Carlo generators for electron-proton scattering
10/1997 - 03/1998	Sokrates/ERASMUS-international exchange program at the University of Turin, Italy
07/1996	Intermediate diploma in physics at the University of Heidelberg (Germany)
04/1996 - 09/1997	Parallel study of physics and psychology of at the University of Heidelberg
10/1993- 10/2000	Study of physics at the University of Heidelberg
06/93	**Abitur**
08/1994 - 06/93	Eleonoren - Gymnasium Worms (Germany)

Professional and Research Experience

since 11/01	Teaching assistant for theoretical physics at the Institute of Theoretical Physics at the University of Zurich for physics majors: Courses in mathematical methods, mechanics, electrodynamics and quantum mechanics
03/2001 - 09/2001	Research assistant at DESY (Hamburg): Implementation of the Subtraction method for Boson - Gluon Fusion in the Monte - Carlo generator RAPGAP
09/2001 - 11/2001	Internship at the Finance and Risk Consulting Group of Arthur Andersen (Frankfurt)
08/1997-09/1997	Internship at the AMANDA collaboration at DESY Zeuthen: Report: On the Rejection of Fake Muons in AMANDA using Neural Networks

Publication

Schilling, S. and Greub, C. and Salzmann, N. and Toedtli,B.,
QCD corrections to the Wilson coefficients $C_{(9)}$ and $C_{(10)}$ in two-Higgs-doublet models,
Phys. Lett. **B 616** (2005) [arXiv:hep-ph/0407323]

Languages

German	mother tongue
Italian, English	fluent
French	good

Acknowledgement

I am indebted to many persons who helped me to learn the basic skills to perform a two–loop (matching) calculation.
First and foremost I would like to thank my advisor Prof. Dr. Daniel Wyler for the possibility to work not only on the interesting subject of B physics, but also the decays of axinos. The latter gave me the possibility to apply the tools developed originally loop diagrams in rare B-decays to two-loop decays in early universe physics and thus to get insight into early universe physics. I have learned to appreciate his profound knowledge of the subject and intuition for the essential. I am also grateful for the many proofreading of the manuscript of this theses.
Next I would like to thank Dr. Mikolaj Misiak who guided my first steps into the field of B physics, effective theories and the technical details of two loop calculations for always patiently giving me well considered answers to all my questions. I really enjoyed the collaboration with him.
Moreover, a special thanks goes to Dr. Jörg Urban. He gave me a lot of technical advises into the programming of two-loop tools, as well as very enriching discussions about his papers, which helped me a lot to avoid the cliffs of tedious two–loop calculations.
Furthermore I want like to thank PD Dr. Christoph Greub for the very nice collaboration in writing our paper, his many advices according the Heavy Mass Expansion and for volunteering to be a referee of this thesis.
Many thanks also to Dr. Frank-Daniel Steffen for proposing the interesting project of the rare stau-decays in the context of early universe physics. Thanks also to Dr. Koichi Hamaguchi who gave a lot advice in the beginning of the project.
It is a great pleasure for me to thank all members of the University of Zurich for numerous – not only physics – discussions, chats and pleasant social environment. Special thanks to Tobias Huber and Dr. Enrico Lunghi as well as Prof. Dr. Thomas Gehrman for many fruitfull discussions about B-physics.
Finalement merci beaucoup à Cyril pour sa patience.